Cranfield UNIVERSITY

Daniele Samuel Pascovici

"Thermo Economic and Risk Analysis for Advanced Long Range Aero Engines"

School of Engineering

PhD Thesis

Cranfield UNIVERSITY

Daniele Samuel Pascovici

"Thermo Economic and Risk Analysis for Advanced Long Range Aero Engines"

Supervisors:

Prof. Riti Singh

Dr. Stephen Ogaji

December 2008

This thesis is submitted in partial fulfilment of the requirements for the Degree of Doctor of Philosophy

To improve yourself and your knowledge

Frank Nopple

Executive Summary

To conceive and assess engines with minimum global warming impact and lowest cost of ownership in a variety of emission legislation scenarios, emissions taxation policies, fiscal and Air Traffic Management environments a Techno economic and Environmental Risk Assessment (TERA) model is needed.

In the first part of this thesis an approach is presented to estimate the cost of maintenance and the direct operating costs of turbofan engines of equivalent thrust rating, both for long and short range applications. The three advanced types of turbofan engines analysed here are a direct drive three spool with ultra high bypass ratio, a geared turbofan with the same fan as the direct drive engine and a turbofan with counter rotating fans. The baseline engines are a three spool for long range (Trent 772b) and a two spool (CFM56-7b) for short range applications. The comparison with baseline engines shows the gains and losses of these novel cycle engines.

The economic model is composed of three modules: a lifing module, an economic module and a risk module.

The lifing module estimates the life of the high pressure turbine disk and blades through the analysis of creep and fatigue over a full working cycle of the engine. These two phenomena are usually the most limiting factors to the life of the engine. The output of this module is the amount of hours that the engine can sustain before its first overhaul (called time between overhauls). The value of life calculated by the lifing is then taken as the baseline distribution to calculate the life of other important modules of the engine using the Weibull approach. The Weibull formulation is applied to the life analysis of different parts of the engine in order to estimate the cost of maintenance, the direct operating costs (DOC) and net present cost (NPC) of turbofan engines. The Weibull distribution is often used in the field of life data analysis due to its flexibility—it can mimic the behavior of other statistical distributions such as

the normal and the exponential. In the present work five Weibull distributions are used for five important sources of interruption of the working life of the engine: Combustor, Life Limited Parts (LLP), High Pressure Compressor (HPC), General breakdowns and High Pressure Turbine (HPT). The Weibull analysis done in this work shows the impact of the breakdown of different parts of the engine on the NPC and DOC, the importance that each module of the engine has in its life, and how the application of the Weibull theory can help us in the risk assessment of future aero engines.

Then the lower of the values of life of all the distributions is taken as time between overhaul (TBO), and used into the economic module calculations. The economic module uses the time between overhaul together with the cost of labour and the cost of the engine (needed to determine the cost of spare parts) to estimate the cost of maintenance of the engine. The direct operating costs (DOC) of the engine are derived as a function of maintenance cost with the cost of taxes on emissions and noise, the cost of fuel, the cost of insurance and the cost of interests paid on the total investment. The DOC of the aircraft include also the cost of cabin and flight crew and the cost of landing, navigational and ground handling fees. With knowledge of the DOC the net present cost (NPC) for both the engine and the aircraft can be estimated over an operational period of about 30 years.

The risk model uses the Monte Carlo method with a Gaussian distribution to study the impact of the variations in some parameters on the NPC. Some of the parameters considered in the risk scenarios are fuel price, interest percentage on total investment, inflation, downtime, maintenance labour cost and factors used in the emission and noise taxes. The risk analyses the influence of these variables for ten thousands scenarios and then a cumulative frequency curve is built by the model to understand the frequency of the most probable scenarios.

After the conclusion of the analysis of the VITAL engines as they were specified by the Original Engine Manufacturer (OEM) (Roll – Royce, Snecma and MTU), an optimisation work was done in order to try to improve the

engines. The optimisation was done using two numerical gradient based techniques Firstly the *Sequential Quadratic Programming – NLPQL* and secondly the *Mixed Integer Optimization – MOST*; the objectives of the optimisation were two: minimum fuel burn and minimum direct operating costs. Because the engines were already optimized for minimum fuel burn, the optimization for minimum fuel burn didn't show any meaningful results; instead the results for minimum DOC showed that the engines can have some improvements.

The ability of the three VITAL configurations to meet the future goals of the European Union to reduce noise and gaseous emission has been assessed and has showed that the three engines cannot fully comply with future legislation beyond 2020.

In the second part of this thesis three further advanced configurations have been studied to determine whether these are potential solutions to meet the ACARE goals of 2020.

For these more advanced aero engines only a performance and gaseous emissions analysis has been done, because it was no possible to do an economic analysis for the new components of these engines. These advanced configurations feature components that have been studied only in laboratories, like the heat exchangers for the ICR, the wave rotor and the constant volume combustor, and for these it has not been done a lifing analysis that is fundamental in order to understand the costs of maintenance, besides in order to do a proper direct operating costs analysis many operational flight hours are needed and none of these engine have reached TRL of 7 and more which is the stage where flight hour tests are conducted.

In this thesis a parametric study on three different novel cycles which could be applied to aircraft propulsion is presented:

1. Intercooled recuperative,
2. wave rotor and

3. Constant volume combustion cycle.

These three cycles have been applied to a characteristic next generation long range aero engine (geared turbofan) looking for a possible future evolution and searching for benefits on specific thrust fuel consumption and emissions. The parametric study has been applied to Top of Climb conditions, the design point, at Mach number 0.82, ISA deviation of 10 degrees and an altitude of 10686 m and at cruise condition, considering two possible designs:

a) Design for constant specific thrust and

b) Design for constant TET or the current technology level

Both values correspond to the baseline engine. For the intercooled engine also a weight and drag impact on fuel consumption has been done, in order to understand the impact of weight increase on the benefits of the configuration, considering different values of the effectiveness of the heat exchangers, the higher the values the greater is the technical challenge of the engine.

After studying the CVC and Wave rotor separately it has been decided to do a parametric study of an aero engine that comprises both configurations: the internal combustion wave rotor (ICWR). The ICWR is a highly unsteady device, but offers significant advantages when combined with gas turbines. Since it is a constant volume combustion device there is a pressure raise during combustion, this will result in having lower SFC and higher thermal efficiency. It is an advanced and quite futuristic, with a technology readiness level (TRL) of 6 or higher only by 2025, so only a preliminary performance study is done, leaving to future studies the task of a more improved analysis.

Acknowledgements

My greatest gratitude goes to professors Pericles Pilidis and Riti Singh which gave me the opportunity to do this PhD, and Dr Stephen Ogaji, which helped me in every way possible throughout all the doctorate period, always showing great patience and a deep insight of my problems, guiding me perfectly in their solutions.

I want to thank Prof. Gregorio Corchero that gave me the possibility to work with him in Madrid; it was a fantastic period by every mean.

Then I want to thank Oliviero Vigna Suria, not only he helped me a lot in the realization of the lifing module, but also for being a true friend.

A list of all the friends with whom I have shared this journey would be too long, but they know who they are and I have thanked them many times.

I want to thank also my Mother that was always with me in these times, good and bad.

And last, but not least, I want to thank my good friend Frank Nopple, without his words and counsel I wouldn't have ever started this PhD, which has been so far the greatest adventure of my life.

Table of Contents

List of Figures

List of Tables

Nomenclature

ACC	Aircraft Cost (€)
APC	Accessory Pressure Compressor
APS	Air Plasma Spray
b	Nox Factor
B	Booster
BN1	Main Bypass Nozzle
BN2	Heated Stream Bypass Nozzle
BPR	Bypass ratio
CC	Combustor
CCS	Cost of each cabin crew staff per hour (€/hr)
CF	Centrifugal Force
CFCM	Cost of each flight crew member per hour (€/hr)
CN	Core Nozzle
CRTFLR	Counter Rotating turbofan for Long Range
CRTFSR	Counter Rotating turbofan for Short Range
CTE	Coefficient of Linear Thermal Expansion
CU	Cranfield University
CVC	Constant Volume Combustion
D/Foo CO	Hydrocarbures (g/kN)
DDTF	Direct Drive Turbofan
DOC	Direct operating cost (k€/year)
DOCMtce/Eng/Hr	DOC of Maintenance per engine per hour
Downtime	Time of overhaul
E	Modulus of Elasticity
EB-PVD	Electron Beam Physical Vapour Deposition
EBT	Engineers Bending Theory
EFC	Engine Flight Cycle
EFH	Engine Flight Hours
EP	Engine price (€)
EPNL	Effective perceived noise level (dB)
far_c	Combustor Fuel Air Ratio

FN	Thrust (kN)
FOD	Foreign Object Damage
FP	Fuel price (c$/US gallon)
$f_X(x)$	Weibull Density Function
$F_X(x)$	Weibull Probability Distribution Function
GTFLR	Geared turbofan long range
GTFSR	Geared Turbofan short range
HBR	High Bypass Ratio
HC	Hydrocarbons (g/kN)
HCF	High Cycle Fatigue
HE	Heat Exchanger
HEM	Numbers of hours between engine overhaul (hr)
HPC	High Pressure Compressor
HPT	High Pressure Turbine
HPT	High Pressure Turbine
i	Failure Order Number
I/O	Input/output
IC	Intercooler Heat Exchanger
ICWR	Internal combustion wave rotor
IF	Inner Fan
INF	Inflation
IP	Interest on total investment
IPT	Intermediate Pressure Compressor
IRC	Intercooler Regenerative Cycle
ISP	Insurance percentage
K	Noise tax factor
k_3	Pressure Loss at the CVC Entry
k_4	Pressure Loss at the CVC Exit
k_{cool}	Coefficient of Heat Transferred To Bypass
LCF	Low Cycle Fatigue
LLP	Life Limited Parts
LMP	Larson-Miller parameter
LPT	Low Pressure Turbine

LTO	Landing/Take-off
MTO	Maximum take off weight (Kg)
MtrlsEngBlockHr	Cost of Materials per Engine/Block Hour
MUS	Method of Universal Slope
N	Total Sample Size
N	Number of scenarios
NA	Number of aircraft
NGV	Nozzle Guide Vanes
NINT	Number of intervals for cumulative curve
NOx	Weight of NOx produced (Kg)
NP	Number of passengers
NPC	Net present cost (k€)
NYEARS	Expected operating engine life (yr)
OEM	Original Equipment Manufacturer
OEW	Operating empty weight [kg]
OF	Outer Fan
OPR	Overall pressure ratio
P	Pressure
PDE	Pulse Detonation Engine
Q(t)	Media Rank
RA	Reduction of area (percentage)
RBL	Block distance (Km)
ref	Reference Values
RHE	Regenerative Heat Exchanger
RLENG	Maintenance labour rate per man hour (€/hr)
ROC	Exchange rate $ -> €
RPM	Rotational speed (round per minute)
SFC	specific thrust fuel consumption
SLS	Sea Level Static
ST	Specific Thrust
T	Temperature
TBC	Thermal barrier coating
TBL	Block time (hr)

TBO	Time Between Overhaul (Hr)
TERA	Techno-environmental and risk analysis
TET	Turbine Entry Temperature
TMF	Thermo-mechanical fatigue
TT0	Take off thrust (N)
U	Reliability function
UHBR	Ultra High Bypass Ratio
VHBR	Very High Bypass Ratio
VITAL	EnVIronmenTALly friendly aero engine
w	Mass Flow
w_{cool}	coefficient of bypass heated mass
WF	Weight of fuel used (Kg)
WR	Wave Rotor
X	Variate
α	Scale Parameter
β	Shape Parameter
γ	Location Parameter
ΔT	Difference of temperature
μ_x	Mean Value
ρ	Density
σ	Stress
σ_x	Standard Deviation
Γ	Gamma function

1. Introduction

1.1 Environmentally Friendly Aero Engines (VITAL)

VITAL will provide a major advance in developing the next generation commercial aircraft engine technologies, enabling the European Aero-engine Industry to produce high performance, low noise and low emission engines at an affordable cost for the benefit of their customers, air passengers and society at large.

The Advisory Council for Aeronautical Research in Europe (ACARE) identified the research needs for the aeronautics industry for 2020, as described in the Strategic Research Agenda (SRA), published in October 2002. Concerning the environment, ACARE fixed, amongst others, the following objectives for 2020 for the overall air transport system, including the engine, the aircraft and operations:

- A 50% reduction in CO_2 emissions per passenger-kilometer (assuming kerosene remains the main fuel in use) with the engine contribution corresponding to a reduction of 15 to 20 % in specific fuel consumption, whilst keeping specific weight constant;

- A reduction in perceived noise (EPNdB) to one half of the current average level, considered as equivalent to a 10 dB reduction per aircraft operation, taking into account that the engine is the major contributor to noise.

The goals that the VITAL project wants to achieve for the noise and gaseous emissions have proven to be realistic as the work done in the past four years has shown.

The main objective of VITAL is to develop and validate engine technologies that alone will provide a:

- 6 dB noise reduction per aircraft operation and equivalent to a cumulative margin of 15-18 EPNdB on the 3 certification points

- 7% reduction in CO2 emissions with respect to engines in service prior to 2000 such as the CFM 56/7 and Trent 772B.

VITAL will also integrate the benefits and the results of other on-going research projects of the EU with respect to weight reduction technologies (as in EEFAE) and noise reduction technologies (as in SILENCE(R)), assess at a whole engine level their benefits and combine their outcomes with those of VITAL to enable the following cumulative benefits by project end in 2008:

- 8 dB Noise reduction per aircraft operation (cumulative ~24 EPNdB on the 3 certification points)

- 18 % reduction in CO2 emissions

The main objective of VITAL will be achieved through the design, manufacture and rig scale testing of the following innovative technologies and architectures:

Two innovative fan architectures:

- Low speed fan for Direct Drive Turbofan (DDTF) and Geared Turbofan (GTF)

- Low speed contra rotating fan for Contra-rotating Turbofan (CRTF)

Including intensive use of light weight material to minimize the weight penalty of very high bypass ratio engines (VHBR = 9-12).

New high speed and low speed low pressure compressor (booster) concepts and technologies for weight and size reduction, suited to any of the new fan concepts

New lightweight structures using new materials as well as innovative structural design and manufacturing techniques

New shaft technologies enabling the high torque needed by the new fan concepts through the development of innovative materials and concepts

New low-pressure turbine (LPT) technologies for weight and noise reduction, suited to any of the new fan concepts

Optimal installation of VHBR engines related to nozzle, nacelle, reverser and positioning to optimize weight, noise and fuel burn reductions

All these technologies will be evaluated through preliminary engine studies for three architectures: Direct Drive Turbofan, Contra Rotating Turbofan and also a Geared Turbofan.

This new set of technologies will enable the European Aero-engine Industry to achieve its long-term objective of producing VHBR engines to enable a significant reduction in both noise and fuel burn. In VITAL, this will be achieved by following two paths:

By increasing significantly the engine bypass ratio (BPR) and therefore developing new lightweight technologies needed to eliminate weight penalties on fuel burn induced by the increased BPR.

By introducing a new fan concept (CRTF), reducing noise levels and fuel burn without the need to significantly increase the BPR.

At the end of VITAL a very important step towards achieving the ACARE goals will have been achieved. The VITAL partners will then take-up the results of VITAL by developing further the innovative technologies produced to bring them to a higher TRL for integration into future engines.

1.1.1 Progress against the state-of-the-art

During the last thirty years, the common trend in turbofan design has been to increase the bypass ratio of commercial aircraft engines. Initiated through the need to reduce fuel consumption by improving the propulsive efficiency, this trend has been amplified recently by the more and more challenging requirements in terms of noise emissions.

Fan noise (determined mainly by fan tip speed) and jet noise (determined mainly by jet velocity) are the two largest contributors to engine noise. The trend to increase BPR has had a strong impact on jet noise reduction through decreased jet velocity and has also benefited noise emissions through reduced fan tip speed. Consequently, engine manufacturers have started to propose turbofans with BPR going up to 9 (Figure 1).

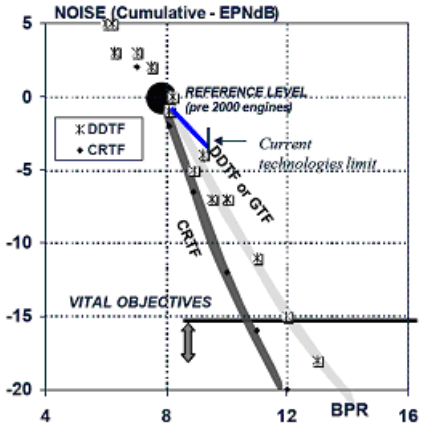

Figure 1: Noise vs. BPR (VITAL 2004)

Therefore to reduce noise even further, engine manufacturers have two options:

1. To continue increasing BPR as explained above

2. To introduce new fan concepts to significantly decrease the fan tip speed

1.1.2 The trend of increasing BPR

With the current technologies, the increase in BPR has reached its limit in terms of fuel burn on mission. Although a higher BPR offers a clear reduction in specific fuel consumption (SFC), it also leads to a significant increase in the engine weight as well as to the nacelle and installation drags. Above an optimum BPR value, the penalties brought about by weight and drag, offset the benefits provided by higher BPR. Based on available technologies, this optimum is around 7 to 9 depending on the payload and the range of the aircraft. The challenge that is proposed today to engine manufacturers is to find technology solutions that will enable the use of higher BPR architectures without inducing fuel burn penalties whilst providing an optimum BPR value (for each fan architecture) (Figure 2). Looking at the evolution over the last twenty years, this objective cannot be reached by the on-going evolution and technologies and therefore requires a decisive breakthrough in technology development as proposed in VITAL.

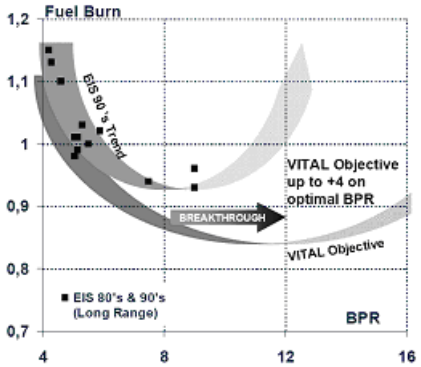

Figure 2: BPR and fuel burn penalties (VITAL 2004)

To be able to produce engines with higher BPR without weight penalties, a 25% weight reduction at constant BPR is required. This step has to be reached for engines going into service in 2020. This requires a yearly

advance in technology at twice the rate than seen over the last 10 years and represents thus an important breakthrough in our technology acquisition plan. As the weight increase is driven by the evolution of the low-pressure system components (due to the effect of changes to the engine diameter), VITAL focuses on these components with the objective of reducing the weight of each low-pressure system component by 25% to 30%. As far as the weight is concerned, the nominal evolution versus BPR is represented in Figure 3.

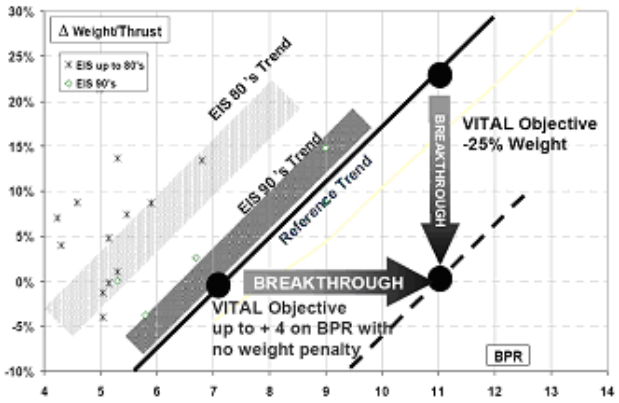

Figure 3: Weight and BPR (VITAL 2004)

1.1.3 Decreasing the fan tip speed

The Geared Turbofan (GTF) enables fan tip speed to be selected without hampering the low pressure turbine and booster operation. This enables the fan tip speed to be reduced but only where the bypass ratio is very high, that is to say 12 or above.

The alternative solution is to reduce the fan tip speed without a gear box which is also efficient for more moderate bypass and can also be used at BPR 9 and above (Figure 1). This solution consists of two contra-rotating fan stages, mounted on contra-rotating shafts linked to a low pressure turbine with contra-rotating blade rows. This architecture allows, at same aerodynamic loads, to decrease the rotational speed by about $1/\sqrt{2}$ (i.e. roughly –30 %). The fan module weight being directly linked to the kinetic energy of the rotating parts, this concept provides, at the same technology

level, a weight reduction. It is estimated that thrust to weight ratio of the corresponding whole engine is increased by 10 to 12%.

In the past, some studies have been conducted on concepts apparently close to CRTF, but they deal with configurations using a gear, having VHBR, very low pressure ratio and low numbers of blades, closer to ducted propellers than fans. The solution proposed here is different, as each fan row works aerodynamically at a low speed fan. Moreover variable blade stagger or nozzle throat variable area, are not needed. In conclusion the incremental improvement of existing technologies will not enable the ACARE 2020 objectives to be achieved. Breakthroughs are needed in the design of engine architectures and in the materials used in the various low-pressure system components and in the nacelle. VITAL will develop these new architectures and technologies and at the same time introduce significant noise and weight reductions to achieve a breakthrough as illustrated in Figure 4.

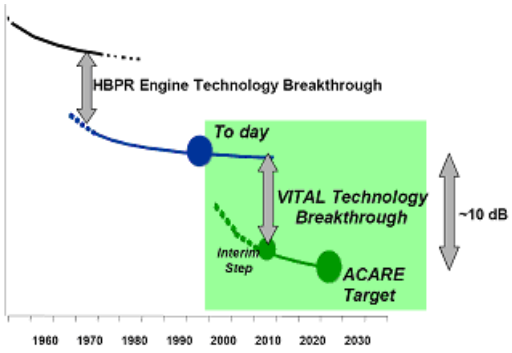

Figure 4: trends in aircraft noise reduction (VITAL 2004)

			VITAL		SILENCE(R)	
	BPR		Focus	Objective	Focus	Objective
DDTF	VHBR	10 to 12	Noise + CO_2	Minimise weight of whole engine		
CRTF	VHBR	9 to 11	Noise + CO_2	New fan concept		
GTF	UHBR	12 to 15	Noise + CO_2	Integration paper study	Noise only	Model testing

Figure 5: fan concepts in VITAL and SILENCE® (VITAL 2004)

1.2 Thesis structure

The content of this thesis is organised in six chapters, of which this section gives an overview.

In chapter 2 the literature review is presented. The main theory behind the economic model and the advanced engines is given. In particular for the economic model, and for each module it is composed by (lifing, Weibull, and economic), the main general theories are presented. For these modules there is also an overview of optimisation techniques more commonly used.

In chapter three the scheme of the economic model is presented extensively. First off all the methodology is explained and then the architecture of the model with its requirements, input and out files. The main part is dedicated to the lifing module, the most complex of all. Its parts are the stress analysis, for disk and blades of the high pressure turbine, cooling, low cycle fatigue and creep.

In chapter four the performance models for the three more advanced engines, intercooled recuperated, wave rotor topped cycle and constant volume combustion, are shown.

In chapter five the results are given and discussed. First of all the economic model is validated against public available data and well established theories. Then the Weibull distributions are applied to cost and risk analysis. Finally the economic model is applied to the VITAL engines in order to forecast their direct operating costs and the associated risk. After that optimisation is used in order to improve the results and have better performing engines under the point of view of minimum fuel burn and minimum operational costs. The results of the advanced propulsion system are given for the design point, top of climb, and for cruise, considering two different design philosophies: constant TET, which means constant technology, and constant specific thrust.

Last, but not least, some performance analysis is done for the most advanced engine: the constant volume combustion coupled with wave rotor.

In chapter six conclusions are summarized and recommendations for future work are pointed out together with the author’s contribution to knowledge.

2. Literature Survey

In order to understand the market of overhaul and maintenance, and in general how the economic strategies of the airliners and aircraft manufacturer work, a lot of magazines dedicated to this topic have been read.

The two most important magazines about overhaul and maintenance are Aircraft Commerce and Overhaul and Maintenance. The former was particularly useful because it gave very precise data about the maintenance of the A330, A320, A319 and A321 family types of aircrafts and a wide range of engines with very different type of thrust from long to short range, all this data has been used to create and validate the economic model. The latter was useful to understand how the market of overhaul is managed.

To understand the market strategies of manufacturers and airliners alike, Flight International was very useful and to comprehend better the airliners policies their annual budget of the last fifteen years published in the ICAO DATA internet site were also useful.

The passage from this big quantity of raw data in a structured formulation was very difficult because an economic analysis from the design point of view cannot take into account all the market volatility and fast changing. As a basis of a structured formulation examples were taken from the Roskam (1990) and Jenkinson (1999) models. The first was quite accurate but his formulation was based on old data (in the seventies) so a lot of the formulas and factors had to be changed to adapt them to the more recent data. The latter was good since it has a simpler structure than the first, it matches quite well the data from more recent years, but also this model had to be improved in order to get more accurate results. Improving these two models made the economic model to match the current data with only a 10% difference.

An important part of the economic model is the inclusion of the cost related to the taxes on noise and emissions. Unfortunately a unique system of taxes all over the world does not exist, but every airport has its own. The Boeing internet site was very useful to have an overview of all these different systems. The purpose of this web site is to track and report airport noise restrictions and government noise regulations for airline customers. This information also allows a better understanding of problems a customer airline may encounter at a particular airport and to assist them in developing possible solutions.

The maintenance costs depend strongly on the lifing of the different parts of the engines, the course notes from the Thermal Power master of professor Pilidis, Haslam and Ramsden helped to better understand how a gas turbine works and which are the possible causes of break.

The iSight reference guide and user's guide has also been studied in order to understand the complex methods for optimization and the use of the program.

2.1 The Economic Module

In the following sections the theory behind the economic method is shown, the lifing approach used is explained and the Weibull formulation is analysed.

2.1.1 The Roskam Method

The Roskam method has been created by Jan Roskam at the end of the eighties as part of his monumental opera dedicated to the aircraft design. In the volume eight of his work he tries to create a reasonable and reliable method to estimate the cost of design, production and operation of a fleet of aircraft that works with all the possible type of engines, from the piston engine of small private aircraft to the big turbofan of the large intercontinental aircrafts, taking into account also the military airplanes. The methodology presented in his work is based on methods presented by NASA and other

association during the sixties and seventies. Those methods were adapted and generalized to be used for any type of commercial planes. Roskam uses American weekly magazines such as Aviation Week and Space Technology that publishes utilization data on a quarterly basis for passenger transports and monthly magazines such as Business and Commercial Aviation that publishes data on the utilization of other commercial airplanes. In his analysis of costs of an aircraft Roskam has included all the possible type of costs since the design phase. For the purpose of my work such a detailed analysis was not necessary, so only the part about the operating costs of commercial airplanes has been taken into consideration.

Roskam considers the total (or program) operating cost of commercial airplanes as the sum of the program direct operating cost and the program indirect operating cost, each of them multiplied by the number of airplanes acquired by the customer, and this for all the types of airplanes that the airline has.

The program direct and indirect operating costs are the direct and indirect operating cost multiplied by the total annual block miles flown per airplane per the number of years of utilization of the aircraft.

The direct operating cost is considered by Roskam as a sum of very different types of components:

- Direct operating cost of flying that takes into account the cost of crew, fuel and insurance of the aircraft;
- Direct operating cost of maintenance that includes airframe labour, engine labour, airframe materials, engine materials and applied maintenance burden;
- Depreciation of the airframe, engines, propellers, avionics, airframe spare parts and engine spare parts;
- Landing and navigational fees and registry taxes;
- Finance.

The indirect operating cost instead comprehend meals, passengers insurance, cabin attendants, passenger handling, sales and reservations, security, maintenance of ground equipment and facilities and their depreciation, airplane service, control and freight handling, commission to travel agencies, publicity and advertising, entertainment, administrative, accounting and corporate staff costs and facilities cost.

Depreciation has been considered as part of the indirect operating costs that are not considered in this work and so it is not taken into account, instead ground handling fees and cabin attendants costs have been considered part of the direct operating cost in the section of flight costs, the former under the voice airport fees and the latter under the voice crew cost.

If in this work the structure of the direct operating cost has more or less been kept the same, the formulation used to calculate each element of the direct operating cost has been changed a lot. That's because most of the data collected by Roskam comes from aircraft in use in the seventies and early eighties like the 737-200, 727-200, DC10-10, 747-100. But in the last twenty years a lot of work has been done in the research field to improve the efficiency of engines and airframes in relation to weight, drag, fuel consumption, life of the materials used and the maintenance needed by the various components. Tirovolis & Serghides (2006) shows very well the difference between the first generation of aircraft (circa 1980) and the second (circa 1990) and the third (circa 2000). In order to match the data from the public literature on modern aircraft and to take into account the technology improvement that is the core of the VITAL program most of the factors and formulas used to calculate all the cost has been heavily changed. The new, modified, factors and formulas have been chosen taking into account the values give in magazines likes: Aircraft Commerce, Flight International, ICAO DATA, JANE. A wide range engines data has been taken and the factors in Roskam's equations have been changed in order to match these values. The new formulation used in the economic module can be found in annex F.

The effect of this change will be shown later in Figure 36 and Figure 37 where a comparison between the Roskam method and the method used in this work is shown.

From this comparison we'll be able to see how what was once considered one of the more complete methods for estimation of direct operating cost is nowadays no more precise enough (with errors of more 50%) to forecast the cost of operation of today and future generation aircraft like the 787 and the A350 and this explain why there was a need for the VITAL project to create a new economic model that could take into account all the technology improvements that will be done in the next few years.

2.1.2 The Jenkinson Method

This method is less detailed than the previous one, but being simpler it offers a fast way of predicting DOC of the aircraft that can be used as a first approximation to understand the order of magnitude of the costs, see the figure below.

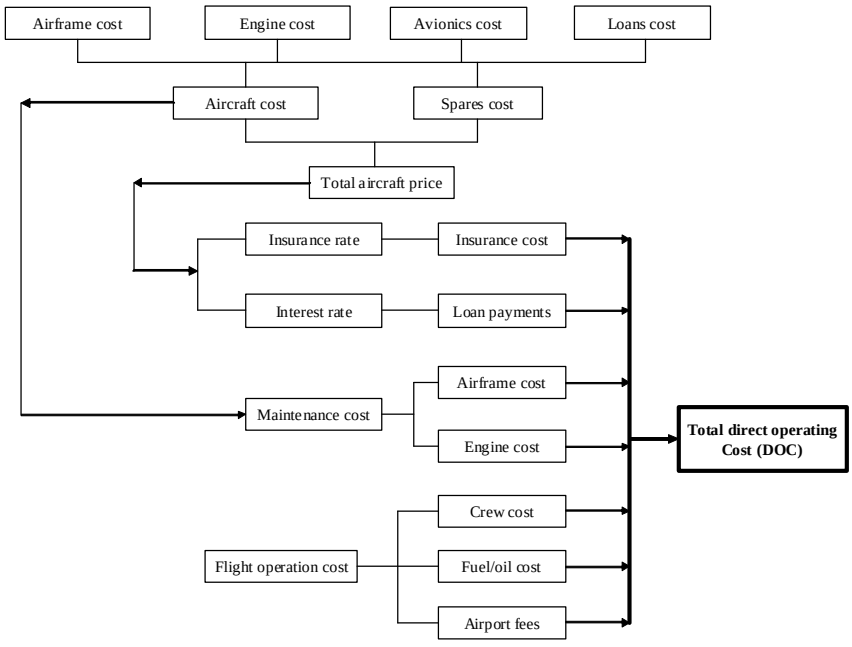

Figure 6 Direct operating cost (DOC) components (Jenkinson 1999)

All the formulation used by Jenkinson is essentially a simplified system of the Roskam's one. Jenkinson in fact specify that "it is difficult to rationalise the design of the aircraft to different cost methods so a choice has to be made. Whichever method is chosen it can be used only to show the relative cost variation between different designs. The method will not predict actual cost as these vary so widely over different operational practices".

Jenkinson tells us that his method is just a guidance to use when better information is not available and "it is appropriate to conventional layout and materials".

The main philosophy behind the Jenkinson method is that "each airline and manufacturer will have developed methods and parameters appropriate to their own operations. In preliminary aircraft design it is necessary to show the trade-offs that are possible in the assumptions above. This will allow significant variations from the standard values to be assessed and allowances made to the aircraft specification if appropriate".

For the VITAL project it was necessary to create a program that could quite well approximate the cost of operation of the airplanes, but at the same time could be enough flexible that the variation of design in the engines or the airframe would be easily be comparable. This has been achieved putting together the Roskam deeply specific method with the trade-off philosophy of Jenkinson method.

Thanks to the optimisation, robust design and trade-off capabilities of iSight, the economic program, together will other the other modules of the VITAL project, can be a powerful tool to analyse the different peculiarity of every new type of design of engines and aircraft.

2.1.4 Engine lifing

Following is the theory used in the lifing module. It can be found in Haslam (2005 & 2006), Rubini (2006) and other papers cited along the theory discussion.

2.1.4.1 Sources and analysis of stresses on blades and disk

The major sources of stress arising in turbo machine blades are as follows:

- centrifugal load acting at any section of the airfoil or shank and produced by the inertia;
- gas bending moment produced by the change in momentum and pressure of the fluid passing across the blade;
- bending moment produced by the centrifugal load acting at a point which does not lie radially above the centre of the root section (or any other reference section);
- shear load arising from the gas pressure or from centrifugal untwisting of the blade;
- Complex loading due to thermal gradients.

In the lifing program a first degree analysis approach is executed and so only the centrifugal stresses are considered.

This simplified approach does not compromise too much the results and can still be considered enough accurate.

Direct centrifugal stresses: This stress exists simply because the blade material has a mass. Operating in an inertia field, about 50 to 80 % of the blade material strength is used to overcome this stress.

The centrifugal force in a rotating component (let's consider now a blade rectangular in shape) is easily expressed as:

$$CF = mass \times r_{cg} \times \omega^2$$

Writing the mass of the blade as:

Mass = *density* x *cross-sectional area* x *height* = $\rho \times A \times h$

Hence:

$$CF = \rho \times A \times h \times r_{cg} \times \omega^2$$

Thus the centrifugal stress acting in a blade of constant cross-sectional area will be:

$$\sigma_{CF} = \rho \times h \times r_{cg} \times \omega^2$$

That means the stress cannot be reduced by increasing the cross-sectional area.

Disc stresses arise from the following sources:

- The centrifugal body force of the disc in a rotary inertia field;
- The radial centrifugal load produced by the 'dead' mass of the blades, shrouds, etc applied to the circumference of the disc as a 'rim stress';
- The temperature gradient between the bore and the rim, in association with the coefficient of thermal expansion, producing a thermal stress;
- The torque load producing shear stresses in the body of the disc either by steady-state torque transmission from the turbine to the compressor, or inertia loading created as the machine speeds up or slows down;
- The bending loads applied to the disc by the pressure difference across the stage or from the gas bending loads on the blades.

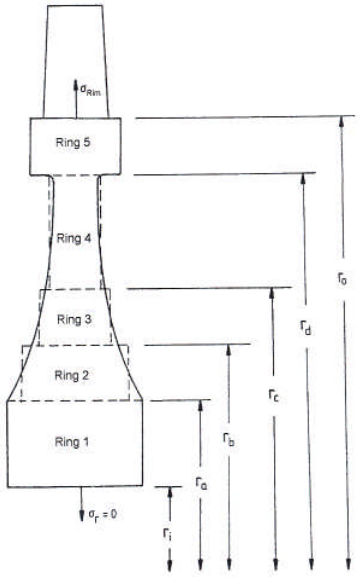

Figure 7 Varying thickness disc (Haslam 2006)

2.1.4.2 Cooling model

The implemented code offers to the user the possibility of using a quite simple blade cooling mechanism, which will allow lowering the metal temperature to a bearable value. In particular, the calculations are based on a simple one dimensional model of convection cooling.

Gas turbine components (in particular the HP turbine) are designed to work at very high operating temperatures, definitely higher than the melting point of the materials they are made of. Hence, in addition to the materials features improvements and the use of thermal barrier coating, an efficient cooling system is normally required in order to lower the exercise temperature to acceptable levels.

The material used for turbine blades has to meet important requirements, which are:

- high melting point;
- oxidation resistance;

- high temperature strength and microstructure stability;
- low density and high stiffness;
- good production, with low cost;
- Reproducible performances.

Nickel based alloys have evolved as the metallic material with the best combination of these properties.

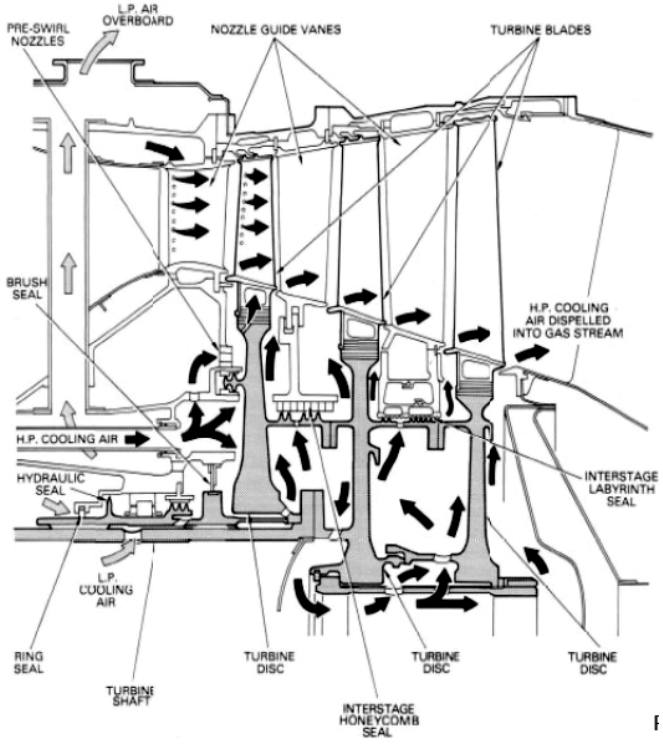

Figure 8 Typical turbine cooling system (Haslam 2006)

An engine cooling system comprises a number of air flow paths parallel to the main gas path Figure 8. For each of these, air is extracted part way through the compressors, either via slots in the outer casing, or at the inner through axial gaps or holes in the drum. The air is then transferred either internally through a series of orifices and labyrinths finned seals, or externally via pipes outside the engine casing. The earlier the extraction point, the lower the performance loss as less work has been done on the air.

For safer operation, the turbine blades in current engines use nickel based super alloys at metal temperatures well below 1100ºC for safe operations. For higher rotor inlet temperatures, the advanced casting techniques, such as directionally solidified and single crystal blades with TBC coating have been proposed for advanced gas turbines (Gonzalez 2005).

Following is presented the theory behind the cooling in the lifing module, all the relations have been taken from Rubini 2006. It is assumed equilibrium between the heat flux entering the blade and that leaving it, absorbed by the coolant. This assumption can be formalized as follows:

$$m_{cb}Cp\left(T_{c2}-T_{c1}\right)=h_g S_g L\left(T_g-T_b\right)$$

Where:

- m_{cb} is the coolant mass flow through the blade;
- T_{c2} is the temperature of the coolant leaving the blade;
- T_{c1} is the temperature of the coolant entering the blade;
- h_g is the external gas heat transfer coefficient;
- S_g is the perimeter of one section of the blade;
- L is the span length of the blade;
- T_g is the temperature of the gas surrounding the blade (TET);
- T_b is the temperature of the metal

From the last equation, it is possible to define the dimensionless coolant mass flow function:

$$m^* = \frac{m_{cb}Cp}{h_g S_g L}$$

Required parameters to be used during the design of a blade cooling system are the following:

- Overall blade cooling effectiveness, ε :

$$\varepsilon = \frac{T_g - T_b}{T_g - T_{c1}}$$

The blade cooling effectiveness (ε) is usually the output of a cooling model; knowing it, and applying the simple steady flow energy equations, the blade metal temperature is easily estimable.

- Convection cooling efficiency, η:

$$\eta = \frac{T_{c2} - T_{c1}}{T_b - T_{c1}}$$

The convection cooling efficiency (η) represents the quality of the internal cooling technology.

- Technology factor:

$$X = \frac{n_c h_c S_c}{h_g S_g}$$

Where:

- h_c is the coolant heat transfer coefficient;
- S_c is the perimeter of one cooling passage;
- n_c is the number of cooling passages.

The previous parameters can be linked thanks to the following useful relations:

$$\varepsilon = \frac{m^*}{1 + m^* \eta}$$

$$\eta = 1 - e^{-\frac{X}{m^*}}$$

Depending on the information available, it is possible to estimate the value of the cooling effectiveness through which the cooled blade temperature will be calculated (Rubini 2006).

2.1.4.3 Thermal Barrier coating

TBC, the zirconium based ceramic, allows making cooling easier and causing a drop in temperature inside the blade, which means longer component life. It ought to be used together with blade cooling techniques, otherwise being ineffective and useless.

Because of their low thermal conductivity, barrier coatings are able to provide a temperature drop of roughly 150°C across a 200μm thick: this means that the metal wall will experience 150 °C less than before being coated.

In Figure 9 there is a sketch of the temperature profile in both the coating and the metal wall.

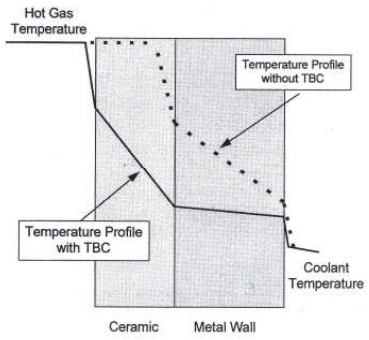

Figure 9 Thermal barrier coating principles

Having a look at the picture (Figure 9), the reduction of thermal gradient across the metal (achieved through the ceramic coating) is clear, thus giving a lower heat flux (proportional to thermal conductivity and thermal gradient).

This will allow the user to:

- Keep the external blade temperature there was without coating ➔ reduction of the heat flux (basically the blade itself will be colder) and consequently of the amount of air needed for cooling (as it is in Figure 9).

- Keep the same metal surface temperature, and same heat flux, but letting the external blade's surface temperature increase ➔ blade working at higher operating temperatures, which means higher engine cycle efficiency.

Summing up, by using thermal barrier coatings, several advantages can be achieved:

- Reduction in metal temperatures;
- Reduction in transient thermal stress;
- Improved engine efficiency, by increasing the engine cycle temperature (essentially the TET);
- Less amount of cooling required;
- Higher operating temperatures (together with point c ➔ higher cycle efficiency);
- Improved corrosion resistance.

2.1.4.4 FAILURE MECHANISMS

The first engine's component that will require maintenance on it is the HPT, forced to work in very hostile surroundings (engine's 'hot section'), namely high temperature of the gas and elevated HP shaft speed: these two main aspects are the causes of the rising of principal stresses (i.e. centrifugal and thermal stresses) acting on the turbine's blades and disc.

In order to be able to carry out a preliminary and possibly accurate analysis for both short and long range mission engines, it is important to identify the most restrictive phenomena that rule the life of the component, causing its failure after a certain amount of time.

Due to the different operating conditions and settings during the whole flight envelope, the high pressure turbine is usually subject to a wide variety of loads, being them either thermal or mechanical loads, that inevitably affect in

a significant way the life of the turbine itself, and cause deterioration and degradation in it.

The principal mechanisms of failure of high temperature components include creep, fatigue, creep-fatigue, and thermal fatigue. Many of the materials employed in the manufacture of turbo machineries continuously deform when loaded steadily at high temperature (creep), and at the same time, most failures of in-service components arise because of the action of cyclic loading on them (fatigue).

In heavy section components, although cracks may initiate and grow by these mechanisms, ultimate failure may occur at low temperatures during start up-shutdown transients. Hence, fracture toughness is also a key consideration (anyway, due to lack of time and necessary experience, this aspect will not be considered in the present work).

Fatigue loading of turbine components associated with continuous aircraft takeoff/cruise/landing cycles is a principal source of degradation in turbo machinery. A disk burst is potentially the most catastrophic failure possible in an engine, thus disks are designed with over-speed capability and low cycle fatigue life as primary objectives. The requirement for higher turbine stage work without additional stages has resulted in increased turbine blade tip speeds and higher turbine inlet temperatures in advanced commercial aircraft engines. This trend has resulted in significant increases in turbine stage disk rim loading and a more severe thermal environment, thereby making it more difficult to design turbine disks for a specific life requirement meeting current goals. Current trend indicates that both turbine blade tip speeds and turbine inlet temperatures will continue to increase in advanced commercial engines as higher turbine work levels are achieved.

In the following paragraphs, a general overview about the issues concerning creep and fatigue is given, in order to make the reader a bit more confident with what is at the basis of the work carried out in this project.

2.1.4.5 LOW CYCLE FATIGUE

In early fatigue design, the engineer tried to identify the endurance limit of a material, in order to discover the limiting stress below which fatigue failure would not occur, thus testing the specimens only for a high number of cycles (i.e. more than 10^5 cycles).

This approach is reasonable for many industrial components, but can lead to severe over-design of components which are subject to significantly less than 10^5. In machines like nuclear pressure vessels, gas turbines and power machinery in general, failures usually occur under high load condition (high stresses) and low number of cycles (Low Cycle Fatigue). In particular, it is not so much the number of times that the load is applied which is important, as the amount of damage done when they are applied; since damage is usually associated with plastic deformation (frequently a thermal expansion of the material, due to repeated thermal stresses), LCF is often known as 'high-strain fatigue' (Haslam 2005).

2.1.4.5.1 General theory

Machines and structures are subject to non-steady loads, which produce fluctuations in the stresses and strains in their components: if the fluctuating stress is large enough, failure may occur after several applications of the load, even though the maximum stress applied is lower than the static strength of the material.

The fatigue process is usually split into the following three phases:

1. Primary stage: crack initiation. It usually takes place at the surface of a component, where the stress is more concentrated;
2. Secondary stage: crack propagation. This phase is very important, since most of the components start working with micro-cracks already existing in them. There are two different stages of propagation: during

the first, the crack continues propagating along a plane of high shear stress, whereas during the second stage growth occurs along a plane normal to the maximum stress;

3. Final or tertiary stage: failure by fracture. Usually a fast running brittle fracture causes a sudden failure of the component.

The stress that causes the material to fail by fatigue after a certain number of cycles is known as the ‘fatigue strength’. For some materials, a limiting stress exists (called ‘endurance limit’ or ‘fatigue limit’), below which a load may be repeated a large number of times (say 10^6 or even more) without causing failure.

The common method of presenting fatigue data is by means of the so-called S-N curve, which is a semi-logarithmic plot of stress against the number of cycles to failure (Figure 10).

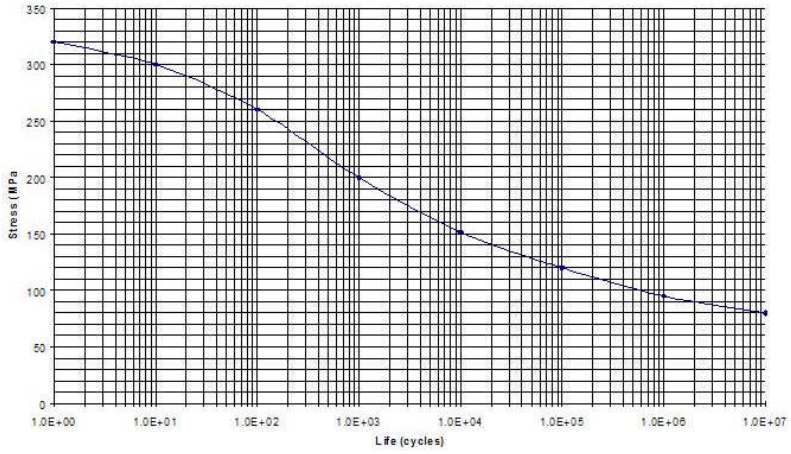

Figure 10, S-N curve for brittle aluminium

As it is evident from the S-N curve, a component could fail under fatigue both at a high number of cycles and low stress applied (HCF, High Cycle fatigue, right-hand side of the chart), and at a lower number of cycles, characterized by a definitely higher stress acting on it (LCF, Low Cycle fatigue, left-hand side of the curve).

It has to be said that the nature of a stress could be thermal as well: if it is the case, the process of failure due to fatigue is known as Thermal fatigue (or TMF), usually characterized by a LCF failure, because of the high peaks of temperature the component (i.e. the turbine) is usually subject.

The cracks usually start on the surface (where the highest temperatures and stresses levels occur) and then grow through the bulk of the component.

Obviously, the components most susceptible to thermal fatigue are the ones into direct contact with the high temperatures gases, namely turbine blades, nozzle guide vanes and the turbine discs.

Moreover, nowadays the high pressure turbine blades always include a complex internal cooling system, that causes stresses to arise because of thermal expansion induced in the blades themselves, often restricted by local constraints (e.g. thin leading trailing edge shapes).

Talking about fatigue, several factors influencing fatigue behaviour have to be taken into account. These are:

- type and nature of loading;
- size of the component (a smaller component usually means higher fatigue limit);
- surface finish and directional properties (surface roughness influences fatigue life: smoothly polished component will have the highest value);
- Stress or strain concentrations

Furthermore, environmental effects and operating condition have also to be considered, since almost any variation in the environmental conditions will affect the fatigue life of a component: the most pronounced effects are ambient temperature and corrosion.

The combined effect of cyclic stress and corrosion usually reduces the fatigue life, because a chemical attack accelerates the rate at which fatigue cracks grow.

Regarding the ambient temperature, at elevated values of temperature the component could experience some creep-fatigue interaction that would affect its life significantly.

2.1.4.5.2 Low cycle fatigue analysis: Coffin-Manson method

Usually, LCF test results are plotted as cycles to failure N_f against the total strain range $\Delta\varepsilon_T$, sum of the plastic and the elastic component, as mentioned before. Manson suggested that both the strain components (plastic and elastic) produce straight lines when plotted logarithmically against N_f (number of cycles to failure). From this he evolved his so-called 'universal slope method', based upon the Manson–Coffin relationship, that Manson himself found to be sufficiently accurate for initial design.

The starting point of the method is again the consideration of the total strain range as the sum of plastic and elastic strains (*Strain-Life Curve*):

$$\varepsilon_T = \varepsilon_p + \varepsilon_e$$

In 1910, Basquin observed that elastic component could be modelled using a power relationship, which results in a straight line on a log-log plot. The Basquin equation can be expressed in terms of true elastic strain amplitude as:

$$\varepsilon_e = \frac{\sigma_a}{E} = \frac{\sigma'_f}{E}\left(2N_f\right)^b$$

Where:

- ε_e = elastic component of the cyclic strain amplitude
- σ_a = cyclic stress amplitude
- σ'_f = fatigue strength coefficient
- N_f = number of cycles to failure

- b = fatigue strength exponent

In the 1950's Coffin and Manson independently found that the plastic component could be modelled using a power relationship as well:

$$\varepsilon_p = \varepsilon'_f \left(2N_f\right)^c$$

Where:

- ε_p = plastic component of the cyclic strain amplitude
- ε'_f = fatigue ductility coefficient
- N_f =number of cycles to failure
- c = fatigue ductility exponent

Hence the Strain-Life curve can be written by summing the elastic and plastic components as follows (Manson 1965):

$$\varepsilon_t = \frac{\Delta\varepsilon}{2} = \frac{\sigma'_f}{E}\left(2N_f\right)^b + \varepsilon'_f \left(2N_f\right)^c$$

The influence of the elastic and plastic components on the strain-life curve is shown in Figure 11.

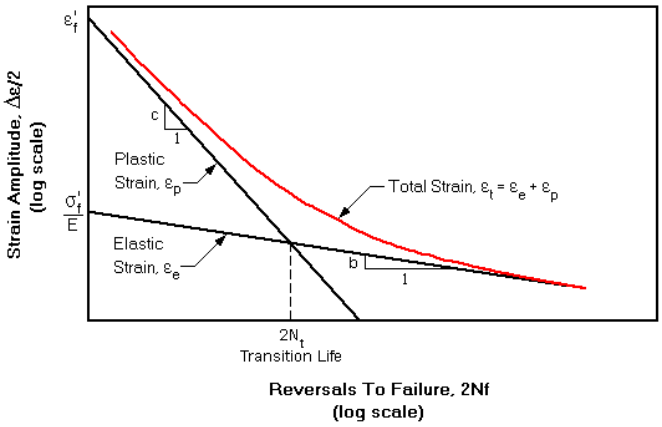

Figure 11 Typical Strain-Life curves

The *transition life* $2N_t$ represents the life at which the elastic and plastic strain ranges are equivalent. As shown in Figure 11, elastic strains have a greater influence on fatigue lives above the transition life, whereas plastic strains have a greater influence below the transition life. Thus the transition life

provides a convenient delineation between low-cycle and high-cycle fatigue regimes.

Note that at long fatigue lives, the fatigue strength (σ_f'/E) controls the fatigue performance and the Strain-Life and Stress-Life approaches give essentially the same results. For short fatigue lives, plastic strain is dominant and fatigue ductility (ε_f') controls the fatigue performance. The optimum material is therefore one that has both high ductility and high strength. Unfortunately, there is usually a trade-off between these two properties and a compromise must be made for the expected load or strain conditions being considered.

To use this low cycle fatigue model, six material fatigue properties must be entered for the material:

- Cyclic Strength Coefficient, *K';*
- Cyclic Strain Hardening Exponent, *n'*;
- Fatigue Strength Coefficient, σ_f' ;
- Fatigue Strength Exponent, *b* ;
- Fatigue Ductility Coefficient, ε_f' *;*
- Fatigue Ductility Exponent, *c*.

Although *K'* and *n'* are usually obtained from a curve fit of the cyclic stress-strain data, the following relationships can be used if no experimental data is available:

$$K' = \frac{\sigma'_f}{\left(\varepsilon_f\right)^{n'}}$$

$$n' = \frac{b}{c}$$

If no experimental data is available, a good approximation of σ_f' is the true fracture strength and a good approximation of σ_f' is the true fracture. In general, *b* varies between -0.05 to -0.12 for most metals and *c*, which is not as well defined as the other parameters, varies between -0.5 and -0.7 for

most metals. Fairly ductile metals (ε_f ~ 1.0) have *c* values closer to -0.7 and strong metals (ε_f ~ 0.5) have *c* values closer to -0.5 (ETBX no data).

2.1.4.5.3 Fatigue material properties: a statistical approach

The main limitation of Coffin-Manson approach to low cycle fatigue is the lack of the fatigue material properties, which are very difficult to find, mainly due to the fact that every company has its own material testing laboratory, where these values are estimated through experiments, and not released outside the company itself, as they are confidential data.

Furthermore, most of the existing methods for estimating the fatigue material properties needed to use Manson's Universal Slope rule are based on a relatively limited amount of experimental data.

Statistical evaluation of the existing Coffin-Manson parameter estimates are frequently used based on monotonic tensile and uniaxial fatigue properties of different metals (steels, aluminium alloys, titanium alloys and nickel alloys). From the collected data, it is shown that all correlations between the fatigue ductility coefficient ε_f' and the monotonic tensile properties are very poor, and that it is statistically sounder to estimate ε_f' *based* on constant values for each alloy family.

The best estimation methods are all based on constant values of the exponents *b* and *c*, while in general σ_f' is well estimated as a linear function of the ultimate strength S_U.

Using 12 continuous probability distributions, it has been possible to fit the available experimental data set, getting mean and median value, together with a coefficient of variation (defined as the ratio between the standard deviation and the mean). Generally, mean values do not give good results, since they are very much affected by the extreme values at the tails of the probability

functions; on the other hand, the median is a much more robust parameter, especially in case of asymmetric distributions.

Finally, it must be pointed out that the presented estimates should never be used in design, because for some materials even the best methods may result in life prediction errors of an order of magnitude. The use of such estimates is only admissible during the first stages of design (as it is the purpose of the present work, being a preliminary design), otherwise all fatigue properties should be experimentally obtained.

Table 1 contains the values of Coffin-Manson parameters (median and coefficient of variation) for several alloys families, and in Figure 12 are drawn the characteristic Coffin-Manson curves for steels, Al alloys and Ti alloys (Meggiolaro and Castro 2004).

Alloy family	σ'_f		ε'_f		*b*		*c*		*E (GPa)*	
	median	*V %*	*median*	*V %*	*median*	*V %*	*median*	*V %*	*median*	*V %*
steels	1.5 x S_U	43	0.45	157	-0.09	40	-0.59	28	205	3.1
Al alloys	1.9 x S_U	24	0.28	179	-0.11	28	-0.66	33	71	4
Ti alloys	1.9 x S_U	36	0.5	123	-0.1	37	-0.69	24	108	7.4
Ni alloys	1.4 x S_U	30	0.15	171	-0.08	28	-0.59	22	211	3.4
cast irons	1.2 x S_U	28	0.04	127	-0.08	29	-0.52	30	140	24

Table 1 Median and coefficient of variation of Coffin-Manson parameters for different materials' families (Meggiolaro and Castro 2004)

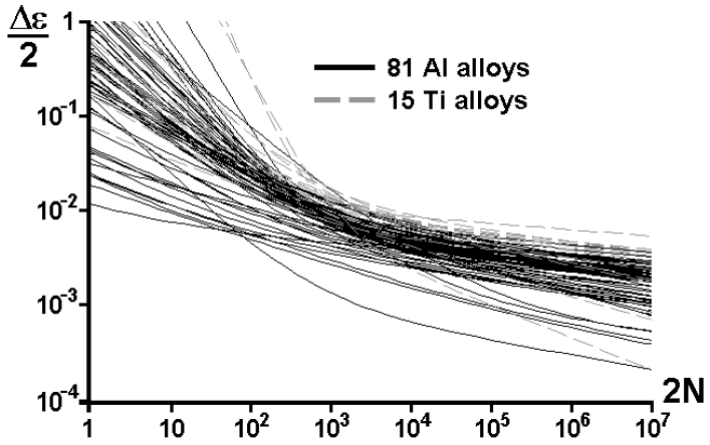

Figure 12 Coffin-Manson curves of 81 aluminium and 15 titanium alloys (Meggiolaro and Castro 2004).

2.1.4.6 CREEP

Lots of the materials currently used in the manufacture of turbo machine present a continuous deformation when loaded with a steady load at high temperature.

This progressive deformation of a material at constant temperature is known as creep. Being a function of stress, temperature, time and strain, creep is a complex quantity to define. The most common mean of representing creep data is to report into Mechanical properties of materials' table the minimum creep stress that causes a plastic strain of a certain percentage of the total plastic strain in a certain amount of time (i.e. 0.1% total plastic strain in 100 hrs for aero-gas turbine, and 0.1% total plastic strain in 10'000 hrs for industrial gas turbine).

In order to predict the failure (i.e. rupture) times under different combinations of stress and temperature, measures of extrapolation from short term creep tests to long component lifetimes are currently used. The simplest way is determining the creep rate at short time and assuming the same rate will apply throughout the components' life.

2.1.4.6.1 General theory

One method of extrapolation, from short to longer times, is to formulate an equation which describes the creep strain in terms of stress and temperature. This involves the use of relationship known as time-temperature parameters, wherein we assume that we can ‘buy’ time with temperature and vice versa, that is assuming that an increase in operating temperature will reduce the time to reach a particular creep state. This assumption can only be true if the same reaction controls the process over the whole temperature range investigated (Haslam 2005).

Roughly speaking, creep can be defined simply as a progressive deformation that takes place in the material at constant temperature, the situation being frequently complicated because of the whole range of temperature and loads acting during a mission, and because of the exposure time.

Creep is based on the mobility of dislocations and discontinuities in the material, caused by the operating stresses and temperatures: at high temperatures, this process is emphasized, thus resulting in worse material’s performances.

This phenomenon is generally accepted to be considered as a four-stage process:

1. Instantaneous elastic stage that involves an initial strain, namely a pure elastic deformation;
2. Primary creep: predominant stage at low stress levels and low temperature (i.e. room temperature); there is an increment of the material’s creep resistance as a function of its own deformation;
3. Secondary creep: constant and minimum creep rate phase (due to the balance between the competing processes of strain, hardening and recovery), thus being the most favourable;

4. Tertiary creep: unreal situation that happens at high stress and temperature. There is an effective reduction in the cross sectional area, together with metallurgical changes (e.g. recrystallisation).

In Figure 13 are shown the generally accepted idealization of the creep process:

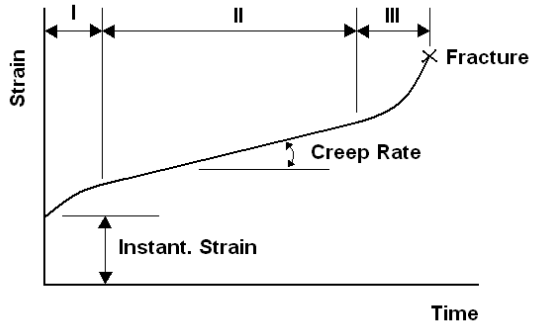

Figure 13 the General Creep Curve

Creep can occur at relatively low temperature (let's say lower than half of the melting temperature) as well, but for most constructional materials it will be insignificant (Haslam 2005).

Creep damage can take several forms. Simple creep deformation can lead to dimensional changes that result in distortions, loss of clearance, wall thinning etc.

2.1.4.6.2 Approaching time-temperature method to creep analysis

Following the theory behind creep analysis is presented as can be found in Haslam 2006. The most popular of the time-temperature parameters is known as the Larson-Miller parameter. It is based upon the Arrhenius equation:

$$\dot{\varepsilon} = A\sigma^n e^{-\frac{Q}{RT}}$$

Where:

- Q = activation energy for creep
- R = universal gas constant

- T = absolute temperature
- A,n = constant
- σ = stress

The creep rate increases exponentially with temperature: 20 °C increase in temperature can double the creep rate. The three constant A, Q and n determine the creep rate of a material. They must be determined by experiment.

The Arrhenius equation can be rewritten in terms of $\log_{10}$, thus giving the so-called Larson-Miller parameter:

$$P = \frac{T}{1000}(\log_{10} t_r + C)$$

Where:

- T = Absolute operating temperature [K]
- t_r = time to rupture in hours
- C = constant (between 15 and 30); this value can be obtained from the intercept

when $log_{10}\, t_r$ is plotted against $1/T$, but for most of the industrial applications it is assumed equal to 20.

2.1.4.6.3 Cumulative Creep

Considering a simple flight envelope, it could be possible to divide it up into several sections (i.e. take-off, climb, cruise, descent, and landing); obviously each flight segment will be characterized by different operating conditions, which are different stresses and temperatures. The difficulty lies in adding together the effects of each segment. One way of solving this problem, is to adopt the so-called Miner's Law, an inverse sum law which states that the sum of life fractions should be unity:

$$\sum_i \left(life \;\; fraction\right)_i = 1$$

Through the use of the Larson-Miller parameter, it is possible to determine the life to failure for each operating condition; hence, by dividing the real time spent at these conditions by the total life to failure, the life fraction is determined. Logically, the sum of these life fractions should be unity.

The Miner's law uses a linear damage sum assumption, relating the damage due to each flight segment with the ratio between times spent and time to failure, and assuming that component failure will occur when the sum reaches the unity. In reality, failure happens when the sum lies between 0.7 and 1.4.

2.1.4.6.4 Limitations and considerations

A very important aspect to point out is that the illustrated Larson-Miller method is not completely fool-proof. Particular attention has to be paid when extrapolating into high temperature regions, since it is possible that metallurgical changes could take place, which essentially means dealing with a different material.

Another crucial point that has to be highlighted is that the Larson-Miller parameter approach is based on the so called *Larson – Miller creep curves* (in order to evaluate the LMP and consequently time to failure through *Larson-Miller law*) which is basically a chart based on rupture: this means that the estimated total creep life refers to rupture of the blade. However, before reaching this critical condition, the components (i.e. the blades and the disc) are going to suffer a creep deformation which will grow progressively till they start damaging the casing (particularly by scraping it off) and the turbine itself (blade and disc could even stop working simply by excessive distortion).

2.1.5 Weibull Distribution

What follows is the explanation of the Weibull module. This module is applied to the lifing in order to extent the lifing prediction capabilities to all the parts of the engines that can cause a breakdown. First the general theory is presented and then the results of the module application are shown.

The Weibull distribution can be defined by three parameters α, β, and γ. Its density function $f_X(x)$ is defined by:

$$f_X(x)=\beta/\alpha[(x-\gamma)/\alpha]^{(\beta-1)}\exp\{-[(x-\gamma)/\alpha]^{\beta}\}$$

where $\alpha > 0$ is the scale parameter, its value determines the "scale" of the probability distribution, $\beta > 0$ is the shape parameter, and γ ($-\infty < \gamma < \infty$) is the location parameter.

The Weibull probability distribution function is:

$$F_X(x) = 1-\exp\left[-(x-\gamma)/\alpha)^{\beta}\right]$$

If $\gamma = 0$, as is true for many cases, the density function reduces to:

$$f_X(x)= \beta/\alpha\ (x/\alpha)^{(\beta-1)}\exp[-(x/\alpha)^{\beta}]$$

and the probability distribution function is:

$$F_X(x) = 1-\exp\left[-(x/\alpha)^{\beta}\right]$$

The reduced density function, called a two-parameter Weibull distribution, is used in probabilistic fracture mechanics and fatigue.

The Weibull distribution is often used in the field of life data analysis due to its flexibility; it can mimic the behaviour of other statistical distributions such as the normal and the exponential.

- If the failure rate decreases over time, then $\beta < 1$.
- If the failure rate is constant over time, then $\beta = 1$.
- If the failure rate increases over time, then $\beta > 1$.

An understanding of the failure rate may provide insight as to what is causing the failures:

A decreasing failure rate would suggest "infant mortality". That is, defective items fail early and the failure rate decreases over time as they fall out of the population.

A constant failure rate suggests that items are failing from random events.

An increasing failure rate suggests "wear out" - parts are more likely to fail as time goes on.

When $\beta = 3.4$, then the Weibull distribution appears similar to the normal distribution. When $\beta = 1$, then the Weibull distribution reduces to the exponential distribution.

The mean value and standard deviation of the random variable X with the two-parameter Weibull distribution are given as follows:

$$\mu_X = \alpha\Gamma(1+1/\beta)$$

And:

$$\sigma_X = \alpha\{\Gamma(1+2/\beta)-[\Gamma(1+1/\beta)]^2\}^{1/2}$$

where Γ is the well known gamma function calculated for the values in brackets.

In mathematics, the Gamma function is an extension of the factorial function to real and complex numbers. The Gamma function "fills in" the factorial

function for non-integer and complex values of n. For a complex number z with positive real part it is defined by

$$\Gamma(z) = \int_0^\infty t^{z-1} e^{-t}\,dt$$

which can be extended to the rest of the complex plane, excepting the non-positive integers. If z is a positive integer, then

$$\Gamma(z)=(z-1)!$$

showing the connection to the factorial function.

The Weibull density function can take many different shapes. In Figure 14 we can see the density functions for the five parts of the engine that are more likely to fail: Combustor, Life Limited Parts (LLP), High Pressure Compressor (HPC), General breakdowns and High Pressure Turbine (HPT).

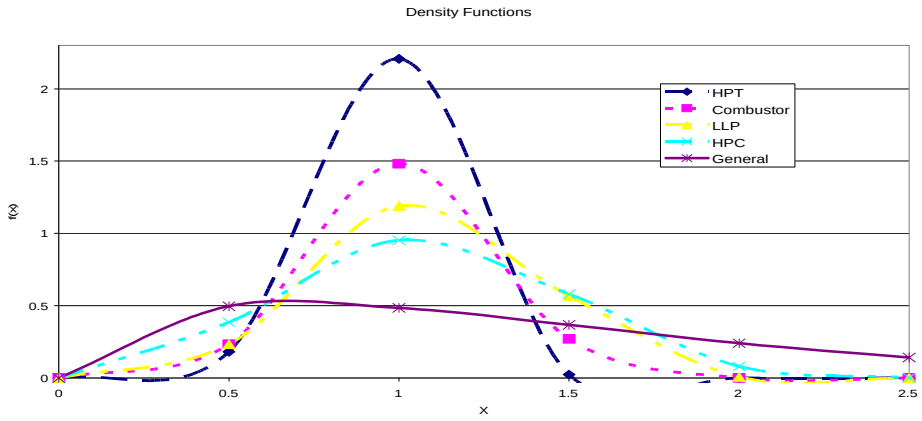

Figure 14 Density function for the five components of the engine

2.1.5.1 Generating Weibull distributed random variates

Given a random value for the reliability function U drawn from the uniform distribution in the interval (0, 1), then the variate

$$X = \alpha\,[-\ln (U)^{1/\beta}] \qquad (1)$$

Has a Weibull distribution with parameters β and α. This follows from the form of the cumulative distribution function $F_X(x)$. In Figure 15 we can see the cumulative distribution function for the four different engines analysed by the risk model that have been used for this work.

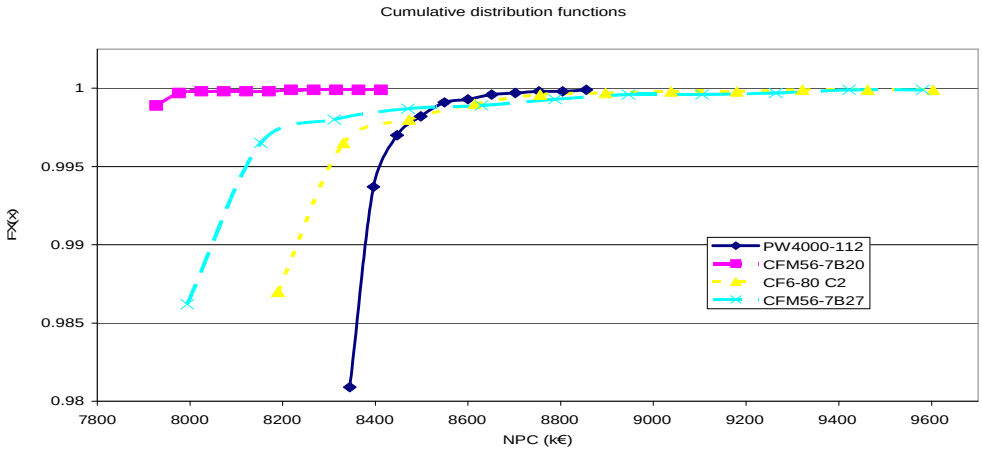

Figure 15 NPC and Cumulative distributions for the four engines

In the Economic model the Weibull distribution takes as input the time between overhaul calculated by the lifing analysis, and the β and α value for all the distributions, one for each component of the engine that could fail.

These values are then put into (1), and then the program gives random values for U and calculates X that in our case is the probable TBO from each distribution.

Then the lower of the values of X of all the distributions is taken as TBO, and used into the economic module calculations.

In the following **Table 2** the values of α and β, found out with this procedure, and are shown:

Component	α	β
HPT	1.0	6
HPC	1.22	3
LLP	1.2	4

Combustor	1.12	4.5
General	1.45	1.5

Table 2 α and β values

2.2 Monte Carlo Simulation Technique

Monte Carlo method has been implemented in the economic model in order to estimate the risk associated with each engine configuration. A simple explanation of this method follows.

Monte Carlo simulation techniques are implemented by randomly simulating a design or process, given the stochastic properties of one or more random variables, with a focus on characterizing the statistical nature (mean, variance, range, distribution, etc.) of the responses (outputs) of interest. Monte Carlo Simulation methods have long been considered the most accurate means of estimating the probabilistic properties of uncertain system responses resulting from known uncertain inputs. To implement a Monte Carlo simulation, a defined number of system simulations to be analysed are generated by sampling values of random variables (uncertain inputs), following the probabilistic distributions and associated properties defined for each.

2.3 Introduction to Optimisation

Following are the most used optimisation techniques. Some of these have been used during the optimisation of the VITAL aero engines.

According the *Webster's New Collegiate Dictionary* optimise means "to make as perfect, effective or functional as possible". But this definition is a too general one, in engineering a more precise definition of optimise is defined as we can read from the *Engineering Optimisation Methods by Reklaitis,*

Ravindran & Ragsdell optimise means “in the most general terms, optimisation theory is a body of mathematical results and numerical methods for finding and identifying the best candidate from a collection of alternatives without having to explicitly enumerate and evaluate all possible alternatives.”

The standard form of General Optimisation Problem is to minimise a non analytical function f(p) where p is a n-dimensional parameter vector. The function f is subject to several constraints expressed in equality form and/or inequality form using non analytical functions g(p) and also side constraints applied directly to the design variables p_j.

2.3.1 Numerical Optimisation Techniques

Numerical optimisation techniques are domain-independent and generally assume the parameter space is unimodal, convex and continuous. Numerical techniques are exploitive, this mean that they immediately focus on a local region of the parameter space. All runs of the simulation codes are concentrated in this region with the intent of moving to better design points in the immediate vicinity. These techniques can be divided into the following two categories:

- Direct methods: they deal with constraints directly during the numerical search process.
- Penalty methods: they add a penalty term to the objective function to convert a constrained problem in an unconstrained one.

2.3.1.1 Direct Methods

Generalized Reduced Gradient

This technique uses generalized reduced gradient algorithm for solving constrained non-linear optimisation problems. The algorithm uses a search

direction such that any active constraints remain precisely active for some small move in that direction.

Method of Feasible Directions - CONMIN

This technique is a direct numerical optimization technique that attempts to deal directly with the nonlinearity of the search space. It iteratively finds a search direction and performs a one dimensional search along this direction. Mathematically, this can be expressed as follows:

Design i = Design i-1 + A * Search Direction I

In this equation, “i” is the iteration, and A is a constant determined during the one dimensional search. The emphasis is to reduce the objective while maintaining a feasible design. This technique rapidly obtains an optimum design and handles inequality constraints. The technique currently does not support equality constraints.

Mixed Integer Optimization - MOST

This technique first solves the given design problem as if it were a purely continuous problem, using sequential quadratic programming to locate an initial peak. If all design variables are real, optimization stops here. Otherwise, the technique will branch out to the nearest points that satisfy the integer or discrete value limits of one non-real parameter, for each such parameter. Those limits are added as new constraints, and the technique re-optimizes, yielding a new set of peaks from which to branch. As the optimization progresses, the technique focuses on the values of successive non-real parameters, until all limits are satisfied.

Modified Method of Feasible Directions

This technique is a direct numerical optimization technique used to solve constrained optimization problems. It rapidly obtains an optimum design, handles inequality and equality constraints, and satisfies constraints with high precision at the optimum.

Sequential Linear Programming

This technique uses a sequence of linear sub-optimizations to solve constrained optimization problems. It is easily coded, and applicable to many practical engineering design problems.

Sequential Quadratic Programming - DONLP

This technique uses a slightly modified version of the Pantoja-Mayne update for the Hessian of the lagrangian, variable scaling, and an improved Armijo-type step size algorithm. With this technique, bounds on the variables are treated in a projected gradient-like fashion.

Sequential Quadratic Programming - NLPQL

This technique assumes that objective function and constraints are continuously differentiable. The idea is to generate a sequence of quadratic programming sub problems, obtained by a quadratic approximation of the lagrangian function, and a linearization of the constraints. Second order information is updated by a quasi-Newton formula, and the method is stabilized by an additional line search.

Successive Approximation Method

This technique lets you specify a nonlinear problem as a linearized problem. It is a general program which uses a Simplex Algorithm in addition to sparse matrix methods for linearized problems. If one of the variables is declared an integer, the simplex algorithm is iterated with a branch and bound algorithm until the desired optimal solution is found. The Successive Approximation Method is based on the LP-SOLVE technique developed by M. Berkalaar and J.J. Dirks.

2.3.1.2 Penalty Methods

Exterior Penalty

This technique is widely used for constrained optimization. It is usually reliable, and has a relatively good chance of finding true optimum, if local

minimums exist. The Exterior Penalty method approaches the optimum from infeasible region, becoming feasible in the limit as the penalty parameter approaches ∞ ($\gamma p \rightarrow \infty$).

Hooke-Jeeves Direct Search Method

This technique begins with a starting guess and searches for a local minimum. It does not require the objective function to be continuous. Because the algorithm does not use derivatives, the function does not need to be differentiable. Also, this technique has a convergence parameter, rho, which lets you determine the number of function evaluations needed for the greatest probability of convergence

2.3.2 Exploratory Techniques

Exploratory techniques are domain-independent and avoid focusing only on a local region. They generally evaluate designs throughout parameter space in search of the global optimum. The techniques included in iSight are:

Adaptive Simulated Annealing

The Adaptive Simulated Annealing (ASA) algorithm is very well suited for solving highly non-linear problems with short running analysis codes, when finding the global optimum is more important than a quick improvement of the design. This technique distinguishes between different local optima. It can be used to obtain a solution with a minimal cost, from a problem which potentially has a great number of solutions.

Multi-Island Genetic Algorithm

In the Multi-Island Genetic Algorithm, as with other genetic algorithms, each design point is perceived as an individual with a certain value of fitness, based on the value of objective function and constraint penalty. An individual with a better value of objective function and penalty has a higher fitness value. The main feature of Multi-Island Genetic Algorithm that distinguishes it from traditional genetic algorithms is the fact that each population of individuals is

divided into several sub-populations called “islands.” All traditional genetic operations are performed separately on each sub-population. Some individuals are then selected from each island and migrated to different islands periodically. This operation is called “migration.” Two parameters control the migration process: migration interval, which is the number of generations between each migration, and migration rate, which is the percentage of individuals, migrated from each island at the time of migration.

Neighborhood Cultivation Genetic Algorithm - NCGA

In this technique, each objective parameter is treated separately. Standard genetic operation of mutation and crossover are performed on the designs. The crossover process is based on the “neighborhood cultivation” mechanism, where the crossover is performed mostly between individuals with values close to one of the objectives. By the end of the optimization run, a Pareto set is constructed where each design has the “best” combination of objective values, and improving one objective is impossible without sacrificing one or more of other objectives. The Pareto plot is an ordered chart of the normalized coefficients, which represent the percentage of total effect on the response.

Non-dominated Sorting Genetic Algorithm - NSGA-II

In this technique, each objective parameter is treated separately. Standard genetic operation of mutation and crossover are performed on the designs. The selection process is based on two main mechanisms, “non-dominated sorting” and “crowding distance sorting.” By the end of the optimization run, a Pareto set is constructed where each design has the “best” combination of objective values, and improving one objective is impossible without sacrificing one or more of the other objectives.

2.4 Advanced Aero Engines

The ability of the three VITAL configurations to meet the future goals of the European Union to reduce noise and gaseous emission has been assessed

and has showed that the three engines cannot fully comply with future legislation beyond 2020.

In the second part of this thesis further advanced configurations have been studied to determine whether detailed investigations and technological development are worthwhile for those configurations.

Modern air transport has developed into a fundamental mean of transportation. Apart from short-term fluctuation, the average worldwide growth is expected to be continued at a rate of about 5 per cent per annum (Klug et al. 2001, Howse 2003, Steffen et al. 2003). To some extent, the previous growth was enabled by the long-term development and application of advanced aero engine technologies which focused primary on minimum fuel consumption as well as on manufacturing and maintenance economics.

Today, beside the fuel consumption, and manufacturing and maintenance economics some additional drivers have increased drastically their importance. They are the pollutants, whenever there are emissions, NOx, gases of green house effects, basically the CO_2 measured by the specific thrust fuel consumption (SFC) or the fuel consumed per unit of thrust, and noise generated by engine components (Klug et al. 2001, Howse 2003, Steffen et al. 2003, Nalim et al. 1996, Sirignano et al. 1999, Sehra et al. 2003, Smith 2005); more efficient, economic and environmental friendly aero engines are worldwide required. More efficient engines mean the design of an aero engine with higher thermal and propulsive efficiency; any increase in thermal or propulsive efficiency will bring down the specific thrust fuel consumption for a given flight velocity, which will also decrease burned fuel and CO_2 production. Specific thrust (ST), which represents the amount of thrust per unit of airflow mass coming into the engine is another important engine variable to be considered; it is a measure of engine size, weight and drag for conventional or near-conventional aero engines, and it also will influence the burned fuel (Johnsen 1965) and the noise due to the jets, higher specific thrust lower engine size. The development of more efficient and less polluting or environmental friendly aero engines requires the overall pressure

and cycle maximum temperature to be pushed up to improve their limits (Nalim et al. 1996, Lefebvre 1998 & 1984) while curbing down the SFC and nitrogen oxides, but also keeping in mind the current technology levels. Many studies have been carried out focusing on these general objectives, evolving from standard Brayton cycle (Howse 2003, Nalim et al. 1996, Heiser et al. 2002, Wilson et al 1996). Sehra et al. (2003) presents interesting ideas on future revolutionary propulsion systems as micro propulsion systems integrated in the aircraft structure and aerodynamics, and also aircraft distributed fans driven by a central engine system. Howse (2003) also presents additional ideas, including possible application of non aero engine standard cycles as well as engine components improvement to increase engine efficiencies. Heiser et al. (2002) presents also a nice comparison between interesting future candidate cycles, like Brayton, PDE, and CV cycles.

Many European programs, supported by the European Commission through their different framework programs, are driven by these objectives; two of them are the CRYOPLANE, devoted to alternative fuels, hydrogen, (Liquid 1999, Corchero et al. 2005) and VITAL (environmental friendly aero engine), under whose program the present work has been carried out (Environmentally 2004). The primary objective of VITAL program consists in developing the technology which permits the in-short-term application of an optimized LPT (low pressure turbine) spool, which drives a fan with an ultra high bypass ratio (UHBR) and a booster in the engine core, and evolving from a previous fixed modern gas generator. Direct and gear drives as well as counter rotating fans are included. This translates into an improvement of the propulsive efficiency, while also they expect to bring down the whole LPT spool weight. Looking to a long-term evolution, the VITAL project includes a task devoted to innovative cycles, which could improve engine efficiencies and emissions although they could come into non-conventional engine configurations; part of the work carried out in this task is presented here.

This thesis presents a work carried out, in the VITAL project, on the application of some innovative cycles to turbofan aero engines with ultra high

bypass ratios (UHBRTF), bypass ratios above twelve. Starting from the assumption that, the LPT spool and bypass stream have been optimized to get a maximum feasible propulsive efficiency considering the expected technology improvement in VITAL project, different innovative cycles have been applied to core engine to improve performances. Performances are focused on specific thrust fuel consumption, and specific thrust improvement, as well as on emissions, and noise levels. In this study, expected VITAL technology level is considered as baseline technology level also.

Recently much work has been devoted to the analysis of innovative cycles, and innovative components for aircraft propulsion systems. Sirignano et al. (1999) and Liu (2001) present the application of inter-stage turbines combustion and continuous turbine combustion cycles, but this cycle has not been studied because the results show an important benefit on specific thrust, but with an increase on specific fuel consumption due to a lower propulsive efficiency, requiring also a new combustor-turbine technology. NASA has also devoted much work to wave rotor simulation and development (Wilson 1993 & 1997, Welch 1997 & 1999, Paxson 1997, Nalim 1996 & 1999).

2.5 More future engine: the internal combustion wave rotor

After studying the CVC and Wave rotor separately it has been decided to do a parametric study of an aero engine that comprises both configurations. This engine is a blue sky concept, highly advanced and quite futuristic, with a technology readiness level (TRL) of 7 or higher only by 2025, so only a preliminary performance study is done, leaving to future studies the task of a more improved analysis.

The Constant Volume Combustor (CVC) concept implements a type of constant volume combustion process utilizing wave rotor type machinery. Compared to a conventional turbine engine combustor, the CVC creates a pressure rise in addition to temperature rise. This results in the potential for

greater work extraction from the flow through the turbine or higher pressure available at the exhaust nozzle to produce thrust.

The machinery is like that of a wave rotor, because the CVC is a type of wave rotor with the additional fact that the combustion takes place within the rotor tubes. The picture below is a highly conceptual drawing of the proposed device with each of the components labeled (Smith et al 2002). Flow enters from the left and travels to the right.

In sequence, the flow passes through the compressor transition duct, inlet endplate, rotor, exit endplate, and exits through the transition duct toward the turbine. Some of the flow will transition through the buffer air ducts after entering the rotor, through which it will then be discharged into an adjacent tube within the rotor. Notice that there are a large number of tubes or channels within the rotor. Identical processes take place within each tube. The process in each tube is out of phase with that in the other tubes relative to the angular position of the tube. Having many tubes in the rotor enhances the quasi-steady in and-out flow. Fuel is detonated at the right end of the rotor tube, indicated on the endplates in the picture. The rotor revolves to provide valve action, i.e., opening and closing of ports into and out of the rotor. The endplates have cutouts which are the ports. As the rotor spins, the tubes pass by the cutouts in sequence for proper “opening” and “closing” of the ports. Transition ducts at either end are required to carry flow from the partial annulus of the wave rotor to the full annulus of the turbomachinery and to dampen the unsteady effects of the flow entering and leaving the CVC.

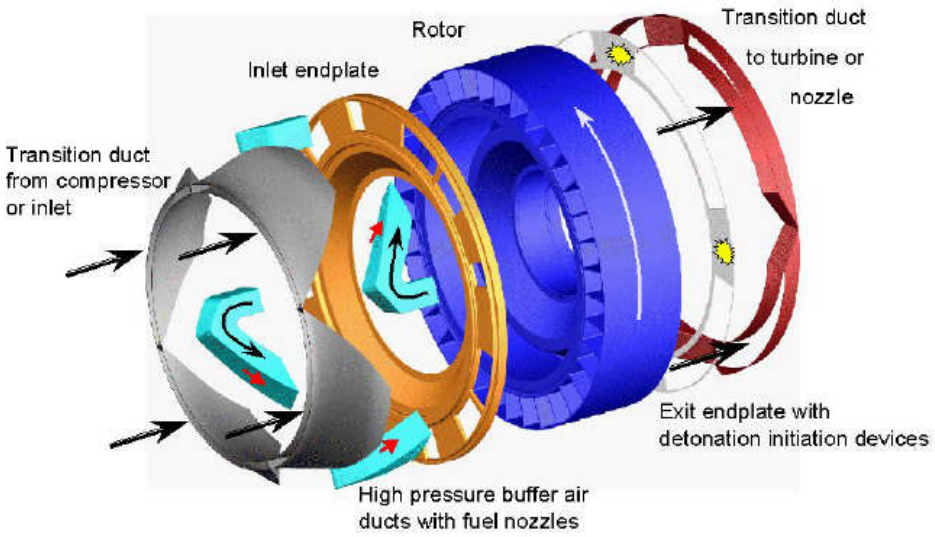

Figure 16: CVC machinery exploded view (Smith et al 2002)

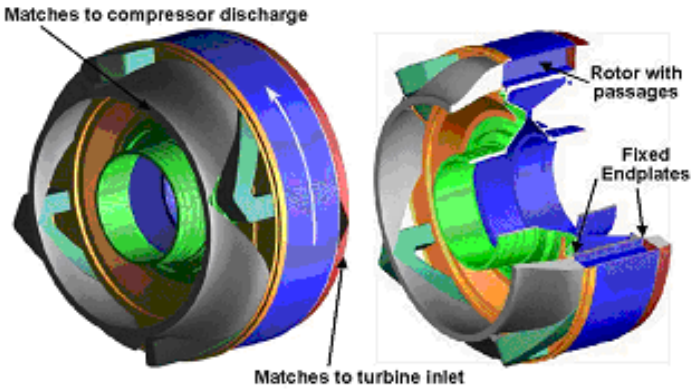

Figure 17 general arrangement of the CVC (Smith et al 2002)

A developed view of the flow processes occurring within the CVC is shown in Figure **18**, illustrated in x-t diagram form x being the distance along the tube axially and t being time. The process sequence begins at the bottom of the diagram where a mixture of air and fuel are trapped within the tube as the tube translates upward (t increasing during rotor rotation) and approaches Port 5.

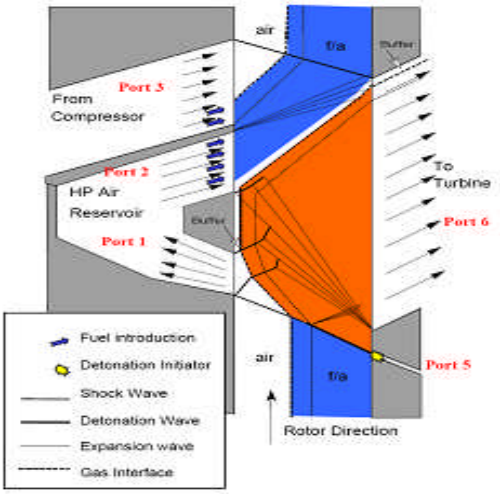

Figure 18 developed view of the CVC process (Smith et al 2002)

The detonation of the mixture is initiated as it passes Port 5 on the exit end of the CVC. The exact mechanisms of initiation were not modeled in detail for the purposes of this study. Implementation will depend on applying lessons learned in recent PDE research. The detonation then travels to the left down the tube as the fuel is combusted. When the detonation passes out of the region having fuel and into the region where no fuel is present, a resulting shock wave travels toward the inlet end through the remaining air in the tube. On the right or exit end of the tube, the opening to the duct adjoining the downstream turbine is opened. This initiates a set of expansion waves, which accelerate the flow within the tube and this flow exits the tube through port 6 and enters the turbine transition duct. A moment later, on the inlet end, the portion of the flow compressed by the shock wave, exits via port 1 and enters a short loop of duct on the inlet end of the CVC. Within this duct the high pressure flow is turned back into the rotor, reentering the rotor some moments later at Port 2. (Note: Some of this buffer gas can also be used for high pressure turbine cooling, a feature previously not available with pulse detonation combustors until fairly recently.) This reentering of high-pressure non combusted gas is the key element to providing a uniform outflow to the turbine inlet. Introducing this compressed gas back to the tube causes the hot gas expansion and expulsion process in the tube to finish in an energetic manner. The energy added by the compressed gas allows a highly uniform

pressure and velocity process to continue within the tube during the entire time the hot gases are discharging.

Essentially, all packets of flow arriving at the exit have the same energy level thus allowing a steady flow at the exit of the CVC. As the compressed gas is reintroduced on the left end, fuel is added within Port 2. As port 2 is closed, port 3 is opened and fresh compressor air is swept into the tube behind the gas rushing toward the exit at the right. As the discharge port 6 is closed, a hammer shock is formed which travels to the left compressing the incoming flow. The tube is closed as the shock arrives at the left end of the tube. The process is now ready to repeat.

A comparison of an advanced reference engine using conventional turbomachinery to the current layout of a CVC based engine is shown in Figure 19. Several differences between the engines can be noted. First of all, conventional engine compressor is replaced with a low pressure ratio compressor due to the pressure rise characteristic of the CVC.

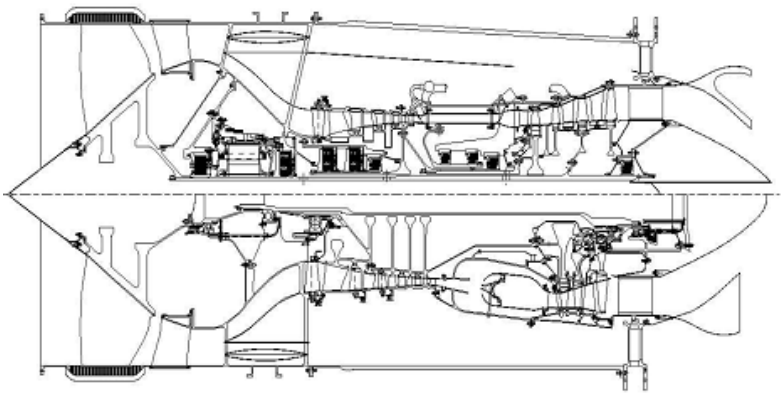

Figure 19 conventional versus CVC engine (Smith et al 2002)

2.5.1 Advantages and Limitations of the Internal Combustion Wave Rotor

Advantages:

- Pressure gain during combustion, thanks to this the turbomachinery of the engine can have a smaller size and lighter weight

- Constant volume combustion is more efficient, because of the shock wave system it uses.

- Higher overall pressure ratio

- Higher overall temperature ratio

- Lower SFC, because in detonation a leaner mixture is used in order to create the same amount of energy

- Higher thermal efficiency, because of the higher temperatures achievable with deflagrations

- Steady flow at exit of ducts

- Self cooling, because in the wave rotor there is always an alternation of cold and hot flow in his tubes creating a perfect cooling environment

- Can replace entire spools, because the increase of pressure and temperature is done in the wave rotor and the combustor the HPC and HPT are smaller

- Possibility of reduced engines size and weight, again the compactness of the wave rotor ensures that the turbomachinery can have a lower number of stages.

Limitations:

- High thermal fatigue loading, because of the high TET creep and fatigue are a main concern

- Structural integrity is an issue because of detonations

- Combustion initiation is difficult, because the creation of detonation under a controlled environment in not an easy task

- Sealing issues are a major problem, because there is a complex valve system connected to the closing and opening of the wave rotor's ports

- Complicated mechanism, as we can see in **Figure 16** and **Figure 17** this type of engine has a quite elaborated structure and it's manufacture would not be easy in mass production

- Failure modes are unknown

- Cost of production is unknown

- Shock waves possibility and uncertainty of the interaction of them with the turbine

- Unsteady device makes calculation, design and analysis unpredictable and difficult

3. Economic Module

In this chapter all the input and output of the economic module are explained. Engine design decisions have significant influence on the first cost and operating expenses. It is therefore important to understand the cost implications of engine manufacture and operation and to take these into account when deciding the aircraft configuration and performance.

The costs of manufacturing are calculated in the Plant cost module of TERA (see Figure 22) and are received as an input by the economic module, so they are not considered here.

Consideration of cost aspects is especially significant in the preliminary design phase of engine projects as fundamental decisions are taken which will be influential in the overall cost of the project. Such decisions affect the cost of manufacturing and equipping the basic engine and the subsequent cost of operating it over the route structure of an airline. It is therefore essential to understand the cost estimation methods to be used by the customer when comparing competitive engines, in order to make sensible design choices.

Here are introduced the methods by which engine operating costs are estimated. These methods are used in the preliminary project phase to allow comparisons to be made between different aircraft configurations and to assess the best choice of values for all the aircraft parameters.

Indirect costs (those not directly related to the engine parameters, for example those associated with marketing and sales expenses) are not covered, whereas direct costs are described in enough detail to allow estimating methods to be incorporated into the aircraft design process. The principal cost functions are described and typical values given.

A comparison between my model, a model created by Roskam (1990) and values taken from magazines for the A330-200, the A320-200 and different types of long and short range engines is presented.

Engine project designers are seen to influence costs directly by the basic configuration of the engine (system complexity, aircraft size, engine size, etc.) and selected performance (cruise speed, range, etc.). All these aspects will have a substantial input to the cost model through the standing charges, the fuel used and the maintenance required. The designers also influence cost indirectly through airline economics (market size, ticket price, engine performance, passenger appeal). These indirect factors feed into the cost analysis through revenue potential, the demand for the aircraft type, market development and ultimately to commonality and type derivations. It is important for the designers to recognise these influences in the early stages of the engine project so that the design can meet the market potential and thereby maximise success of the project.

3.1 Methodology

Under the direct operate cost (DOC) category all the costs associated with flying and direct maintenance must be considered. The cost components may be considered in three broad headings:

- Standing charges
- Flight costs
- Maintenance costs

A description of each of these headings is given below in Figure 20.

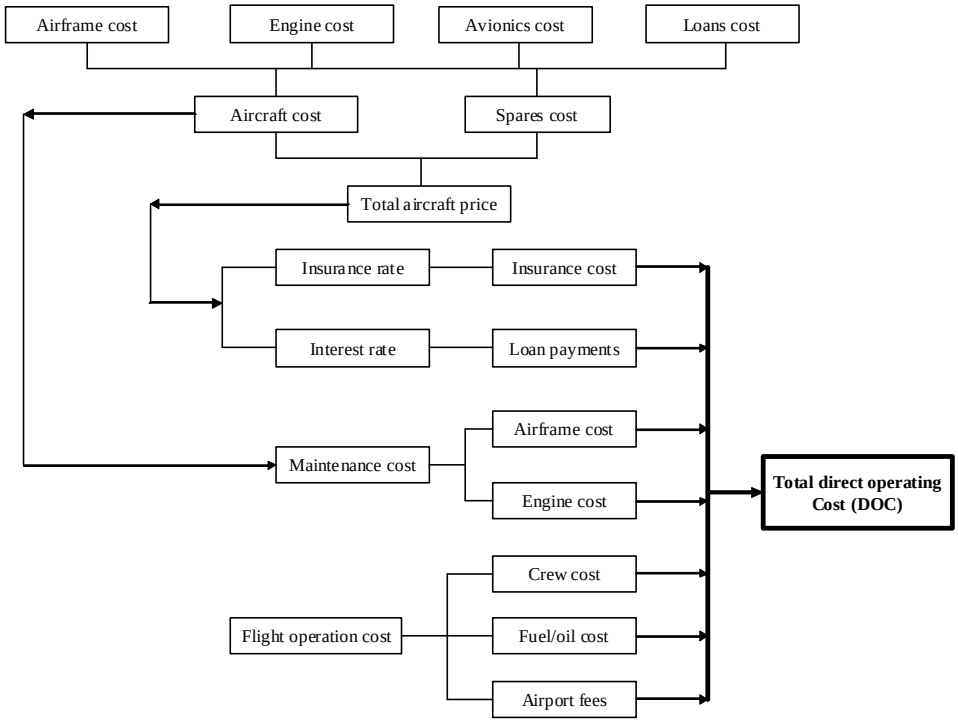

Figure 20 Direct operating cost (DOC) components (Jenkinson 1999)

Standing charges:

These are the proportion of the costs that are not directly linked to the engine flight but may be regarded as ‘overhead’ on the flight. Such costs, in order of importance, include:

- Interest charges on capital employed
- Engine insurance

Interest charges are impossible to quantify in a general analysis as the banks and government agencies will charge different fees to different customers. Such charges will be dependent on the world economic climate, local exchange rates, the credit standing of the purchaser and the export encouragement given by the national government of the airline or the manufacturer. Usually current national base interest rates should be used to account for this type of cost.

The insurance cost is directly related to the risks involved and the potential for claims following loss. Insurance companies will vary their fee in relation to the nature of the operation and the level of airline security. The fees vary usually between 1 and 3% of aircraft value.

Flight costs

This cost element comprises all the costs which are directly associated with the flight. They are:

- Fuel and oil usage
- Airport charges

Included in the airport charges are not only the landing and navigational fees but also the taxes on noise and emissions that nowadays are becoming more and more important due to the concern about environmental pollution from the public and government alike.

Maintenance costs

Prediction of maintenance costs is complicated by the lack of definition for items to be included under this heading. Setting up a maintenance facility is an expensive outlay for the airline. Some such facilities run as a separate business. The capital cost of building, the administration costs and the cost of special equipment may be regarded as an indirect cost on the total maintenance operation and included in the Indirect Operating Cost evaluation. These suits the aircraft manufacturer as the evaluation of DOC would proportionally reduce.

Maintenance charges include labour and material costs associated with routine inspections, servicing and overhaul. The equations used for calculate the maintenance costs are shown in annex F.

In an inflationary economic climate, values for costs are highly time-dependent; therefore some effort must be made to secure current prices for

the various elements that make up the total operating cost. Alternatively, old prices must be ‘factored’ to account for changes since publication. This factoring requires the use of an inflation index. This index has been applied to most of the costs already described.

The economic module has inside a lifing module to study the lifing of rotor blades and the disk of the high pressure turbine. It is important because the maintenance costs depend strongly on the time between overhauls of the components of the engine and the high pressure turbine has the most severe operating environment of all the parts of the engine.

To the lifing module the Weibull distribution is applied in order to generalise the lifing prediction taking into account all the parts of the engine which can cause breakdown.

The Risk Module

The economic module has also a risk module inside in order to do a Monte Carlo Risk Analysis for the DOC over a period of time of thirty years, which is considered the average life for both the aircraft and the engine. An explanation of the Monte Carlo Method has been done in paragraph 2.2.

The risk model uses Gaussian distributions applied to several parameters that affect the DOC and NPC like:

- Interest Percentage
- Fuel Price
- NOx
- Downtime
- Inflation
- Labour
- Carbon Tax
- Noise Tax
- Time Between Overhaul

The risk is applied to 10000 scenarios, this number of scenarios is considered in statistic evaluation as the minimal required in order of being sure that the analysis has a meaning, and then a classical S shaped cumulative curve is created, as we can see in **Figure 21Figure 34**.

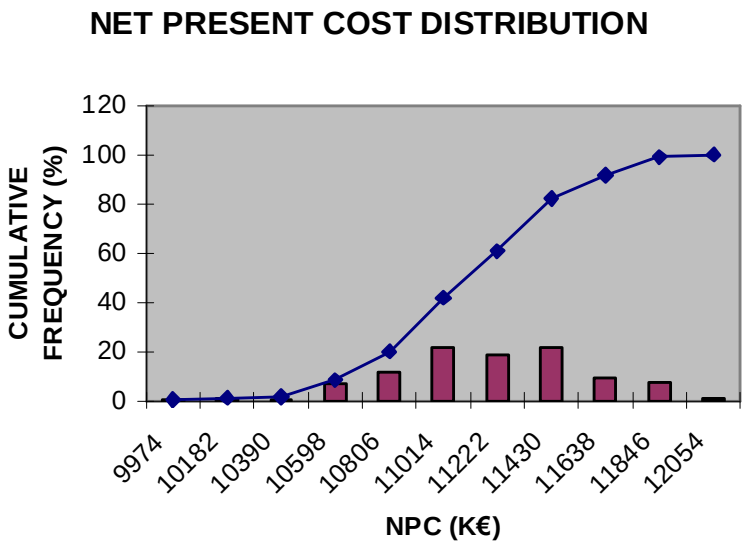

Figure 21 Cumulative curve for the net present cost (NPC)

The economic module has to be integrated with other modules like an aircraft module and a performance module created here in Cranfield, a weight module done by Chalmers University in Sweden, a plant cost module done in Stuttgart University and two modules that analyse the noise and emissions done in SUPAERO University in France. This integrated complex system is called TERA: Thermo Economic and Risk Analysis. The integration of these entire modules is done through a licensed program used by many industries called iSight. This is a very powerful tool that can do optimization, design of experiment, trade-off analysis, optimum robust design and approximation methods. Thanks to TERA the VITAL project will be able to create optimal design of engines with a good trade-off between performance and costs.

Figure 22: the TERA structure (TERA 2006)

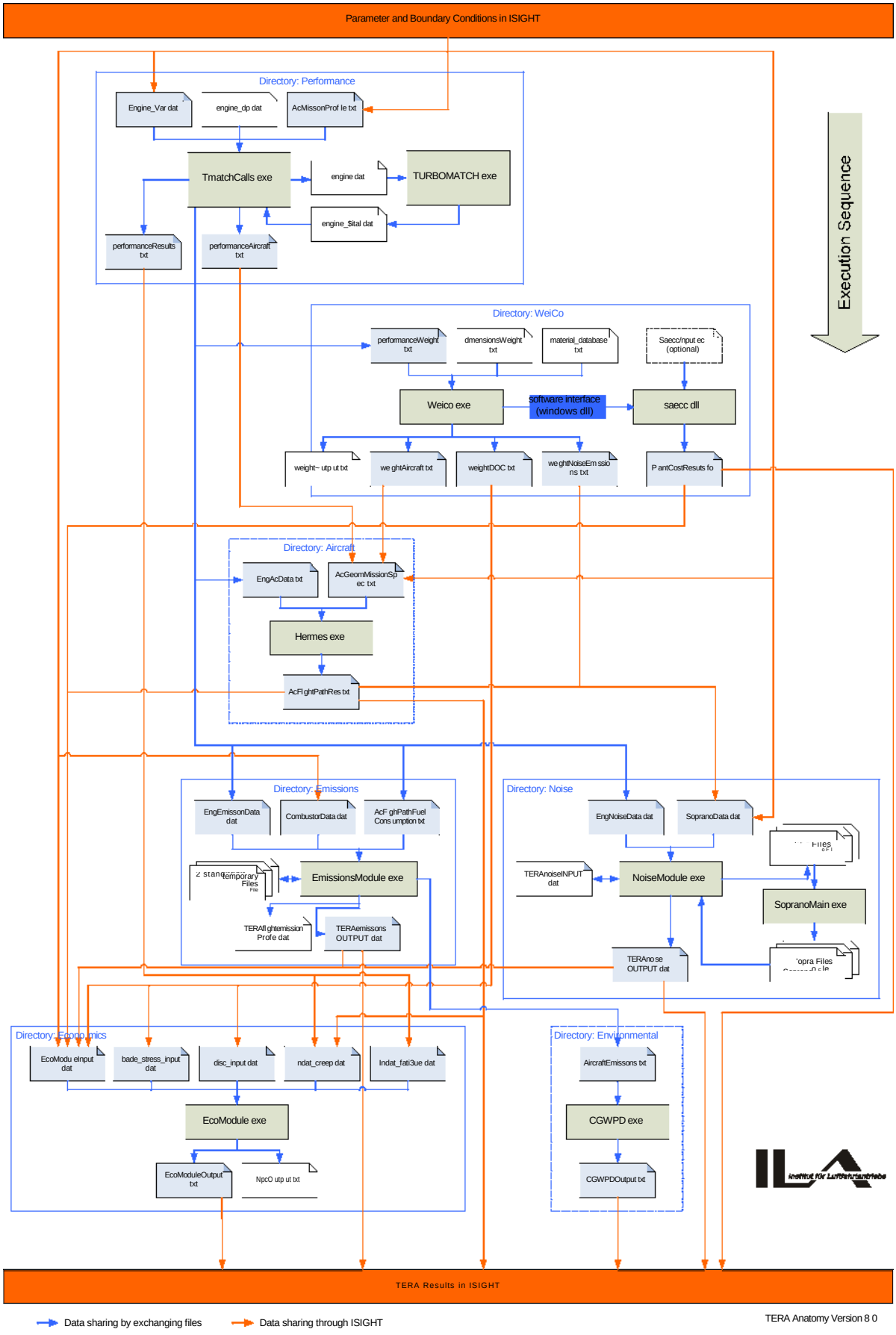

3.2 Economic Module Description

In this section, a description of the Economic module is given. The features of the economic module are based on the TERA high level specification given by the VITAL project. The capabilities of this current version of the Economic module would be shown via the inclusion of the input file and examples of the program outputs. The programming language for the economic model is Fortran 90.

3.2.1 Economic Module Architecture

The flow chart with the architecture of the economic module is shown in the figure 23:

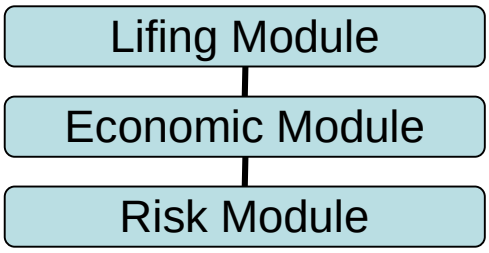

Figure 23 Economic Module Structure

3.2.2 Module Requirement Definition

A set of requirements was developed and implemented into the economic module. These include the following capability to vary as inputs:

- Cost of aviation fuel
- Cost of maintenance hours
- Interest rates
- Noise charges at airports
- Carbon emission charges

- NOx charges

The Risk Module

Also a stochastic risk module, developed following the Monte Carlo approach is integrated into the economic model. This enable scenario studies with the input parameters taking likely distributions and the analysis conducted over the product life.

Through the selection of variables in the input file it is possible to choose which variables will be changed by the risk module. If the value of the selector is 1 the variable is not changed by the module, with a value of 2 the module will change the value of the variable. The values that are not changed by the module have to be given by the user in the input file. The risk requires the minimum and maximum of the variables that it has to change.

If the economic program has to work without the risk analysis, N (number of scenarios studied by the program) has to be set to 1. With a value of N>1 the economic analysis will use the risk module.

The NOX factor B is a variable that increases the value of NOX considering the future increase of the tax.

The Noise tax is calculated using a threshold system of taxation. A value for the threshold is given in input and if the noise produced by the engine is higher than the threshold, the higher is the tax. The same policy has been used for the Carbon Tax.

3.2.3 Input file Definition

Some key parameters required by the economic model and their sources (other modules that are in TERA) are shown in the table 3:

Parameter	Source/Module
Cost of aviation fuel (c$/US gallons)	User defined
Cost of flight and cabin crew (€/FH)	User defined
Cost of maintenance hours (€/FH)	User defined
Interest rate (%)	User defined
Noise level (dB)	Noise model
Emission level	Emissions module
Block fuel (kg)	Ac Performance module
Block time (hrs)	Ac Performance module
Shaft speed (relative)	Engine performance module
TET (k)	Engine performance module
Plant cost (k€)	Plant cost module

Table 3: Key Economic Module Parameters

The typical input file for the economic model is a notebook file that requires data for the engine and the aircraft.
It incorporates data that are used by both the economic and risk modules.
It has several parameters, but the most important are:

- Take off Thrust: from this depend the maintenance hours needed by the engine.
- Overall Empty Weight: to assess the maintenance hours needed by the airframe.
- Weight of Fuel Used.
- Time between engine overhaul: this parameter can be given by the user or can be calculated by the lifing module.
- All the elements needed to calculate the airport fee and taxes, like noise and emissions.

The input file for the lifing module (blade_stress_input.dat, disc_input.dat, indat_creep.dat, Indat_fatigue.dat, material_database.txt) contains the data needed to calculate the creep and low cycle fatigue from an analysis of the

stresses for the blades and the disk of the high pressure turbine, which is typically the most life limited component.

In order to calculate creep and fatigue several geometrical parameters and the properties of the materials used in the components are needed, such as the Larson-miller parameters, for the creep, and the coefficients of the Coffin-Manson equation, for the low cycle fatigue.

Also needed are the temperatures and duration to which the components are exposed during the flight cycle. The lifing module will be better explained in the next section.

3.2.4 Output Files

Amongst the outputs the economic model would give are:

- Direct operating cost, DOC (k€)
- Engine maintenance cost (k€)
- Net present cost, NPC (k€).
- Cost of taxes (k€)
- Stresses of the blades and the disk.
- The cost of labour and materials used in the overhaul.

The NPC is obtained over a time frame defined by the user to depict the engine operating life.

The cumulative curve enables the planners to assess risk when a specific minimum value of NPC is targeted. In such conditions, if the airline plans to spend 11.5 millions of Euros the NPC value is 80%, so the risk estimated is 20% as we can see from **Figure 21**.

3.3 The lifing Module

The lifing module has been done by the master student Oliviero Vigna Suria and integrated by the author in the economic module with little modifications. The general theory behind the lifing analysis has been explained in paragraph 2.1.4. The results that validate the module can be found in Vigna Suria's thesis (2006).

Oxidation and hot corrosion, creep, thermal mechanical fatigue can all potentially lead to turbine hot section component failure. Assessing gas turbine blade life is a multi-disciplinary task requiring expertise in metallurgy, material, mechanical design, fracture mechanics, aero-thermal dynamics, combined with operation and service history. The life limits provided by original equipment manufacturer (OEM) are calculated on the basis of a design envelope of expected base load, calculated or measured component stresses and temperatures as a function of operating conditions, expected response of the material to those conditions, and safety factors to take into account uncertainties in the model and natural variability of the materials. Because of uncertainties in each of these factors and variations between the operating conditions of specific engines, the OEM estimated life may be too conservative in some instance, while in others, the OEM design life may not be achieved.

Conventional maintenance scheduling techniques are typically based on the OEM's guidelines and applied to all engines of a certain make and model. This approach does not always address the specific operating environment and requirements of each operator.

Using the basic failure theories, together with a stress analysis depending upon the operating conditions, explained in paragraph 2.1.4, the lifing module is able to determine with certain accuracy the time between engine overhaul, taking into account every kind of uncertainty through what are known as 'safety' or 'ignorance' factors.

3.3.1 Structure of the lifing module

The module has been written in Fortran 90 language.

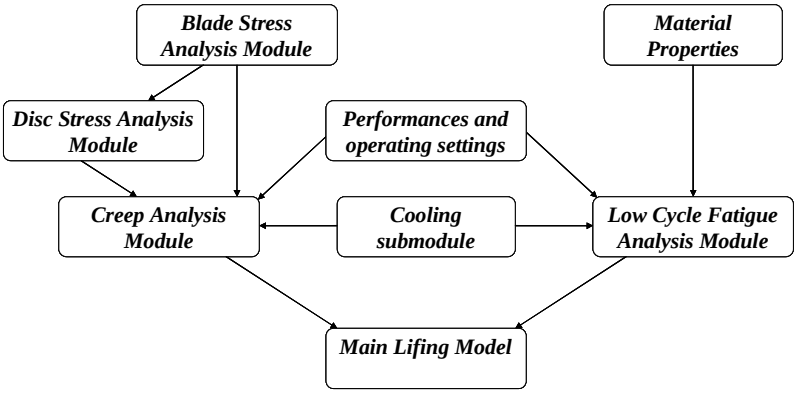

Figure 24, Lifing Module Breakdown (Vigna Suria 2006)

Knowing the maximum stress acting on the blades and on the disc, plus some additional settings and performance data (i.e. time spent and TET, that will allow to define the actual scenario, in terms of stress-time-temperature), the creep module will calculate the creep life time for both the components, as normally they are made from different materials, thus having a different life time.

On the other hand, using simply the material's properties and the peak of temperature experienced when starting-up the engine, the low cycle fatigue module will estimate the fatigue lives.

The main algorithm will then compare creep and low cycle fatigue life times: the lower will be considered as the real time between engine overhaul, and passed to the economic module as an input.

The important facility offered by the module is the possibility to run either the module as a whole, or each module independently, depending on the amount of information available when running the algorithm.

All the uncertainties can be taken into account by the use of what are known as ‘safety’ or ‘ignorance’ factors, available in the code.

An important issue that has to be pointed out is how creep and low cycle fatigue affect the life time of the engine’s HP turbine during each type of mission, since the failure mechanism that gives the lowest life, will be the one to adopt in predicting time between engine overhaul.

In Figure 25, the influence of both creep and fatigue can be appreciated as a comparison between the relative importance’s they have.

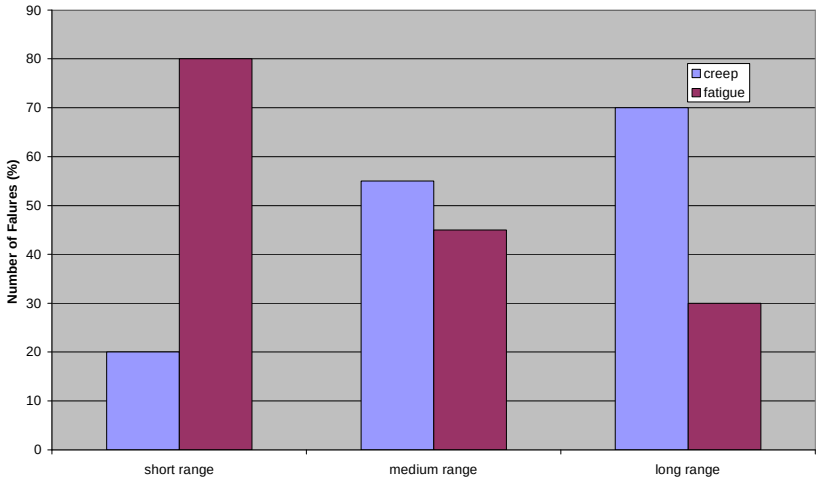

Figure 25 Creep and Low cycle fatigue life for different types of mission

The results show the presence of a predominant failure mechanism for both short and long range (the exact amount of hours has not been reported on the y axis, since this is just a relative comparison, not aiming at giving any real result but only the trends). In particular, short range missions are dominated by low cycle fatigue failure, due to the high amount of start-stop cycles the engine is subject; on the other hand, long range engines are affected mainly by creep failure, since the fraction of time spent at elevated temperature is significantly high, thus allowing creep to act intensively on the component.

For medium range aircrafts, the situation is more or less balanced, with the two failure mechanisms influencing the life time more or less in the same percentage.

3.3.1 STRESS ANALYSIS

First in the lifing model comes the stress analysis. Different approaches are available, as the code is user-friendly, and allows the user himself to choose among different levels of details through the use of selectors to be set appropriately in the input file.

Two different subroutines have been carried out: the first one estimates the stresses acting on the turbine's blades, while the second one analyses the disc.

3.3.1.1 Blade stress analysis module

The blade stress analysis module is based on the simple equations mentioned in paragraph 2.1.4.1, it has been created by the master student Oliviero Vigna Suria and the validation of the method can be found in his thesis (Suria 2006). It aims to estimate the maximum stress acting on the HP turbine blades. The code itself is in appendix F.7.

The flow chart in Figure 26 shows the module breakdown.

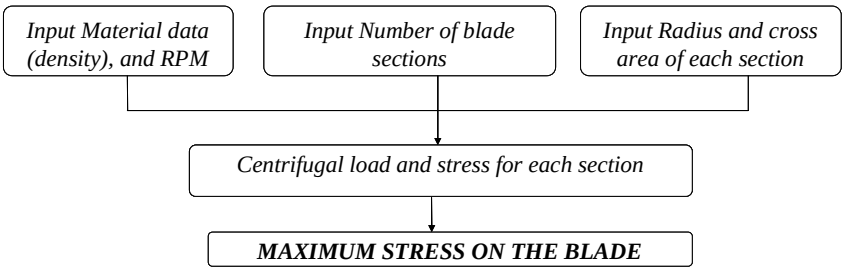

Figure 26 Blade stress module structure (Vigna Suria 2006)

Entering into a detailed description of the code itself, the subroutine is called from the main program, giving an input, namely the HP spool speed in RPM, and getting an output, that is the maximum stress acting on the blade.

An input file in the form of data sheet (blade_stress_input.dat) is required and showed in Appendix A; the following are the most important inputs:

- radius
- cross sectional area

By knowing all these data, and applying the stresses equations, the code estimates the centrifugal stresses acting on each section of the blade, and subsequently the maximum stress acting at the blade root.

3.3.1.2 Disc stress analysis module

The disc stress analysis module, which aims at calculating the maximum stress acting on the HP turbine disc, it has been created by the master student Oliviero Vigna Suria and the validation of the method can be found in his thesis (Suria 2006). The code itself is in appendix F.6.

The structure of the module is reported as a flow chart in Figure 27.

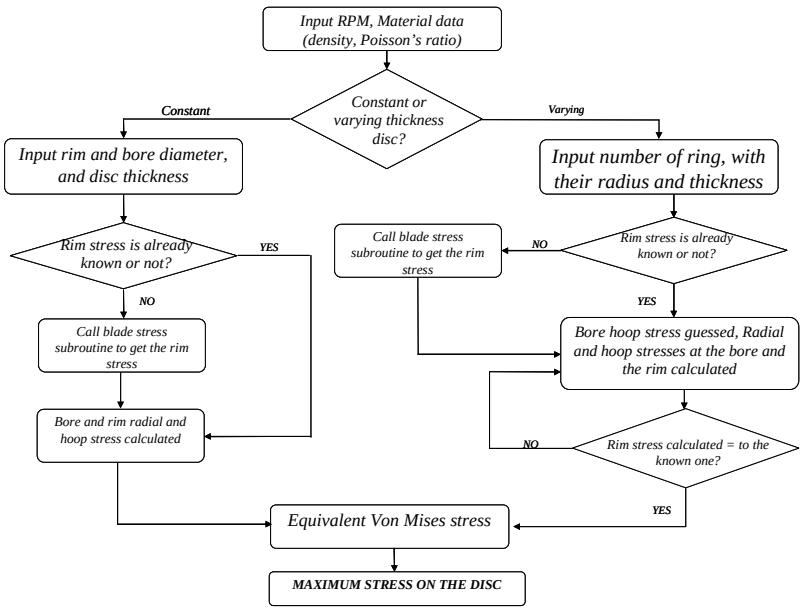

Figure 27 Disc stress module structure (Vigna Suria 2006)

As for the blade stress subroutine, also this one is called directly from the main program, giving the same input, namely the HP spool speed in RPM, and getting the maximum stress acting on the disc as output.

Again an input file in the form of data sheet (disc_input.dat) is required and showed in Appendix A, where the following details have to be specified by the user:

- a check to determine whether the disc is a constant or a varying thickness disc;
- Another check to define whether the rim stress due to the blades that the disc is carrying will be provided by the user or will have to be calculated.

In case of a constant thickness disc, the rim diameter, the bore diameter, and the thickness of disc have to be inserted as input, together with either the rim stress, if it is given as an input, or details regarding the blades (namely number of blades, blade mass and radius of the centre of gravity of the blades, given with respect to the blade root), if it has to be calculated.

If the disc has a variable thickness, the approach is different: the disc has to be split into several rings, each one being considered as a constant thickness ring.

The last step is to compare the estimated value of the rim stress, with the real one due to the presence of the blades the disc is carrying, and to proceed iteratively adjusting the bore hoop stress, until the calculated rim stress will be the same as the real one.

Again, after getting the right radial and hoop stress across the disc, they will be combined through the use of Von Mises equation in order to get the equivalent stress acting on each ring, thus being able to find the maximum stress acting on the disc.

3.3.2 Application of cooling within the code

Both creep and low cycle fatigue algorithm include a fairly simple blade cooling system. The process is based on a certain amount of air spilled from the last stages of the HP compressor, just before entering the combustor, and transferred to the HP turbine, where it will cool the blades.

In the structure of the fairly simple blade cooling sub-module can be appreciated. The module follows the equations and assumptions done in paragraph 2.1.4.2. The module has been tested and created by the master student Oliviero Vigna Suria and the validation of the method can be found in his thesis (Suria 2006). The code itself is in appendix F.5.

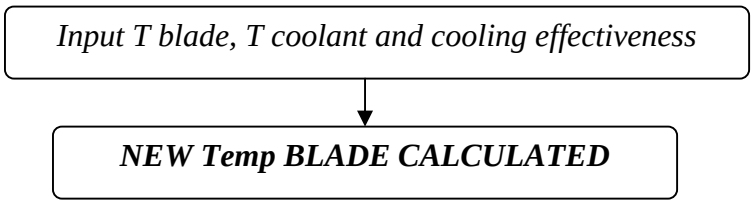

Figure 28 Blade cooling sub-module structure. (Vigna Suria 2006)

For simplicity of purposes, the model starts from a defined value of overall effectiveness that the user has to input, avoiding all the calculations involving all the other parameters mentioned in paragraph 2.1.4.2, since it is assumed that the engine designer will provide the exact amount of air needed to get such an effectiveness; moreover, the main point of the algorithm is to estimate the new temperature of the cooled blade, rather than focusing on the blade cooling system.

Hence, knowing the temperature of the coolant entering the blades (i.e. the temperature of the air leaving the HP compressor), the temperature of the gas surrounding the blades (TET) and the effectiveness being inputted by the user, very easily the code provides the new temperatures of the component. After that, the main algorithm (both the creep and the low cycle fatigue analysis) proceeds normally, as it will be explained in the next two chapters.

3.3.3 Low cycle fatigue module

As mentioned in the previous paragraph, although most engineering structures and components are designed such that the nominal loads remain elastic, thermal stresses due to high peaks of temperature (as it is for the HP turbine of an engine) often cause plastic strains to develop. Due to the constraint imposed by the elastically-stressed material surrounding the plastic zone, deformation is considered strain-controlled.

The module is able to predict the low cycle fatigue of an engine component, using the theory explained in paragraph 2.1.4.5, the Coffin–Manson rule, together with the Neuber method applied to cyclic loading, explained later in the paragraph.

It has been created by the master student Oliviero Vigna Suria and the validation of the method can be found in his thesis (Vigna Suria 2006). The code itself is in appendix F.4.

In particular, this method is a strain method, based on the capability of which the material component is made from to tolerate the start-stop cycle it is subject every time it is started and ready for the take-off, that is the most critical moment for the turbine, as it experiences the peak of TET.

The purpose is to determine the fatigue life of the component loaded with thermal stresses arising from the temperature difference due to the engines starting, namely the difference between the TET and the ambient temperature.

The breakdown of the low cycle fatigue module is reported in the Figure 29:

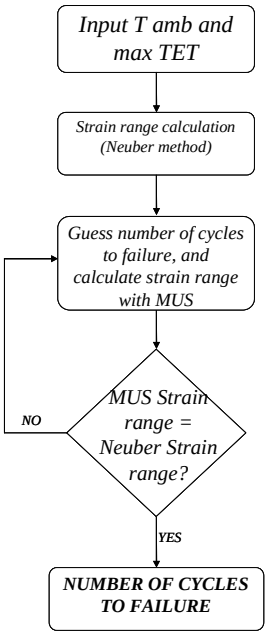

Figure 29 Low Cycle Fatigue module structure (Vigna Suria 2006)

Knowing the linear coefficient of thermal expansion of the material the component is made from, and assuming a perfect elastic behaviour of the material itself, the maximum thermal strain and the maximum associated stress can be estimated, the former simply by multiplying the ΔT by the linear coefficient of thermal expansion itself, the latter by multiplying the thermal strain by the elastic modulus of the material.

The Neuber Rule

In reality, when the yield stress of the material is overtaken, the component starts deforming plastically, following its stress-strain curve. The Neuber rule (derived for determining the strain distribution around a notch) allows determining the strain that occurs at the yield stress, by identifying a hyperbola on the *σ-ε* diagram, that is:

$$\sigma \times \varepsilon = const.$$

The product between the maximum thermal stress and strain just calculated will define the value of the Neuber constant, through which it is possible to proceed estimating the strain that actually occurs at the yield stress, simply by dividing the Neuber constant by the material yield stress.

When the unloading part of the cycle occurs, the stress range returns along the elastic straight line of the σ-ε diagram, unless the yield limit in compression is reached.

For the compressive phase, a new Neuber hyperbola has to be found, because there will be the same problem of the specimen behaving plastically rather than totally elastic. That means that the unloading phase, which started at the tensile yield stress, will last until the maximum thermal stress that loaded the component will completely be unloaded (i.e. until a stress equal to the difference between the yield stress and the maximum thermal stress will be reached).

Hence the maximum compressive strain can be calculated, by dividing the maximum compressive stress (just estimated as difference between the yield stress and the maximum thermal stress) by the elastic modulus of the material. By multiplying the maximum compressive stress and strain together, the new Neuber's constant is defined, thus being able to determine the compressive strain corresponding to the compressive yield stress.

Now that all the needed figures are known, it is possible to calculate the total strain range ε_T as difference between the tensile and the compressive strains, and to proceed with the final step, namely the estimate of the number of cycles to failure, by applying the MUS. The solution will be found iteratively, as the procedure is to guess the number of cycles, thus getting a value of total strain range that will be compared with the real one, calculated before through the Neuber rule: the iterations stop when the difference between the real and the estimated value of total strain stays within 1%.

As in the creep algorithm, even in the low cycle fatigue algorithm, the user has the possibility to choose among three different analyses:

- only the blade;
- only the disc;

- disc and blade together

3.3.4 Creep module

The creep algorithm is able to estimate the creep life of an engine component, applying the Larson-Miller parameter criterion, together with the Miner's cumulative creep law, as explained in the background theory in the previous pages.

It has been created by the master student Oliviero Vigna Suria and the validation of the method can be found in his thesis (Vigna Suria 2006). The code itself is in appendix F.5.

The flight envelope has to be split into several segments (e.g. climb, cruise and descent), each one characterized by a time length, and a well defined operating condition, that is a determined engine RPM, and TET. Knowing the turbine entry temperature, and the amount of time spent during each phase, the creep life can be estimated running the algorithm.

In Figure 30, the flow chart with the structure of the creep module is drawn.

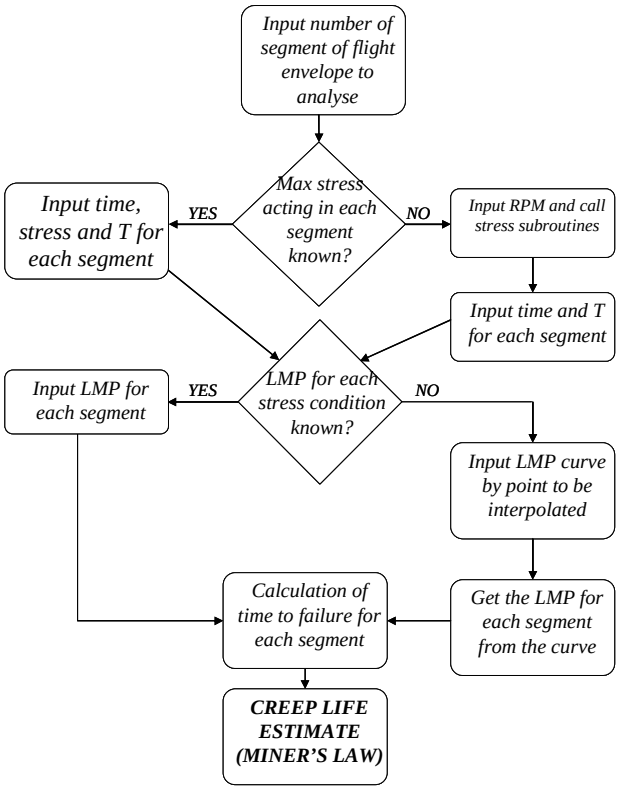

Figure 30 Creep module structure (Vigna Suria 2006)

In particular, as mentioned before, creep is a function of stress, temperature and time; hence the first step will be the estimate of the stress acting on the blade and the disc, thank to the two stress subroutines that need the RPM as unique input. A matrix is created, containing stress, temperature and time spent for each flight segment (time can be inputted as hours of flight or percentage of the whole flight cycle).

The creep algorithm also gives to the user the possibility of cooling the blade, thus lowering the TET and increasing significantly the life of the component.

Once the time-stress-temperature matrix has been generated, it is possible to proceed with the research of the appropriate Larson-Miller parameter for each phase: in doing so, two different ways are available, namely inserting either directly the parameters (if they are already known) or the Larson-Miller curve for the material the component is made from, the latter being a bit more complicated, since the user has to provide the curve in the form of several

known points (at least six, in order to be quite accurate), that the code will subsequently interpolate in order to find the corresponding value for each of the stresses acting during the flight envelope.

The code offers to the user the possibility to choose among the analysis and the estimate of the creep life for blades, disc or both of them together.

The last step is the calculation of creep life (either in hour of flight, or in cycles, depending on the user's will), through the use of Miner's cumulative creep law, after having estimated the times to failure of each segment.

In estimating the creep life of a component, take-off and approach phases are considered negligible, thus being not taken into account, as the amount of time spent for each of these two flight segment is definitely low if compared to the time length of each of the other phases. Moreover, it is difficult to simulate and achieve accurate data of the engine for these two sections.

For the other segments, several check points will be calculated, in each point a blade metal temperature and blade centrifugal stress will be estimated in line with the operating conditions taken from the engine simulation. For each point an operation time will be assigned and with the two previous variables, stress and temperature, by the use of the Larson Miller parameter the time to failure will be calculated.

4. Advanced Propulsion Systems

The work presented in this section has been conducted in the Universidad Politecnica de Madrid (UPM) under the supervision of Prof. Gregorio Corchero Diaz. The program used to analyze the advanced cycle has been created in UPM and is property of UPM University.

4.1 Candidate Cycles Description

Three cycles have received especial attention for their application to turbojets during last years. All of them are based on the application of some modifications to the standard Brayton cycle to get a higher efficiency by introducing new components. These cycles are:

a) intercooler-regenerative cycle (IRC)

b) The wave rotor topping cycle (WRTC)

c) The PDE (pulse detonation engine) and the CV (constant volume) cycle or Humphrey cycle, which really represents a first approximation to the PDE cycle (Heiser 2002).

This section will be devoted to the study of these three cycles, searching for a performance improvement when they are applied to a next generation turbofan engines as VITAL engines are expected to be. The work will be based on their possible benefits on SFC, ST, emissions, and noise level as well as on the technological level required. Next paragraphs present a brief description of each one.

IRC cycle:
In this cycle the intercooler (IC), a heat exchanger, cools the mass flow coming into the high pressure compressor (HPC) transferring energy from the core engine stream to the bypass stream at the exit of the outer fan, see Figure 31.

This saves energy in the compression process, improving also the bypass contribution to the engine specific thrust, but it will need additional fuel to get a given temperature at the exit of the combustor. This increase of fuel is compensated by an energy transfer from the exit of the LPT to the entrance of the combustor, the regenerative heat exchanger (RHE), while the mechanical energy available at the exit of the LPT decreases smoothly producing an increase of thermal efficiency. It is a typical application in sea and terrestrial power generation (Saravanamamutto 2001, Sawyer et al. 1972, Dellenback 2002, Beck 1996, Bhargava et al. 2004), and in other special applications (Martinez-Friaz et al. 2004, Barret 2005). Some works can be found on IRC application to aero engine, especially in international symposium and including the development of heat exchangers for aero engine applications (Missirlis et al. 2005, Yakinthos et al. 2006). Finally NEWAC (new aero engine core concept) is also a European project devoted to the development of these technologies (NEWAC 2006).

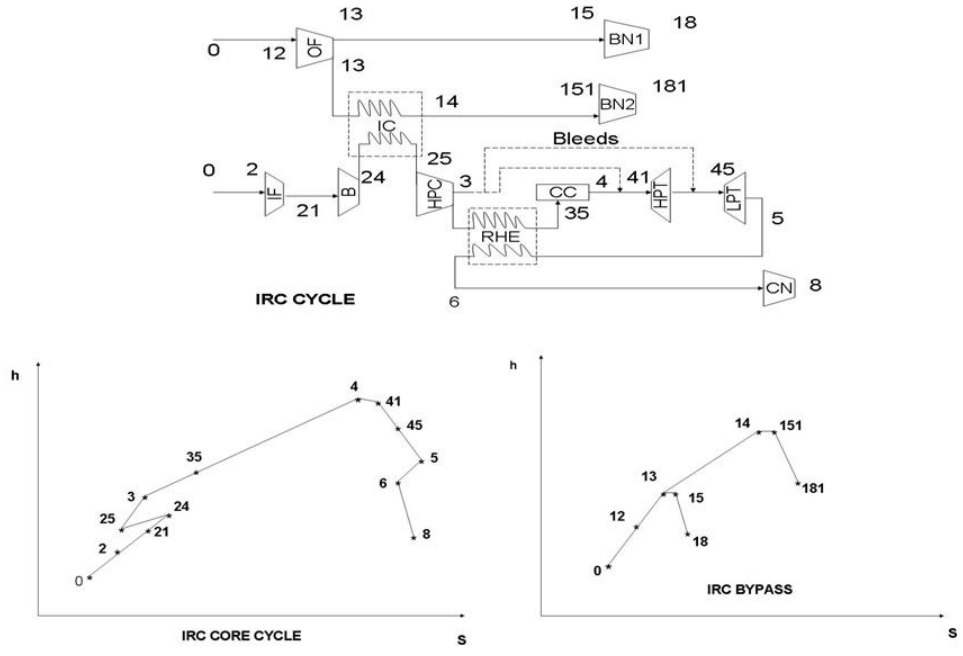

Figure 31 the Intercooled Recuperated Cycle

The WRTC:

Wave rotors are devices which use unsteady waves to compress and expand air in a single device. The wave rotor consists in a duct or multiple ducts, near parallel to the rotating axe, surrounded at the ends by a stationary casing; the casing end walls are penetrated by inlet and outlet ports that carry gas to and from the rotor passages or ducts. At any time sectors of the rotor flow annuli are exposed to the ported flow while the remaining sectors face the casing end walls (Paxson 1996, Welch 1997). At the inlet port, low-pressure gas in the rotor passage is exposed to the high pressure port flow; a compression wave compresses the passage gas and, thus, allows the incoming gas to enter the rotor. At the exhaust port, high pressure-passage gas is suddenly exposed to low-pressure exhaust port flow; an expansion wave propagates into the rotor passage, reduces the passage pressure, and discharges the passage gas into the exhaust port. The air, coming from the compressor, flows into the passage on the wave rotor where it is compressed by compression waves and shock waves, then it leaves the wave rotor passing to the combustor (CC). From combustor, the hot gas returns to the wave rotor and expands out to a lower pressure; passing trough the wave rotor, the gases are first compressed and then expanded. Thus a wave rotor combines in a single device the functions performed by a compressor and a turbine in a high spool, see Figure **32**. Also, since the wave rotor is washed alternatively by cool air from compressor and hot combustion gases it is self-cooled, and permits the increase of the upper cycle pressure and temperature improving thermal efficiency. NASA paid much attention to the wave rotor for aero engine applications in the nineties, including the design of demonstrators (Welch 1999). Also during last years much work has been devoted to wave rotor studies (Paxson 1996 & 1999, Welch 1997, Nagashima et al. 2007, Resler et al. 1994).

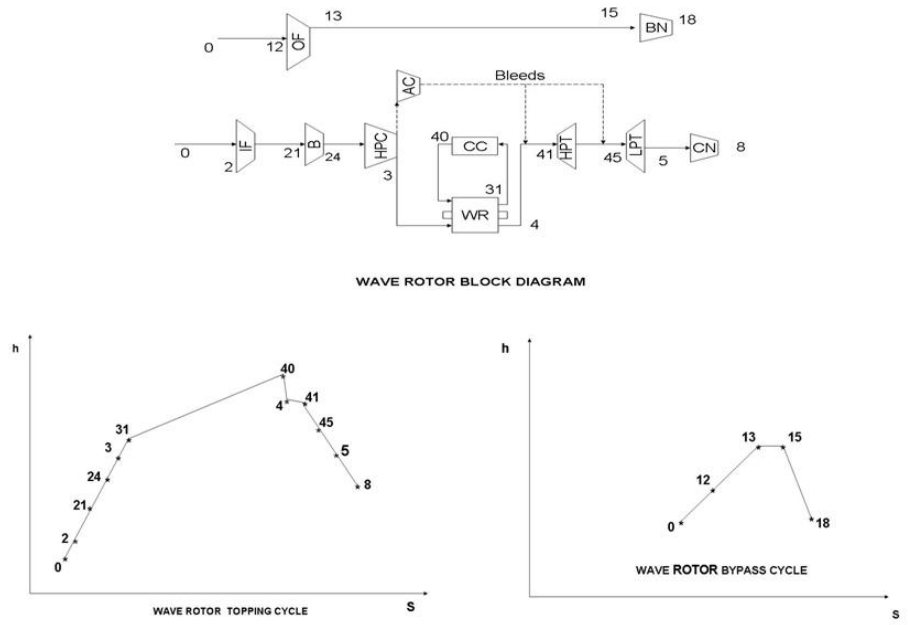

Figure 32 the Wave Rotor Cycle

The CV cycle:

The constant volume combustor cycle (CV) is also studied due to its simplicity and as an estimate of the PDE cycle. The CV cycle consists in replacing the standard combustor by a constant volume combustor (CVC); a small vessel or duct is fed with air coming from the compressor, see Figure **33**. Once it is closed the fuel is injected in the vessel and burned; then it is opened and gases are discharged to the turbine entry. This combustor will increase the cycle pressure saving energy in the compression process, and saving also some HPC stages for the same engine global overall pressure ratio. Heiser (2002), Cambier et al (1998) and Kentfield (2002) are devoted to interesting related topics.

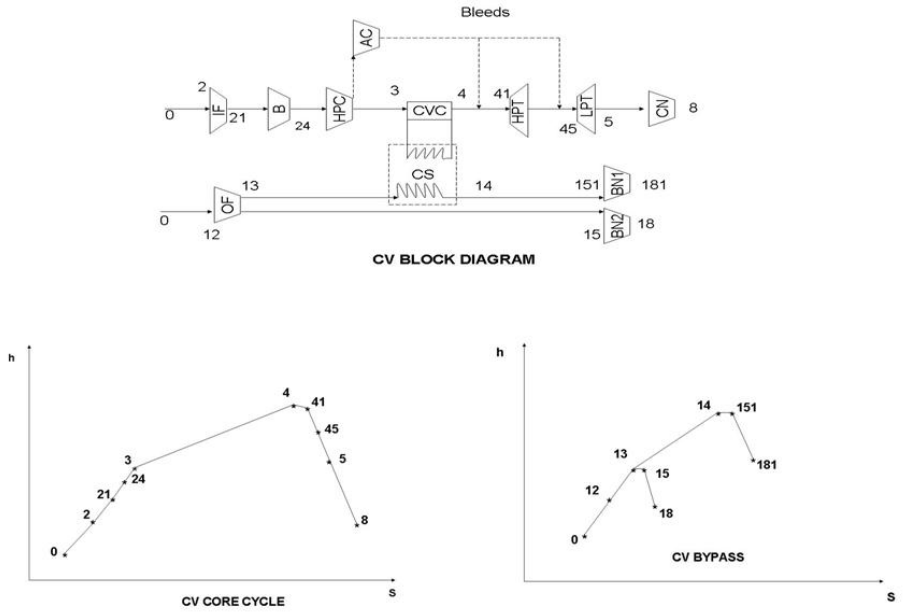

Figure 33 the Constant Volume Combustion Cycle

The emissions are important drivers in aero engines design and use. This section presents a part of the work carried out in the VITAL project; it consists in a parameter study on the application of three innovative thermodynamic cycles to aircraft propulsion looking for benefits on fuel consumption, carbon dioxide, nitrogen oxides, and noise. These cycles are the intercooler-regenerative, the wave rotor topping, and the constant volume combustor cycles. The work, starting from a next generation ultra high bypass ratio turbofan, the baseline, and considering two possible design conditions, presents the influence of the application of these new cycles or design changes to the baseline on the emissions and the required technological level, represented by turbine entry temperature (TET). The baseline is a representative ultra high bypass ratio turbofan in the VITAL project. The results show that some significant benefits on emissions can be achieved although they are linked to significant technology improvements and in-depth studies of the new components, involved in the cycle implementation.

4.2 Performance model

The study uses has baseline engine the long range GTF (gear turbofan) engine, it has been done at the design point of Top of Climb ISA+10, 10668 m. and M_0=0.82 and at the off design point of Cruise (10668 m. and M_0=0.82); hereafter this engine will be referred as baseline engine, and its values at the respective flight conditions will represent the reference values in this work. Similar qualitative and quantitative results are obtained when the study is applied to other VITAL engines as short range engines, for example to the short range GTF engine. In the parameter study, it is assumed that bypass data (bypass ratio, outer fan pressure ratio, outer fan efficiency and mass flow), booster data (pressure ratio and efficiency), and inner fan data (inner fan pressure ratio and inner fan efficiency) are constant as in the baseline; they will represent the VITAL optimized LPT spool. Additionally, the bled air for turbine cooling are also assumed constant, justified by the constraint that the expected VITAL technology limit is assumed; this limit is represented by TET value (the Turbine Entry Temperature to the high pressure turbine). All changes to the baseline engine, searching for an engine efficiency improvement, are applied to core stream between the exit of the booster or intermediate pressure compressor (IPT) and the entrance of the core exit nozzle with some interaction with bypass stream at the exit of the outer fan.

These cases are:

a) The IRC where the intercooler intercepts the core and bypass streams and

b) The CV where the bypass stream is used to cool the CV combustor;

The thermodynamic model for standard turbofans is well known and its description can be found at any text book or conceptual paper (Hill et al 1965, Mattingly et al. 2002 and Walsh 1998). We are dealing with real engines and consequently we will work with enthalpy and entropy considering that transport coefficients change with temperature, and that also composition and air mass flow are changing along the engine. The influence of fuel air ratio, *far*, constant

pressure specific heat, *Cp*, and specific heat ratio, γ, variations with temperature are considered. The methodology applied to manage and study these differences will be presented in next paragraphs.

The IRC

There are two important differences: the intercooler heat exchanger and the regenerative heat exchanger.

- The intercooler (IC) cools the whole core mass flow but only heats up a part of the bypass mass flow, w_{cool}, where w_{cool} represents the ratio between the total bypass mass flow and the bypass heated mass. A simple model has been applied to study the heat transfer process. The model assumes that both streams run in parallel until they reach the same temperature; this is equivalent to a mixing of two streams with no heat addition and with the same composition; equivalent heat transfer could be got with a reasonable heat exchanger size by using a cross or counter flow heat exchanger. This condition, joint to the stagnation pressure losses at both heat exchanger sides, defines the exit conditions of both streams. Then the bypass heated stream and the main bypass stream expand out to ambient conditions in two separate convergent nozzles, assuming the same stagnation pressure losses in both nozzles.

- The regenerative heat exchanger (RHE) is responsible for the energy transfer from the LPT exit to combustor entry. It is defined by the stagnation pressure losses on both streams, cool and hot, and the regenerative thermal ratio or recuperative efficiency η_R given by the expression

$$\eta_R = \frac{T_{35} - T_3}{T_5 - T_3}$$

The WRTC

The wave rotor topping cycle represents the easiest case from a simulation point of view. The wave rotor accomplishes the functions of a standard high spool, and as such a high spool is usually simulated. Then it will be considered

as a standard high pressure spool integrated by a compressor, a standard combustor, and a turbine (Wilson 1993).

The CV

In this case the standard combustor and the HPC or some stages of the HPC are replaced by a constant volume combustor. The constant volume combustor is modeled as a vessel which is filled with air, and once it is closed, some amount of fuel is added and burned. The condition of constant volume leads to the expression

$$\frac{P_4}{R_4 T_4} = \frac{P_3 k_3 k_4}{R_3 T_3}\left(1 + far_c\right)$$

This expression links the combustor entry conditions with exit conditions and the fuel air ratio in the combustor, far_c, the pressure at the exit of HPC, P_3, the pressure at the exit of the combustor, P_4, and the gas constant at the respective sections. The constant k_3 and k_4 represent a measure of the pressure losses originated by the closing and opening combustor system respectively.

Therefore, the energy equation applied to the combustor leads to the following expression which also links entry and exit combustor conditions, and where k_{cool} represents the ratio between the energy transferred to bypass by the CV combustor cooling process and the energy which can be obtained from the burned fuel, *c*FHV*, where *c* is the rate of the burned fuel mass and *FHV* is its lower fuel heating value. K_{cool}=0.10 represents that 10% of the energy coming from the burned fuel is transferred to the bypass in the cooling process.

$$h_4 = \frac{\left\{h_3 + far_c \cdot \left[FHV \cdot \left(1 - k_{cool}\right) + C_{pf} \cdot \left(T_f - 298.3\right)\right]\right\}}{1 + far_c}$$

In the above expression h_4 and h_3 represent the stagnation enthalpies per unit of mass flow rate at the exit of the compressor and combustor, respectively, and C_{pf} is the constant pressure specific heat of the fuel while T_f *is* its temperature at injection conditions and 298.3 K the standard temperature at which *FHV* is

measured. Once the entry conditions, the pressure losses, far_c, the lower fuel heating value, and the transferred energy to the bypass are given the expressions above and below provide the combustor exit conditions.

The bypass stream, coming from the exit of the outer fan is used to cool the CV combustor. Once it has cooled the combustor it is expanded out to ambient conditions in a separate convergent nozzle, as in the intercooler model. The enthalpy at the exit of the cooling process, according with the consideration made in the last paragraph, is given by

$$h_{14} = h_{13} + k_{cool} \cdot far_c \cdot FHV \cdot w_3 / w_{14}$$

Where w_3 is the mass which goes through the CV combustor and w_{14} is mass flow of the bypass stream, $w_{14} = w_{cool} * w_{12}$ which is used to cool the combustor.

The influence of the mass flow w_{14} in engine performance is considered; h_{14} and h_{13} represent the stagnation enthalpies per unit of mass flow at the respective engine sections.

Additional considerations must be made on cooling bleeds for each case; it must be kept in mind that only the nozzle guide vanes and the rotor of the HPT turbine will require cooling air. These cooling airs are assumed constant as in the baseline and as it was stated before, but they need some additional comments:

• *The IRC*.
There are three possibilities:

1) Both bleeds are taken from the exit of HPC or the entry of the regenerative heat exchanger,

2) Both bleeds are taken from the exit of the regenerative heat exchanger, before the combustor entry, and

3) A third possibility will be considered in which one bleed is taken from the entry of the heat exchanger, the cooling air for the NGV (nozzle guide vanes) of the HPT and the other one from the exit of the heat exchanger. For the third case only some comments will be presented.

• *The CV and WRTC*.

In both cases, the pressure at exit of the HPC compressor usually is lower than the pressure at the entry of the HPT turbine. An APC (accessory pressure compressor) will be use to increase the cooling air pressure, from the pressure at the bleed section to the value at the entry of the HPT.

• *Mixing process*.

The NGV cooling air is mixed with the main stream at exit of the NGV while the HPT rotor cooling air is mixed at exit of the rotor. In both cases, the mixing is made at constant pressure, the stagnation pressure of the main stream, and assuming that not heat either work are extracted or added in the mixing process.

Some considerations also must be made on emissions. First of all, the SFC is a measure of the CO_2 production and the study on SFC can be translated to CO_2 emissions. Estimation of nitrogen oxides, NOx, and noise level is a complex task, requiring the knowledge of the components geometry which is not known, especially in the case of non-standard combustor; Lefebvre (1998) presents a good summary on emissions. For NOx emissions the correlation from Lewis (1991), which uses the pressure *P3* in the combustor and the combustion temperature T_4, is used, the equation is shown below; it also offers qualitatively the same results as Wulff (1999):

$$NO_x = 1.05 \cdot 10^{-6} P_3^{0.5} e^{0.008 T_4} \quad ppmv$$

According to Lefebvre, Lewis and Wulff, it offers a good agreement with experimental data and conceptually it could be applied to any combustor; it

must be kept in mind that pressure and temperature, given a far_c value, is a measure of equilibrium composition. P_3 is expressed in atmospheres and T_4 in Kelvin degrees. For the CV cycle the pressure at the end of combustion process is considered.

5. Results and Discussions

5.1 The Economic Module

The input file for the economic module can be found in the annex A. Below the essential values needed in order to understand the basic assumptions of the calculation of the DOC are repeated.

```
0.1                          : INTEREST PERCENTAGE (IP)
```

The interest paid from the airline on the total capital invested on the engine has been put to 10%.

```
0.02                         : INFLATION (INF)
```

Inflation has been considered on an average of 2%. Inflation influences most of the economic parameters, changing them during the working life of the engine, 30 years in the simulations done.

```
0.8222                :exchange rate $ -> € (ROC)
```

The exchange rate between dollar and euro is very volatile and impossible to predict, but because the fuel price is in dollars and all the results are in Euros there is the need to fix an exchange rate. The one used in the programming is of the year 2006, but it can be changed by the user according of the value of current year.

```
172                          FUEL PRICE (FP) [cents of U$/US gallons)
```

Also the fuel price is a parameter near impossible to predict although in the program an attempt of changing it with fuel price (see Figure 38), still the initial value has to been fixed by the user. Again the value used in the calculation is the one of year 2006.

```
70                            MAINTENANCE labour Rate per Man Hour (RLENG) (€/Hr)
```

The cost of maintenance labour is a more stable parameter than the previous one. It increases roughly every decade, because of the inflation, the value used

is the one valid for this decade and for the future life of the engine it is changed by inflation in the program showing quite realistic trends.

```
10                          : DOWNTIME
```

The time needed to repair or check the engine for any faults is usually predetermined and in usually between one and two week, it depends how big the overhaul is, then an average period of ten days has been considered quite reasonable.

```
82533.090000                : WEIGHT OF FUEL USED,AcBlockFuel (Kg)
27000                       : Threshold for the Carbon Tax (Kg)
5                           : Carbon Tax Charge (€/kg)
```

The carbon tax uses a threshold system. When the weight of fuel used is higher than the threshold then the tax is equal to the difference between the threshold and the fuel burn multiplied by the charge. We can see this tax in influenced by two parameters that can vary a lot as the impact of the tax on DOC. Different levels of the threshold and of the charge can make the tax one of most important factors in the operation costs or one of the least.

```
89.9                        : NOISE TAX Limit (dB)
50                          : Unit of cost of Decibel (€/dB)
```

The same reasoning applies to the noise tax.

```
5.                          : NOX TAX CHARGE (€/kg)
1.5                         : NOX FACTOR (B)
```

The NOx tax is instead always paid, but because the tax in not yet implemented in any known tax policy a factor has been added in order to increase its importance considering that the engine life spans for the next 30 years and for sure in the future the importance of this tax will be great. Again then the importance of this tax on the costs is quite relative.

In Figure 34 the risk module uses Gaussian distribution, as shown in appendix F, in order to create an example of the cumulative curve for the net present cost of one engine with an interest percentage on total investment of 10% fixed for all the scenarios, this is useful to understand which are the most probable cost of the engines and the aircraft. The figure show the risk associated with each of

the NPC values. The value over each histogram represents the occurrence in percentage of that particular value of NPC. This value is the risk connected to that particular NPC. This value gives the impact of design decisions on operating cost in uncertain scenarios.

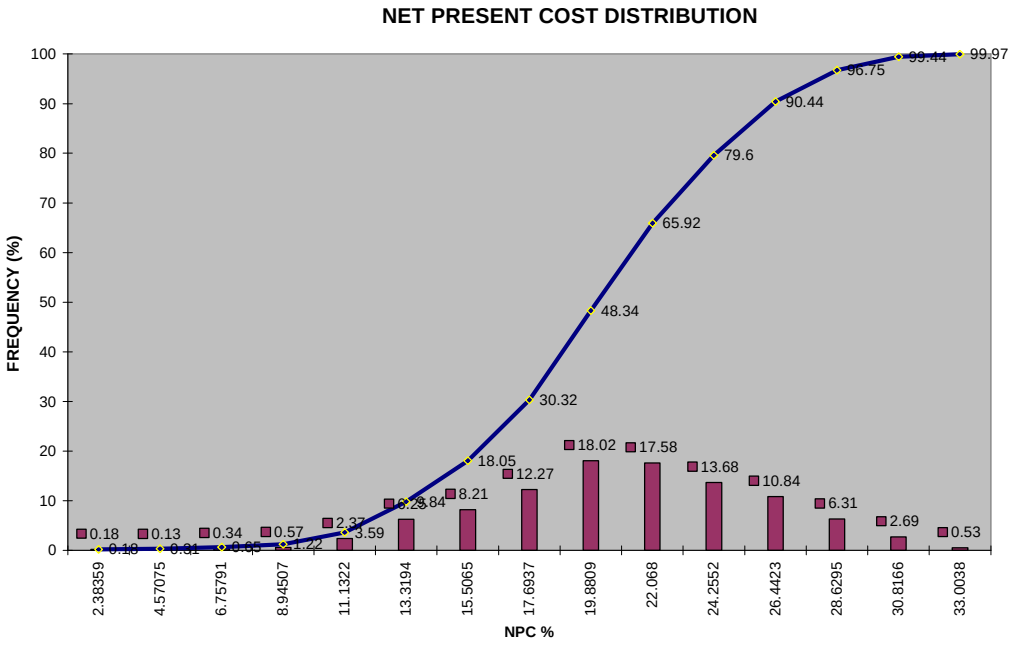

Figure 34 Cumulative curve for the net present cost (NPC)

Figure 35 shows how the costs of maintenance, calculated by the economic module with the equations in appendix F, are divided between labour cost and materials cost, which enables us to identify the factors that can influence the cost of maintenance and which need to be minimized to reduce the cost of overhaul.

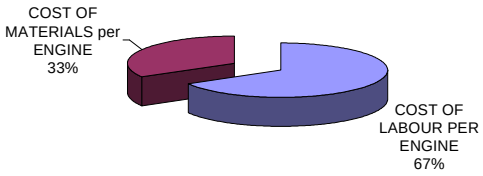

Figure 35 Costs of maintenance division between labour cost and materials cost

Figure 36 and Figure **37** shows the results obtained when the economic module and the method proposed by Roskam (1990) are used to estimate the cost of maintenance for short and long range engines currently in use. This has been compared with data available from the public literature; the comparison is used to validate the method used to calculate the costs. The Roskam method was created using data from the 70s and for the design of a short range airplane. Hence the comparison of the Roskam method with today data shows an overestimation of the values for short range engines and even a greater overestimation of the long range ones. The economic model has adapted the factors of the Roskam method to today values using data that can be found in public literature, but because of the wide scattering of data available the economic module can only follow the general trend of the values, therefore there a 15% difference between the model and the public data.

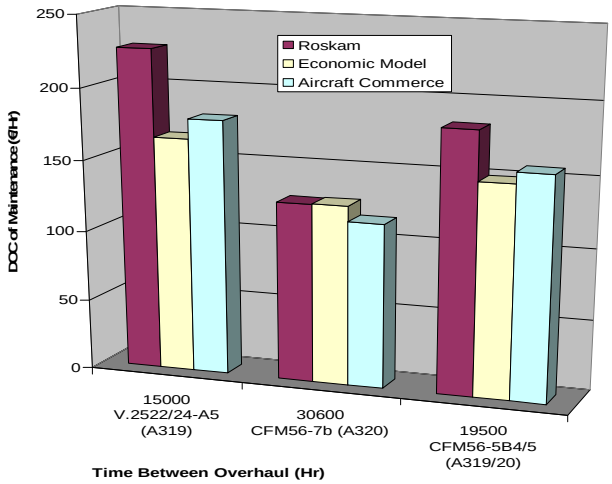

Figure 36 Cost of maintenance for short range engines currently in use

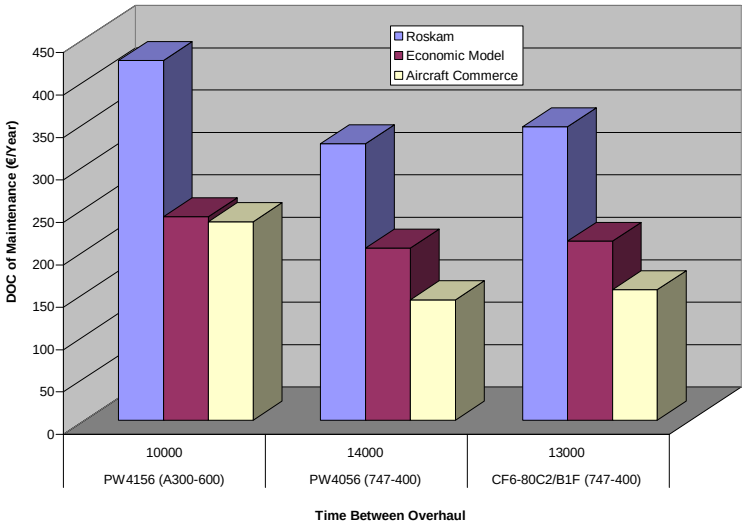

Figure 37 Cost of maintenance for long range engines currently in use

In Figure **38** we can see how the risk module changes the fuel price with inflation over a period of 30 years; this method of change tries to simulate the volatility of the fuel price as shown in the petroleum report (2006).

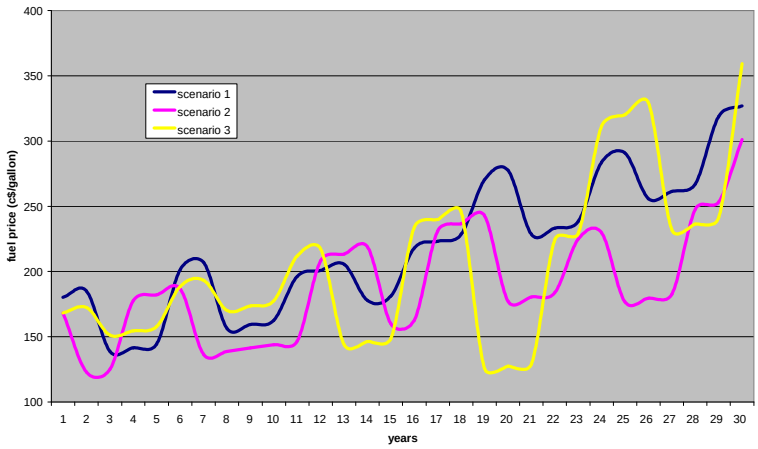

Figure 38 Change of the fuel price with inflation over a period of 30 years

Keeping in mind the aforementioned assumptions, using the risk module, a sensitivity analysis has been done in order to understand the impact of the different parameters on the operating costs; the results are shown in the next four figures. As we can see they show that fuel price and carbon tax are the factors that more will influence the operating costs of aero engines. The fuel

price is the third most influencing factor, but if the costs of fuel will increase more with the same pace as the last four years, it's influence could be even greater.

In order to take into account the impact of on DOC of the different economic parameters a study has been done rising the importance of some these parameters. The results are shown in **Figure 39**. As we can see in future legislation noise tax would become one of the main drivers in the engine design.

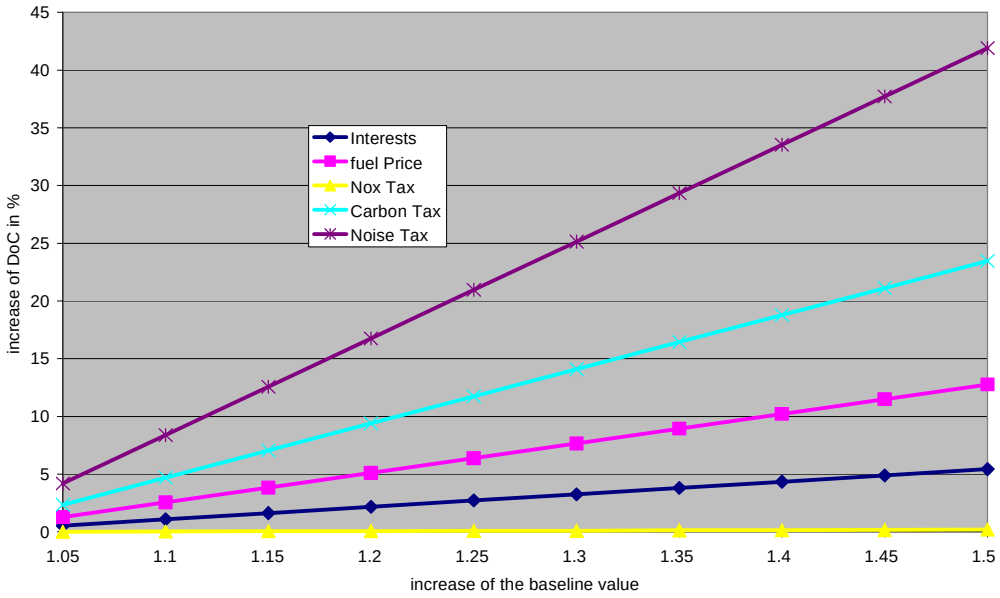

Figure 39: impact on DOC with the change of values of the economic inputs

Considering today legislation and common core technology for the different VITAL engines, we can see from **Figure 40** that the bigger drivers in the engines NPC are fuel burn and carbon tax, instead NOx and noise have quite low impact. But we need to keep in mind that for sure the legislation will soon change. What we can see in **Figure 40** is the impact of the different risk parameters on the NPC of the three VITAL engines. The NPC on the y axis is relative to the nominal NPC for the performance values specified by the OEM for each engine. As we can see for all the engines the fuel price and the carbon tax are very important drivers and their impact is high. The noise and NOx taxes are calculated according to today legislature, as the future engines production of noise and gaseous emissions are well below today thresholds for the taxes

then for these parameters the calculated NPC doesn't diverge much from the optimal value.

The TBO impact is high on the engines that have higher TETs, therefore lower life, because the lower is the TBO the higher are the costs of maintenance and hence the DOC and NPC.

The lower value of the NPC of the labour costs in respect to the nominal value depends from the fact that, keeping constant all the other parameters, in the future this cost is expected to decrease thanks to cheap workforce that can be found in third and second world countries. For example in Europe many airlines are operating nowadays a policy of relocation of their maintenance sites to eastern Europe, where it is possible to find talented workforce at lower costs than in the western part.

In **Figure 35** can be seen the division of maintenance costs, valid for today engines. But this division will change, firstly because of the decrease of labour cost and secondly to the future material costs are expected to increase a lot with the rising prices of the raw materials, e.g. Titanium, Nickel and so on. If the increase of the costs of material would be higher than the lowering of the labour cost then the maintenance cost could be expected to rise in the future as we can see in Figure 41.

Because the great impact of TBO on the GTF, this engine is the one that will need more overhaul, than it will be this engine that will benefit more from the decrease of impact of the labour costs, but it would also have a great disadvantage from the rising of the cost of materials as we have seen from the TBO's NPC histogram.

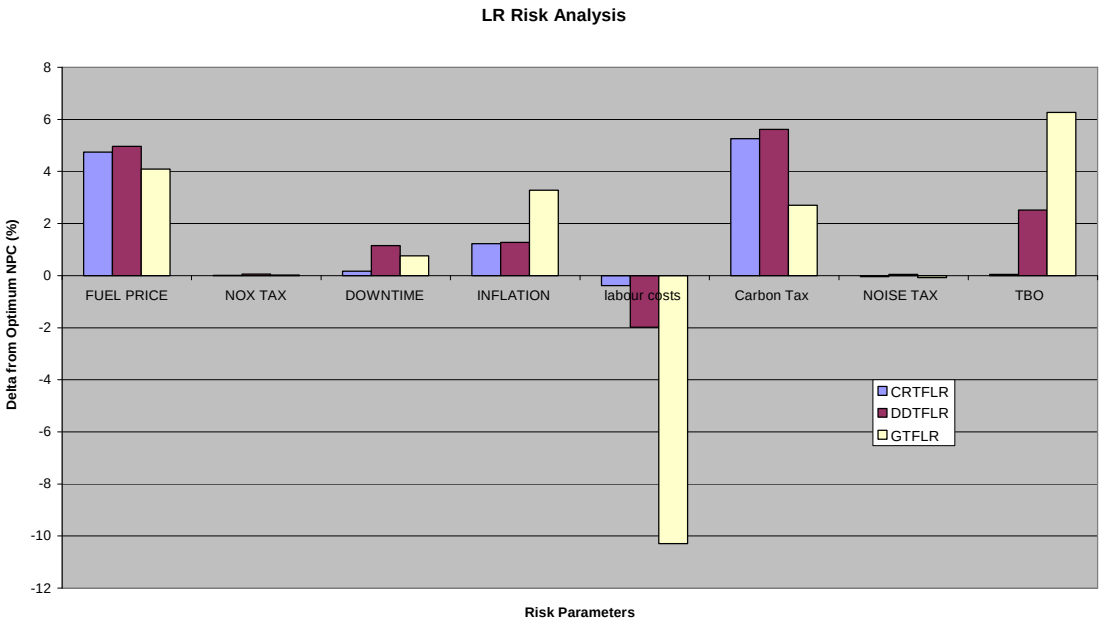

Figure 40 influence of economic parameters according to the risk analysis for long range engines

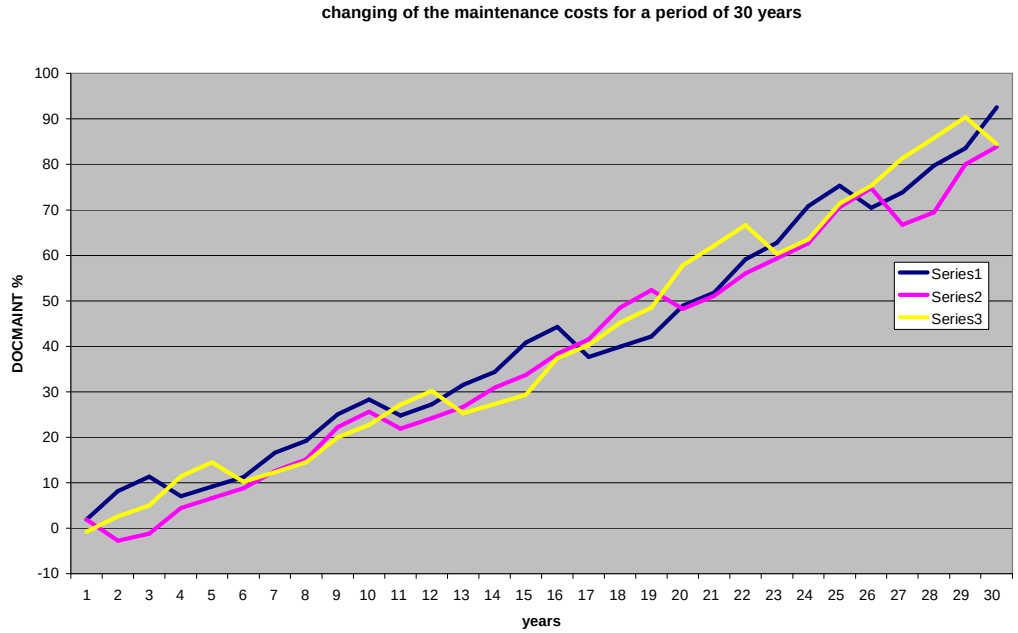

Figure 41 growing of the maintenance cost in the next 30 years.

5.2 Results of the Weibull Module

5.2.1 Engine Components description.

The five components that are continuously under surveillance during the life of the engine are:

- High Pressure Turbine: This is the rotating part of the engine that has to sustain the highest combination of stresses (centrifugal stresses from the high rotational speeds), temperatures (from the hot flow that comes from the combustor) and pressures. Because of the extreme working environment this part of the engine usually is the one that limits more the life of the engines.

- High Pressure Compressor: This rotating part of the engines is one of the most important, because it has to create the biggest jump in pressure in the engine. Nowadays the pressure load that the HPC has to sustain is very big and for today engines, and surely future ones, this part of the engine is one of the most lives limiting.

- Life Limited Parts: means any part for which a mandatory replacement limit is specified in the type design, the Instructions for Continued Airworthiness, or the maintenance manual. In long haul, engines account for a smaller portion of total engine reserves than they do in short haul engines. This is because LLPs have lives fixed in engine flight cycles (EFC), and can last for more than 30 years due to the low number of flight cycles (FC) aircraft accumulated each year. LLPs account for a varying portion of total engine maintenance costs, and also influence the maintenance management of engines. The majority of engines powering wide bodies are used on medium- and long-haul missions, although some are still used on short-haul operations. LLPs always account for a high proportion of total engine maintenance costs on short haul

operations because of short average cycle times and the high rate of accumulation of FC.

- Combustor: This is the non rotating part of the engine that has to sustain the highest temperatures and pressure, but because it has no rotating parts the stresses are generally low so the life of this component is quite long.

- General: under this name we consider every other possible cause of breakdown of the engine like for example: hitting of external object of the fan, break of the fuel system, leakages of oil and etc.

5.2.2 Engines Description and outcome of the analysis

The risk analysis has been applied to four different engines of different thrust, respectively of: 90 kN, 120 kN, 250 kN and 330 kN. The engines taken into consideration are very general in their characteristics and they are meant to represent all the engines used nowadays for short, medium and long hauls. This is done to show that the model used can be applied to every type of engines and as well can be used to do a probabilistic analysis of future engines.

The short range engines analyzed are (Aircraft Commerce):

- CFM56-7B20: The CFM56-7B series is the most numerous of all CFM56 engines, and its only application is the 737NG, on which it has a monopoly. More than 2400 737NGs have been ordered, of which more than 1600 are operational. The number of CFM56-7Bs installed would therefore have increased to about 7400 by this stage, making it the most numerous engines in operation. The importance of the engine's maintenance costs is therefore clear. This engine powers the 600 and 700 versions of the 737NG and has a thrust of 90 kN.

- CFM56-7B27: This is the largest variant of the CFM-7B and it powers the 800 and 900 version of the 737NG and it's rated with a thrust of 120 kN.

The 737NG has a longer range capability than earlier 737 models, so the NG series is used on longer average route lengths by airlines. While a few airlines use the 737NG on average flight cycle (FC) times of less than one flight hour (FH), the average FC time for the -700 and -800 fleets is 1.8 FH and 2.1 FH respectively. The -900 is also used on similar styles of operation, while the smallest -600 has a shorter average FC time of about 1.2-1.3 FH. The -700, -800 and -900 fleets are all generating 8-9FH per day, equal to about 3000 FH and 1600-1700 FC per year (Aircraft Commerce).

All variants of the CFM56-7B have the same turbo machinery and components, with three low pressure compressor (LPC) booster stages, nine high pressure compressor (HPC) stages, a single high pressure turbine (HPT) stage and a four stage low pressure turbine (LPT). The fan is 154.94 centimetres in diameter. This allows the lowest rated -7B18 engine to achieve a bypass ratio of 5.5:1, while the highest thrust rated -7B27 has a bypass ratio of 5.1:1 (Aircraft Commerce).

The long range engines analyzed are (Aircraft Commerce):

- CF6-80C2: The variety of operations on which the CF6-80C2 is used means it has average FC times of 1.0-9.0FH. It has a thrust rating of around 250 kN. Engines operated on average FC times of 1.0-3.0 FH have intervals of 2,500-3,500 FC, the longest intervals being achieved by the lowest thrust rated engines operating on the shortest cycle times. Engines used on medium-haul operations, on aircraft such as the 767 and A310 or A300-600 with average FC times of 4.0 FH, have removal intervals of about 2,200 FC. Engines in long-haul operations with cycle times averaging 6.0-9.0 FH have intervals of 1,500-1,800 FC.

- PW4000-112: This engine has a diameter of 284.48 centimetres and it is rated between 330-350 kN thrust, and powers the 777-200 and -300

series. Aircrafts powered by this engine are used for short-haul operations with cycle times of 1.0-1.5 FH by Japanese carriers and on high density US domestic and long-haul operations with cycle times averaging between 3.0 and 7.0 FH. Annual utilisations will be in the region of 1,700-2,200 FC for short-haul operations, 1,000-1,200 FC for medium haul operations and 650 FC for long haul services.

The lifing module estimates the life of the high pressure turbine blades through the analysis of creep and fatigue over a full working cycle of the engine. These two phenomena are the most limiting factors to the life of the engine. The output of this module is the amount of hours that the engine can sustain before its first overhaul (called time between overhaul (TBO)).

The value of TBO calculated by the lifing is then multiplied to the values of α. These are used in the distributions by the Weibull module. The module calculates a value of possible TBO for each distribution and then the lowest of the values is taken as the TBO that will be used into the economic module calculations.

In Figure 15 we saw the cumulative distribution functions for the four different engines. On the x axis we can see the NPC in thousands of Euros calculated for a period of 30 years, generally considered the life in service of an engine, for 10000 scenarios. On the y axis we can see the Probability Distribution Function $F_X(x)$. As expected the engine with lowest thrust suffers lower breakdowns of the engines with higher thrust and this means that all the modules are least subjected to stresses than an engine with higher thrust.

In Figure **42** we can see the cumulative density function $f_X(x)$ for the four different engines. On the x axis we have again the NPC and on the y axis we can see the number of scenarios. The y axis is in logarithmic scale to better visualize the large difference scale of the numbers. As we can see for all engines the shape of the histograms reflects the shape of the density function of the Weibull distribution. Between the engines there are some differences, as

shown also in Figure 15; the engine with lower thrust could go out of service with a lower NPC in more scenarios then the engines with higher thrust.

Figure 43 we can see in Pareto diagram what causes the breakdown in the four engines. The Pareto diagram was calculated for 10000 scenarios. For all these scenarios it was calculated how many times the engine breakdown for a particular reason (HPT, HPC, LLP, Burner and General), the values on the y axis are in percentage considering 100% as all the 10000 scenarios; so for example the value 20% for the HPC means that in 20% of the 10000 scenarios the cause of breakdown was the HPC. Because the shapes of the density function are the same for all the engines the results for each engine are mostly the same. The first cause of failure in an engine is general and could be an external object hitting the engine or an error in the control system. General reasons for failure could be many and are often very difficult to predict, what instead is very interesting to notice is which part of the engine that the designer can control causes more breakdowns. The HPT and the HPC are the two components that are more likely to break and end prematurely the on-wing life of the engine. This figure shows us how the Weibull distribution applied to an analysis of creep and fatigue can help the designer to do a more accurate risk assessment of the maintenance and operational costs of aero engines.

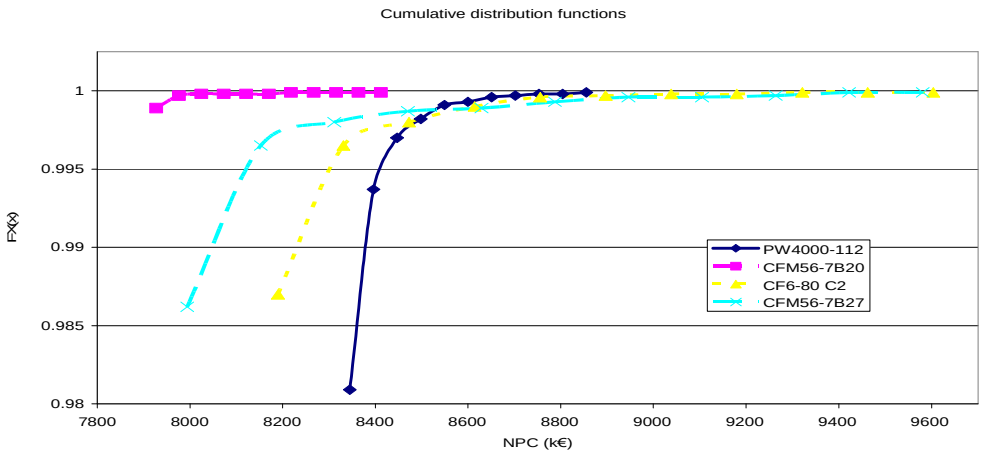

Figure 15 NPC and Cumulative distributions for the four engines

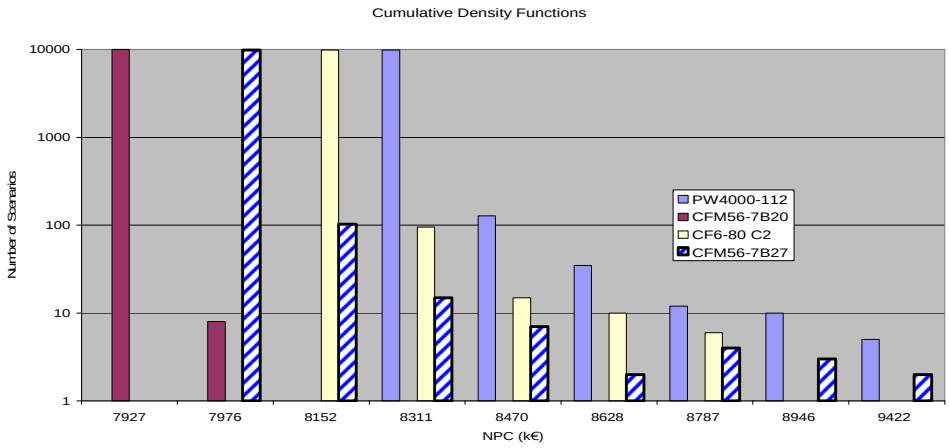

Figure 42 NPC and Frequency for the four engines.

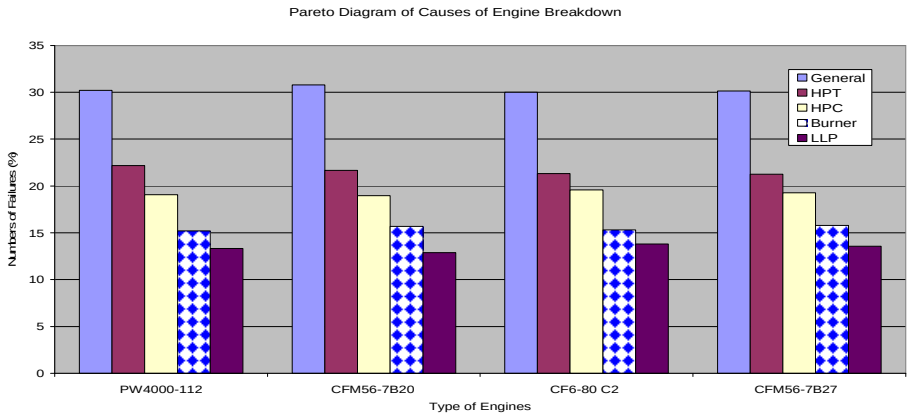

Figure 43 Causes of engine breakdown (Pareto Diagram)

5.3 Operating Cost and Risk Analysis for Aero Engines

Here are presented the results of the Economic model for the three VITAL engines in comparison with the baseline engines. The values showed in input are only preliminary results and differ considerably from today actual value of the project, but they still give an idea of the general trends of the engines' costs.

5.3.1 Baseline and Future Engines description

The baseline engines for the long range haul are a three spool engine and for the short range haul are a two spool engine; the main performance parameters of these engines are shown in table 4.

Parameter	Long range	Short range
BPR	5	5
OPR	35	28
FN* (kN)	316	121
Mass Flow (kg/s)	919	459

* At SLS condition

Table 4: Main cycle parameters* for baseline engines

The direct drive turbofan (DDTF), Figure 44, concept maintains the current fan layout. The innovation here is in reducing the number of blades (with each blade having to support a higher aerodynamic load), and increasing their size, thus the overall fan diameter. These new fans will provide a very high bypass ratio (from 10 to 12:1), at a lower speed of rotation. Tests are also slated to check out new, lighter materials.

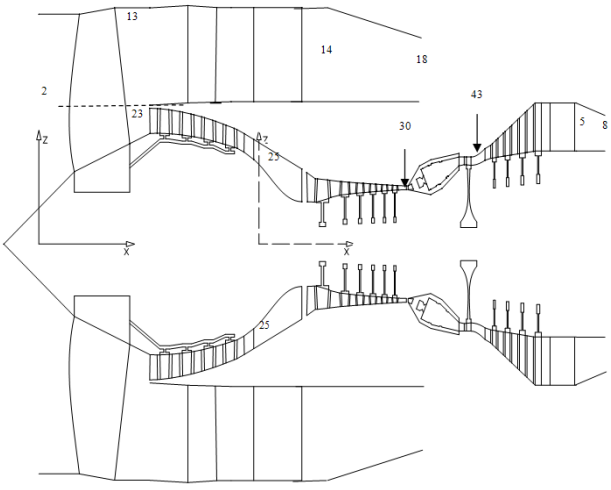

Figure 44 Schematic of the DDTF

As its name implies, the geared turbofan (GTF) concept introduces a gear train into the equation. A setup of this type will offer an ultra-high bypass ratio (UHBR), in the neighbourhood of 12:1.

The counter-rotating turbofan (CRTF) concept is particularly innovative, see Figure 45. This layout simply means that there are two independent shafts, rotating in opposite directions. At the other end of the low-pressure section, they are joined to a low-pressure turbine with several stages of counter-rotating blades. For a given aerodynamic load, this configuration will reduce the fan rotating speed by 30 percent or more. Since this fan concept can be applied over a wide range of bypass ratios, its benefits can be combined with those generated by higher bypass ratios (around 10). The advantage of this technology is that it offers the same performance as a conventional fan, but with slower tip speeds.

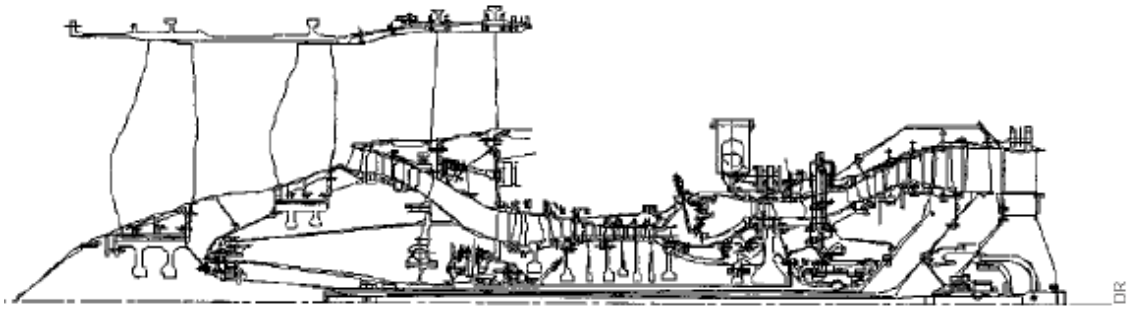

Figure 45: Preliminary counter-rotating turbofan (CRTF). (Baudier 2004)

All the three future engines have the same core technology. Tables 5 and 6 show the main performance parameters used to simulate the future engines.

Parameter	CRTF	GTF	DDTF
BPR	10	12	11
OPR	30	30	30
FN* (kN)	121	121	121
Mass Flow (kg/s)	500	500	500

* At SLS condition

Table 5 Main cycle parameters* for the three future engines short range

Parameter	CRTF	GTF	DDTF
BPR	10	12	13
OPR	40	40	40
FN* (kN)	316	316	316

Mass Flow (kg/s)	1200	1200	1200

* At SLS condition

Table 6 Main cycle parameters* for the three future engines long range

The status-data analysis and comparison of the above different engines is based on following constraints. Same Airplane Cycle application with consideration of:

- same engine thrust ratings
- same average missions
- same ratios for EFC/EFH
- same levels of utilisations

The thrust ratings for the short range engines is around 121 kN at take off condition, and for the long range engines is around 316 kN at take off condition both of them at sea level static.
The EFC/EFH ratios are for short range 1.6, and for long range 7.5.
The block distance for the short range aircraft is 970 Km and for the long range one is 5600 Km.

5.3.2 Results

In tables from 7 to 9 we can see the values used as input for the economic model compared with the baseline values.

	DDTFLR	BASELR	%Δ	DDTFSR	BASESR	%Δ
Plant Cost (k€)	7000	5592	25.179	3000	3379	-11.216
Weight of Fuel Used (Kg)	32000	37261	-14.119	3000	4252	-29.445
Maximum Take Off Weight (Kg)	196000	192890	1.6123	65000	63270	2.7343
Operating Empty Weight (Kg)	127000	124390	2.0982	43000	40770	5.4697
EPNL (dB)	90	103	-12.621	90	100	-10
NOX (g)	23000	26306	-12.567	8000	7481	6.9376

D/Foo CO (-)	8	24	-66.667	17	38	-55.263

Table 7 Input data comparison for the CRTF, long and short range with baselines

	DDTFLR	BASELR	%Δ	DDTFSR	BASESR	%Δ
Plant Cost (k€)	7500	5592	34.12	3800	3379	12.459
Weight of Fuel Used (Kg)	32000	37261	-14.119	3500	4252	-17.686
Maximum Take Off Weight (Kg)	196000	192890	1.6123	65000	63270	2.7343
Operating Empty Weight (Kg)	127000	124390	2.0982	43000	40770	5.4697
EPNL (dB)	90	103	-12.621	90	100	-10
NOX (g)	23000	26306	-12.567	8600	7481	14.958
D/Foo CO (-)	2	24	-91.667	11	38	-71.053

Table 8 Input data comparison for the DDTF, long and short range with baselines

	GTFLR	BASELR	%Δ	GTFSR	BASESR	%Δ
Plant Cost (k€)	6400	5592	14.449	3200	3379	-5.2974
Weight of Fuel Used (Kg)	32000	37261	-14.119	3500	4252	-17.686
Maximum Take Off Weight (Kg)	196000	192890	1.6123	65000	63270	2.7343
Operating Empty Weight (Kg)	127000	124390	2.0982	43000	40770	5.4697
EPNL (dB)	90	103	-12.621	90	100	-10
NOX (g)	28000	26306	6.4396	8400	7481	12.284
D/Foo CO (-)	3	24	-87.5	8	38	-78.947

Table 9 Input data comparison for the GTF, long and short range with baselines

In tables from 10 to 12 we can see a comparison between the output values for the future engines and the baseline engines.

Configuration	CRTFLR	BASELR	%Δ	CRTFSR	BASESR	%Δ
Emission Tax (€/Hr)	18	29	-38	28	43	-35

Cost of Materials per Block Hr (€/Hr)	54	41	+31	54	50	+6
DOC of Maintenance Hr (€/Hr)	148	134	+10	132	128	+3
DOC per Year (K€/Year)	7735	13063	-40	1594	2556	-37
Cost of FUEL per Yr (k€/Year)	5827	6616	-11	619	755	-17
Noise Tax (€/Hr)	0	2066	-100	0,00	1651	-100
NPC FOR 30 YEARS (k€)	7922	6709	18	3602	3476	3

Table 10 Output data comparison for the CRTF long and short range with baseline

Configuration	DDTFLR	BASELR	%Δ	DDTFSR	BASESR	%Δ
Emission Tax (€/Hr)	20	29	-25	30	43	-31
Cost of Materials per Block Hr (€/Hr)	56	41	+36	60	50	+18
DOC of Maintenance Hr (€/Hr)	152	134	+13	139	128	+8
DOC per Year (K€/Year)	7750	13063	-40	1693	2556	-33
Cost of FUEL per Yr (k€/Year)	5738	6616	-13	631	755	-16
Noise Tax (€/Hr)	0	2066	-100	0,00	1651	-100
NPC FOR 30 YEARS (k€)	8234	6709	+22	4011	3476	+15

Table 11 Output data comparison for the DDTF, long and short range with baseline

Configuration	GTFLR	BASELR	%Δ	GTFSR	BASESR	%Δ
Emission Tax (€/Hr)	29	29	-0	42	43	-1
Cost of Materials per Block Hr (€/Hr)	48	41	+16	50	50	0
DOC of Maintenance Hr (€/Hr)	143	134	+6	129	128	+1
DOC per Year (K€/Year)	7534	13063	-42	1568	2556	-38
Cost of FUEL per Yr (k€/Year)	5756	6616	-13	630	755	-16
Noise Tax (€/Hr)	0	2066	-100	0	1651	-100
NPC FOR 30 YEARS (k€)	7108	6709	+6	3386	3476	-2

Table 12 Output data comparison for the GTF, long and short range with baseline

From these tables we can see how the new engines achieve the result of reducing the costs derived from the fuel consumption, the gaseous and noise emissions, because the novel configurations of these engines generate less emissions and lower specific fuel consumption than the baseline ones.

The high cost of the new engines explains why also their costs of maintenance are higher. Higher is the cost of the spare part higher is cost of repairing the engines and then the costs of maintenance.

The same applies for the NPC: the time needed to recover from the initial investment is higher for the novel cycle engines.

In both cases the baseline engines have higher DOC, because they surpass the barrier of 89 dB that is fixed by the Noise tax and so the old engines have to pay the tax. On the other hand, the new engines are quieter, they generate a maximum EPNL less than the permitted threshold, and so they don't have to pay the noise tax.

Figure 46 and Figure 47 show the most important of these results in two bar charts: the values showed are the direct operating cost of maintenance, the direct operating costs and the net present cost. The comparison is shown in percentage considering a value of 100% for the baseline engines.

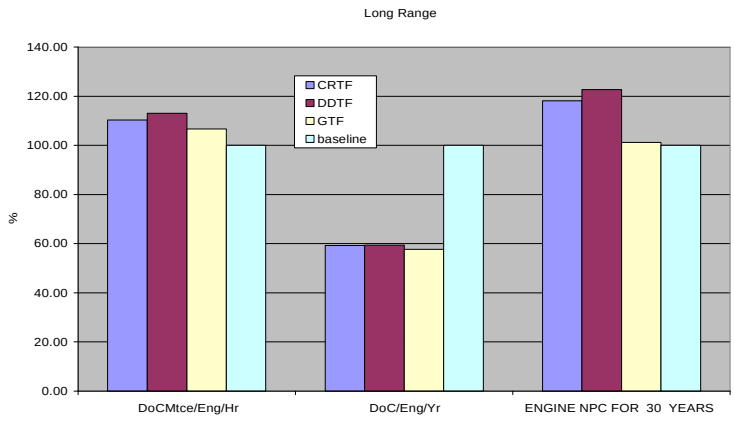

Figure 46 Comparison of costs for the long range engines

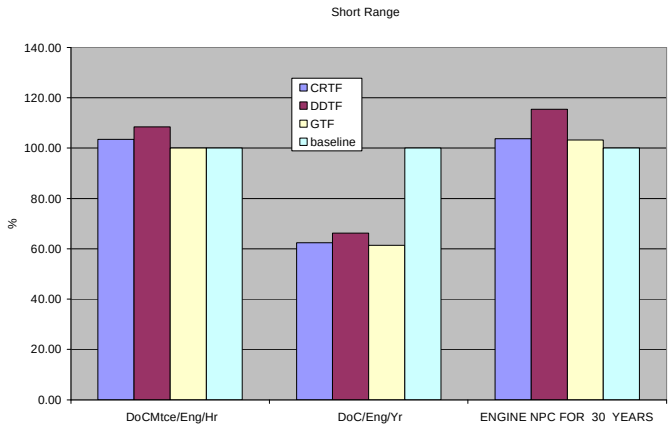

Figure 47 Comparison of costs for short range engines.

5.4 VITAL Engines Optimization Results

Using iSight optimization has been done on the VITAL engines. Two techniques have been used in the optimization. Firstly the *Sequential Quadratic Programming – NLPQL* and secondly the *Mixed Integer Optimization – MOST*; the NLPQL is used in order to exploit local area around initial design point, rapidly obtain local optimum design and handle the inequality constraints used; the MOST is used because it is well suited for continuous design spaces and it is also able to find good discrete solutions in discrete design spaces.

The aim of the optimization is to minimize the fuel burn and the direct operating costs changing the FPR and BPR. As expected the fuel burn optimization for both engines can only give small improvements because the VITAL engines were created already with the target to minimize the SFC, but when the engines are installed then the fuel burn is worsened by the dimensions of the engines and this is shown in the optimization where smaller BPR and higher FPR are preferable. Interesting are also the results for the DOC minimization, in particular for the GTF, here we can see how a smaller BPR and higher FPR engine would improve the maintenance costs, which influence nowadays the operating costs. But in the future when the legislation will change and the taxation on noise and gaseous emissions will be stricter then the results of this

optimization could change in favor of higher BPR engines that have a lower production of noise and gaseous emissions.

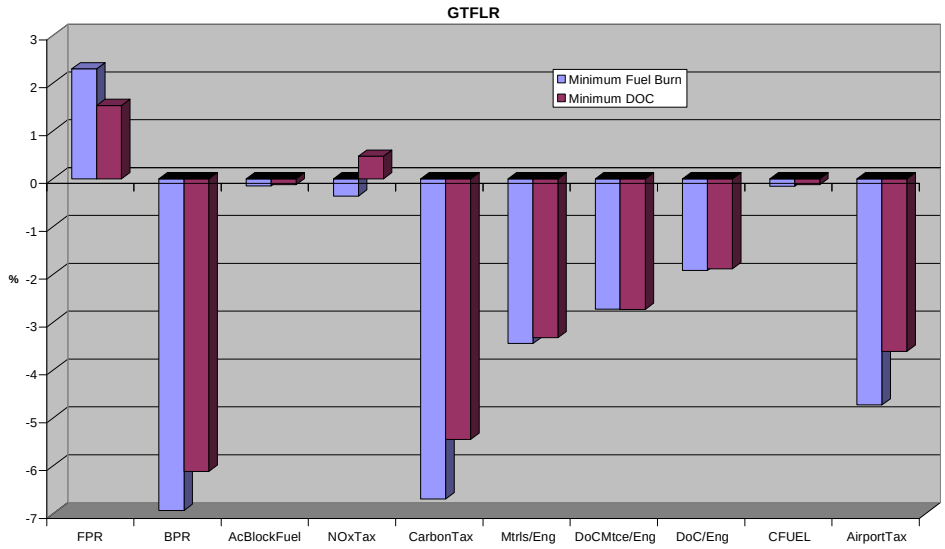

Figure 48 Optimisation results for the GTFLR for the economic parameters

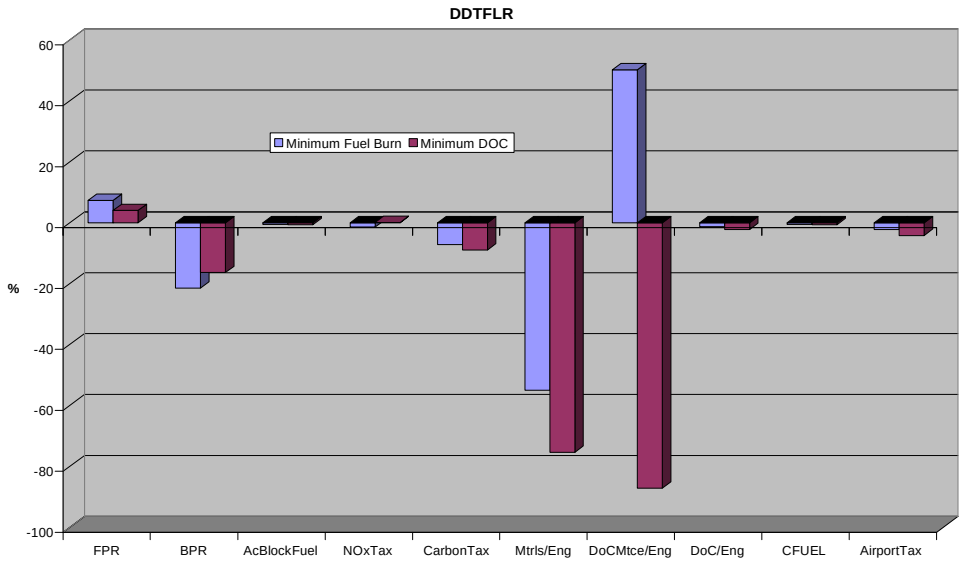

Figure 49 Optimisation results for the DDTFLR for the economic parameters

5.5 Results of the advanced propulsion systems

The work presented in this section has been conducted in the Universidad Politecnica de Madrid (UPM) under the supervision of Prof. Gregorio Corchero

Diaz. The program used to do the study has been created in UPM and it is a property of UPM University.

We have different possible designs starting from the long range GTF engine, the baseline engine, and once the new components are defined. These new components are defined by their characteristic parameters and an example could be the heat exchangers in the IRC cycle. The regenerative RHE is defined by its regenerative thermal efficiency and the stagnation pressure losses in both streams while the intercooler is defined only by the stagnation pressure losses in streams, core and bypass; this can be inferred from the performance model.

Two representative designs are considered:

a) Design for constant TET, the same as in the baseline engine, and

b) Design for constant specific thrust ST, the same as in the baseline engine;

In the first one the VITAL technology limit for the gas generator is fixed while in the second one we also search for the benefits of using lower TETs. These designs were done at two flight conditions, sea level static and cruise, but no attempts have been made to match part loads. For both designs conditions, the overall core pressure ratio is the free parameter to fix the thermodynamic cycle, once the characteristic parameters which define the new components are fixed; the influence of these characteristic parameters will be also presented in the next paragraphs. Section 5.5.1 presents the results for both design conditions at Top of Climb (ISA+10, 10668 m and M_0=0.82), the design point, and section 5.5.2 shows the results for both designs at cruise (10668 m and M_0=0.82), the off design point. All the results presented in this thesis are scaled by the reference values and any delta represents the difference between the variable under study and its respective reference value; these reference values correspond to the baseline engine values at the respective flight conditions, climb or cruise, depending on the flight conditions at where the parameter study is done.

5.5.1 Results for designs at Top of Climb

5.5.1.1 The IRC cycle

Figure 50 to Figure 55 present the results for constant specific thrust (ST) designs and w_{cool}=0.1; this means that 10% of the total bypass stream goes through the intercooler. This value increases the cycle possibilities of using a regenerative heat exchanger while it could be feasible of being installed in the bypass, and also it improves the engine specific thrust capabilities; this possibilities increase of using a regenerative heat exchanger is due to a lower HPC exit temperature.

Similar qualitative results will be obtained if this value is increased or decreased. The stagnation pressure losses are assumed to be the same for all the heat exchangers and equal to 3%, which could be reasonable for sea level static conditions (Kentfield 1975). These losses will increase if high compact heat exchangers are used; in this way 1% of pressure losses increase in any heat exchanger will translate approximately into an increase of 0.1-0.2% in SFC.

Finally the influence of the regenerative thermal ratio or recuperative efficiency is included in the parameter study with values ranging from 0.6 to 0.9.

Practically no benefits on SFC are obtained for η_R=0.6, see Figure 50 and Figure 51, while for η_R=0.9 the maximum benefits on SFC are obtained. η_R=0.9 represents a characteristic value in terrestrial application, which will be difficult to achieve in aero engines and consequently it would represent a target for aero engine applications. The case of η_R=0.9 and no stagnation pressure losses in the heat exchangers is also included as a reference and a measure of the maximum achievable benefits on SFC; it is called HE_{ideal} in the different plots.

Figure 50 and Figure 51 show the benefits on SFC for both cooling bleed configurations and constant ST designs. These benefits vary from practically nil

for η_R=0.6 to above 15% for η_R=0.9 and low overall pressure ratios, when the cooling air bled at the exit of the RHE. The higher benefits for this configuration come from the fact that the cooling air is bled at a higher temperature than when the cooling air is bled at the RHE entry, but this configuration could have dangerous effects on turbine cooling. In this way, Figure 52 and Figure **53** shows a measure of the ability of the cooling air to accomplish its function for both cooling configurations, respectively; they present the ratio of the temperature difference, $\Delta T_{cooling}$, between the temperature at the entry of the HPT nozzle guide vanes and the temperature at bleed section, and the same value for the baseline engine. Figure 52 shows a much higher $\Delta T_{cooling}$ than the baseline for the case of cooling air bled at RHE entry, which would permit a decrease of cooling air mass and consequently to obtain higher benefits on SFC than the ones presented in Figure 50.

Figure 53, where the cooling air is taken from the exit of the RHE, shows a clear loss of cooling ability for high RHE efficiencies and low overall pressure ratios, when the higher benefits on SFC can be reached, so their benefits seem to be overestimated. These figures also show an important overall pressure ratio reduction, and consequently an important decrease of HPC size and weight for low specific fuel consumption designs, overall pressure ratio about twelve, and when it is compared with baseline engine. Figure 54 and Figure 55 also present additional benefits on NOx emissions and TET for the case of cooling air bled at the RHE entry; practically the same results are obtained for the case of cooling air bled at exit of the RHE. For the case of maximum benefits on SFC, the engine TET and NOx emissions practically take the baseline engine values but for higher overall pressure ratios, when still there are clear benefits on SFC and NOx emission, also there are clear benefits on TET decrease and consequently on the engine life, see Figure 50, Figure 51 and Figure 54; we have to keep in mind that a decrease of about 20 degrees on TET will double the turbine life. The same study has been carried out for the third cooling configuration and the results lead to the same conclusions; their results are not included to avoid excessive data presentation.

Figure 56 and Figure 57 present some results for constant TET design. These results lead to the same previous conclusions with the difference that here we obtain a benefit on ST but paying it with an increase of TET when they are compared with those of constant specific thrust design, see Figure 54, Figure 56 and Figure 57. All cooling bleed configurations have been studied as in the case constant ST design but not all results are presented to avoid excessive data and they will lead to the same considerations.

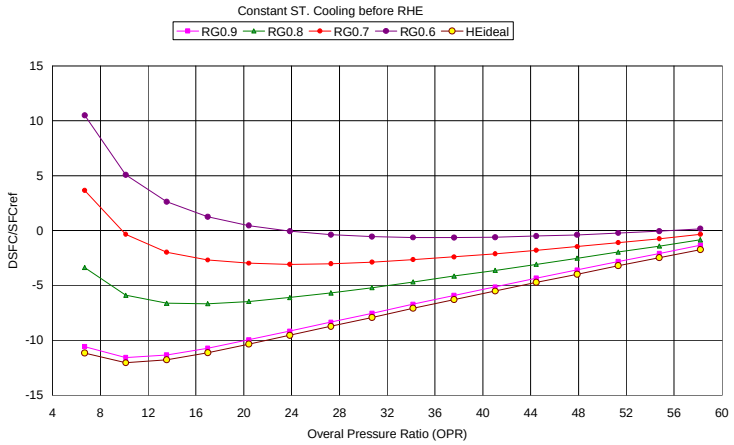

Figure 50 – Influence of the overall pressure ratio and the regenerative thermal efficiency (0.9, .., 0.7) on the SFC at ToC and for constant ST design and cooling bled before RHE

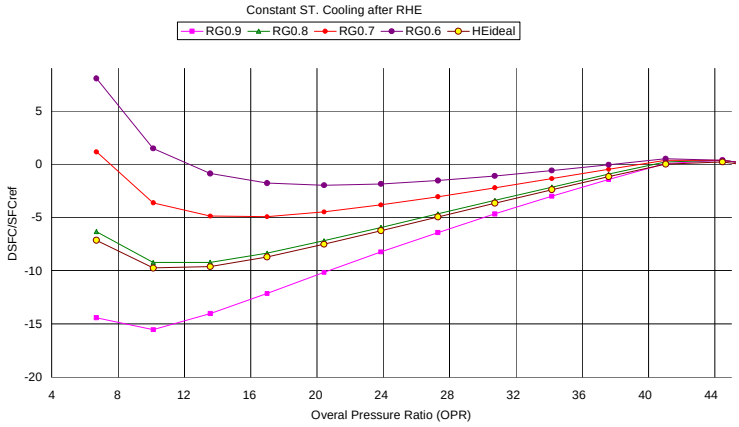

Figure 51 – Influence of the overall pressure ratio and the regenerative thermal efficiency (0.9, ..,0.7) on the SFC at ToC and for constant ST design and cooling bled at the exit of the RHE

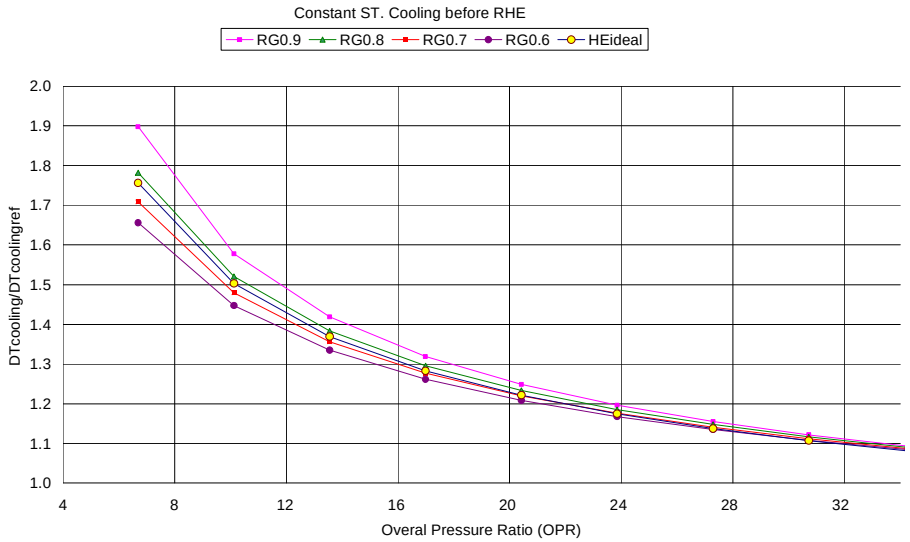

Figure 52 – Influence of the overall pressure ratio and the regenerative thermal efficiency (0.9, ..,0.7) on the cooling availability at ToC for constant ST design and cooling bled before RHE

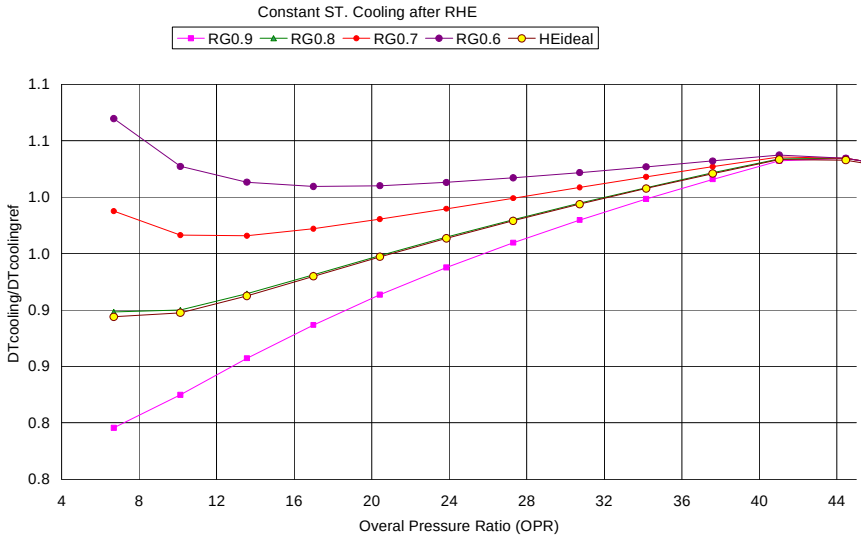

Figure 53 – Influence of the overall pressure ratio and the regenerative thermal efficiency (0.9, ..,0.7) on the cooling availability at TOC for constant ST design and cooling bled at the exit of the RHE

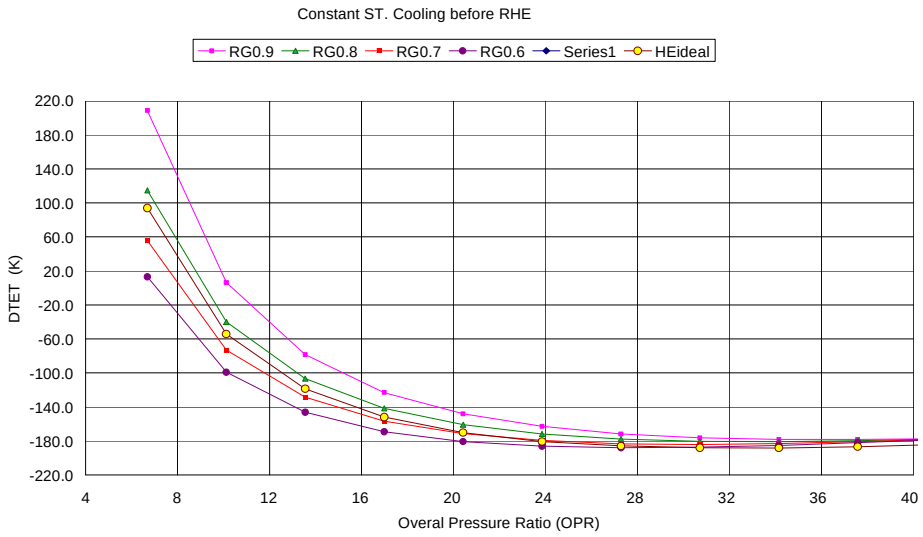

Figure 54 – Influence of the overall pressure ratio and the regenerative thermal efficiency (0.9, ..,0.7) on the TET decrease at TOC for constant ST design and cooling bled before of the RHE

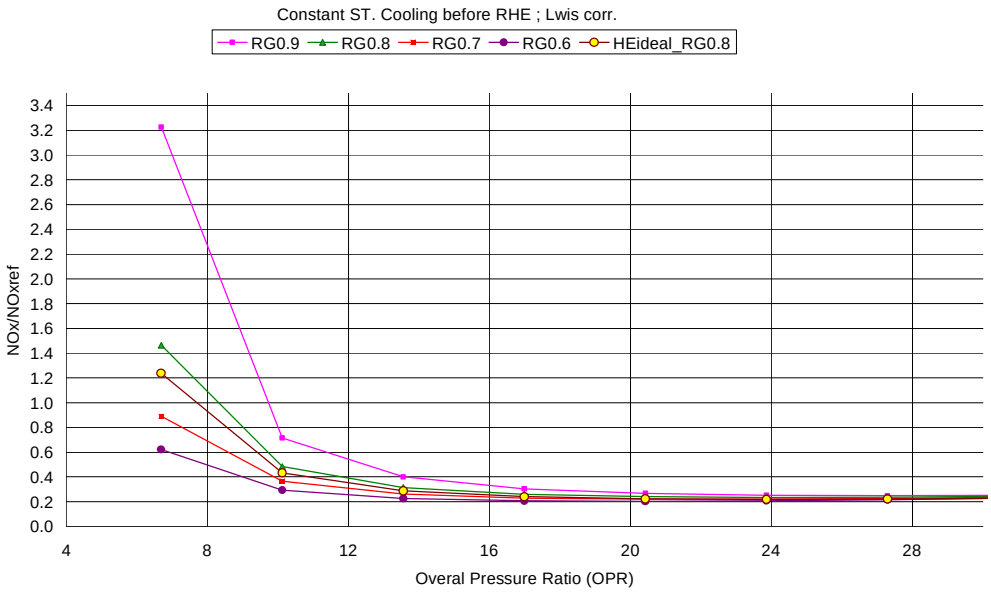

Figure 55 – Relative variation of the NOx with the overall pressure ratio and the regenerative thermal efficiency (0.9, .., 0.7) on the SFC at TOC and for constant ST design and cooling bled before RHE

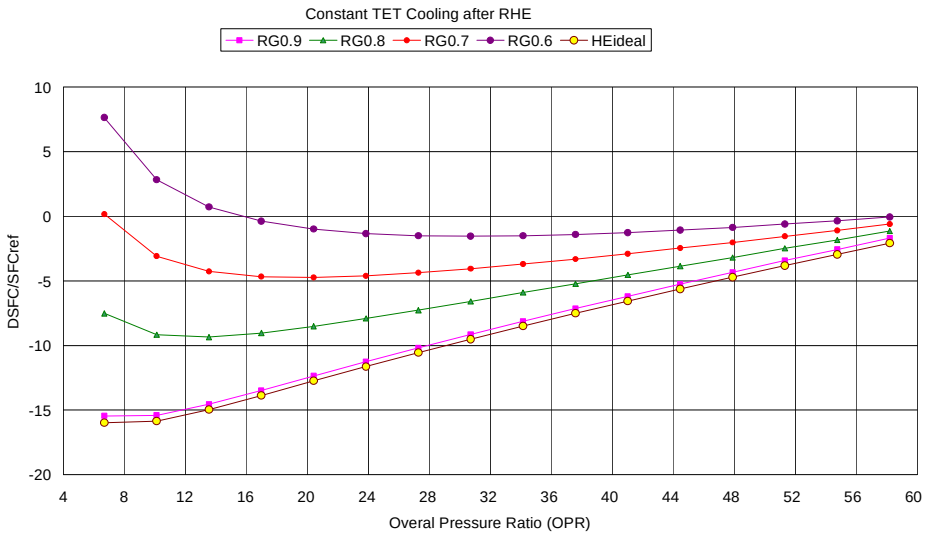

Figure 56 – Influence of the overall pressure ratio and the regenerative thermal efficiency (0.9, ..,0.7) on the SFC at TOC and for constant TET design and cooling bled at the exit of the RHE

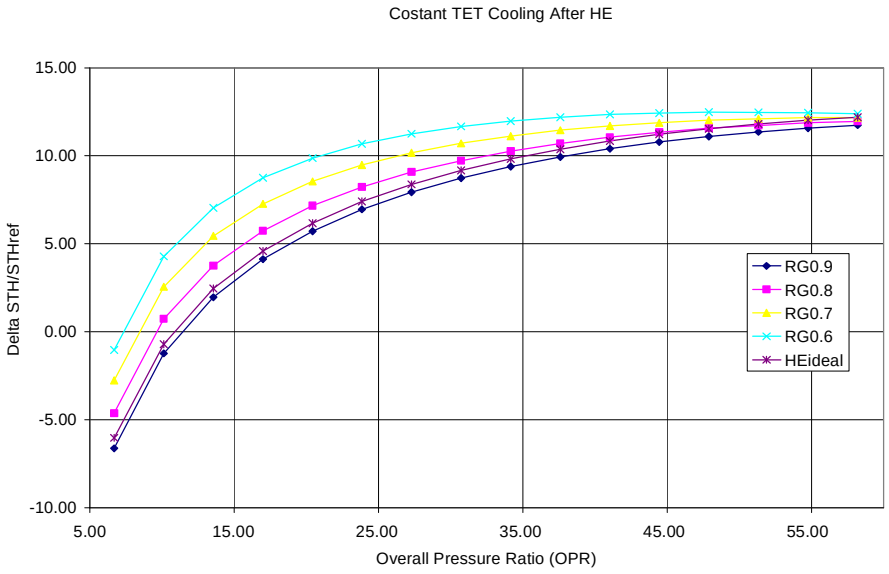

Figure 57 – Gain of ST with the overall pressure ratio and the regenerative thermal efficiency (0.9, ..,0.7) at TOC and for constant TET design and cooling bled at the exit of the RHE

5.5.1.2 The WRTC cycle

The *WRTC* is simulated as a standard turbofan cycle to which an extra standard high spool has been added, the wave rotor. An efficiency of 0.83 has been

assumed for the compression and expansion processes (Wilson 1993) while the wave rotor pressure ratio has been varied from 1 to 3.6, a wave rotor pressure ratio which seems to be achievable (Wilson 1993, Welch 1997, Paxson 1997); the same efficiency has been assigned to the APC compressor, used to compress the cooling air. Here also two design conditions, constant TET and constant specific thrust, have been considered.

Figure 58 to Figure 62 show the results for both design conditions. This cycle increases significantly the maximum cycle pressure and temperature, see Figure 58 and Figure 59, and then a thermal efficiency and SFC improvement is expected. Figure 60 presents the SFC improvement for both designs; for an achievable wave rotor pressure ratio of 2.5 (Wilson 1993, Welch 1997, Paxson 1997) an improvement between 3 and 6% can be accessible, depending of the design conditions. Additionally, while the Figure 60 presents a benefit of 3% and 6% on SFC for the constant TET and constant ST designs respectively, therefore the Figure 61 presents an important decrease of TET for constant ST design, which will translate into a clear increase of engine life with no much increase of NOx emissions, see Figure 62. The constant ST design shows a clear advantage on the constant TET design getting higher benefits on SFC and also an important decrease of the TET. The increase of the maximum cycle pressure and temperature originates a clear increase of the NOx emissions independently of the correlation used for its calculation, see Figure 62.

Finally, assuming that the wave rotor topping cycle is self-cooling and consequently the maximum cycle temperature is not a dramatic problem it clearly increases the NOx emissions, when compared to the baseline engine, and also gives lower benefits on specific thrust fuel consumption than the intercooler- regenerative cycle.

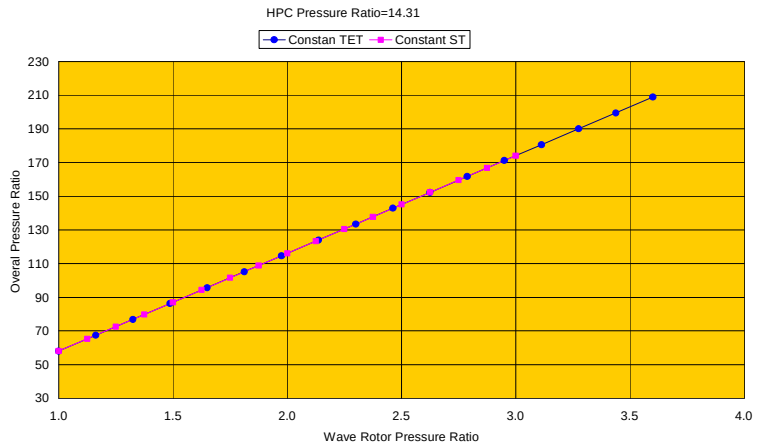

Figure 58 – Variation of the overall pressure ration with wave rotor pressure ratio for constant TET design (TET) and for constant ST design (ST) at TOC

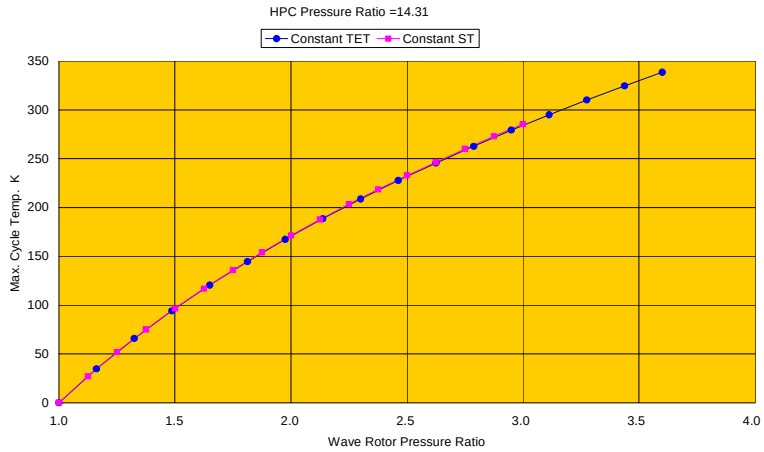

Figure 59 – Increase of the maximum cycle temperature with wave rotor pressure ratio for constant TET design (TET) and for constant ST design (ST) at TOC

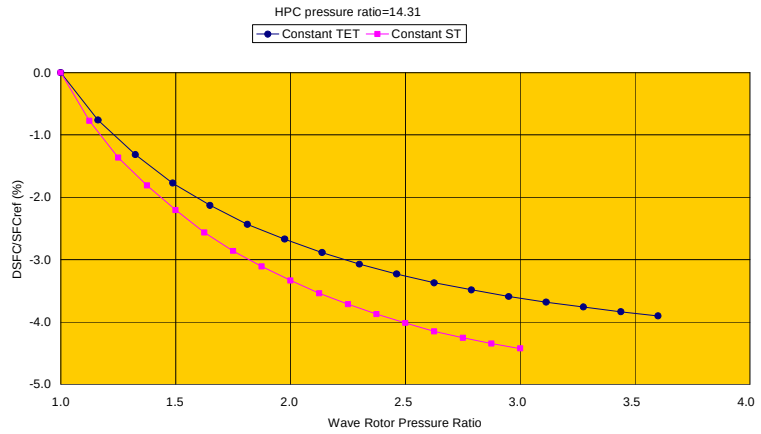

Figure 60 – Influence of the wave rotor pressure ratio on the SFC for constant ST design (ST) and for constant ST design (ST) at TOC

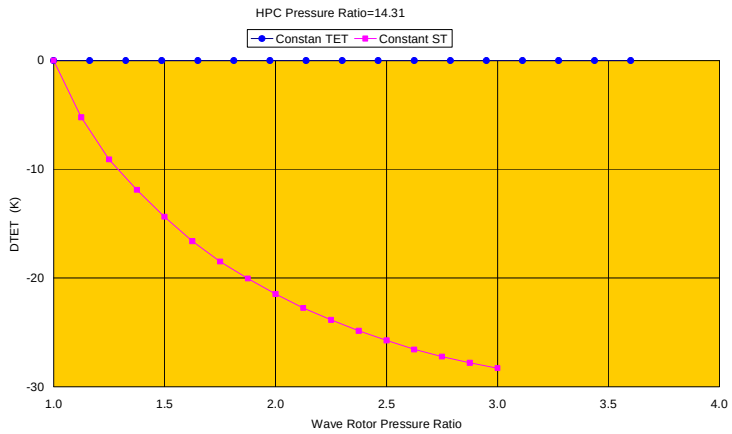

Figure 61 – Gain of turbine entry temperature (TET) with wave rotor pressure ratio for constant TET design (TET) and for constant ST design (ST) at TOC

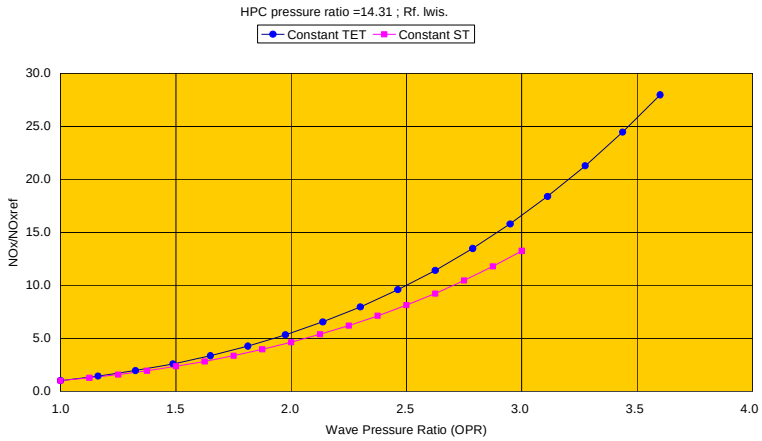

Figure 62 – Influence of the wave rotor pressure ration on the NOx for constant TET design (TET) and for constant ST design (ST) at TOC

5.5.1.3 The CV cycle

Steady process has been considered in the CV cycle although it is well known that the combustor discharge is an unsteady process; later we will come back to this process. Only the design condition of constant specific thrust has been considered. The constant ST design gives a significant TET reduction which makes that the constant TET design not necessary; beside these benefits, the constant TET design will give also limited physical solutions.

In the CV simulation it is assumed that 10% of the total bypass mass flow is used in the CV combustor cooling process. This ensures the combustor cooling with low temperature increase in the bypass stream and also the intercooler installation in the bypass seems to be feasible. We need to keep in mind we are working with a very ultra high bypass ratio and also that the heat addition to a stream at low pressure is less efficient for mechanical energy production than the heat addition to the core stream at a much higher pressure. Besides the HPC pressure ratio, the influence of the pressure losses at the combustor, k_3 and k_4, and the heat transfer to the bypass in the combustor cooling process have also been studied; once the HPC pressure ratio is fixed the design condition will provide the overall pressure ratio. In the figures which will be presented later, the symbol ST 0.08 0.9 means that it corresponds to constant ST design and that the 8% of *c*FHV* is transferred to the bypass in CV combustor cooling process and that 10% of the in stagnation pressure is lost in the opening and closing system respectively, $k_3=k_4=0.9$. Really the product k_3k_4 represents the total loss of stagnation pressure in the combustor independently on which is higher and it really is the influent parameter; see expression (2); this is why for the simulation it is assumed that both, k_3 and k_4, take the same value in an intent of plots reduction. Finally the overall pressure ratio is defined as the ratio between the stagnation pressure at the exit of the combustor, once the pressure losses has been discount, and the stagnation pressure at the entry of the compressor, P_4/P_2.

From **Figure 63** to **Figure 67** are presented the results for CV cycle. Figure 63 and Figure 64 show significant benefits on SFC; these benefits are clearly lower than those ones of the IRC cycle and practically equal the benefits provided by the WRTC cycle. These benefits go down when the HPC pressure ratio decreases and consequently the overall pressure ratio also decreases, see Figure 64, and also when the heat transfer to the bypass, due to combustor cooling process or the pressure losses in the combustor, $1/k_3k_4$, increase. The heat transfer to bypass and the pressure losses could negate completely the benefits on SFC, or on CO_2 production, see Figure 63 and Figure 64. In the case of combustor pressure losses increase, additional fuel is needed to compensate these pressure losses while, in the case of increasing the heat

transferred to the bypass stream in the CV combustor cooling, this energy is transferred from the core stream at a high pressure to a stream, the bypass stream at a lower pressure which is less efficient for mechanical energy production; the mechanical energy production will increase with the nozzle pressure ratio available in the different nozzles, core and bypass streams.

Figure 66 and Figure 67 show also some additional benefits of the CV cycle. These figures present the influence of the overall pressure ratio, indirectly the influence of the HPC pressure ratio, and the amount of heat transferred to bypass in the combustor cooling process on the NO_x and the TET. The CV cycle gives up a great reduction of TET, consequently also a great reduction on the cycle maximum temperature, with no much increase of the overall pressure ratio, see Figure 65 and Figure 67; the TET reduction will be of about 100 K for the maximum benefits on specific fuel consumption. This translates in a reduction of NO_x emission, see Figure 66, and also in a clear increase of engine life. The influence of the amount of heat transferred to bypass on TET is practically nil. Similar results are obtained if the influence of pressure losses in the combustor are considered, but it will be more sensible to the pressure losses. This higher sensibility comes from the fact the pressure losses affect the whole expansion process in core stream and as a consequence the power ratio available to be given to the bypass stream through the fan compressor. Globally the CV cycle gives similar results on NO_x emissions when it is compared to the IRC cycle, but a lower benefit on specific fuel consumption. The benefits on TET are clearly higher than the ones obtained from the other cycles; we have to keep in mind that we have not considered any losses due to the unsteady process.

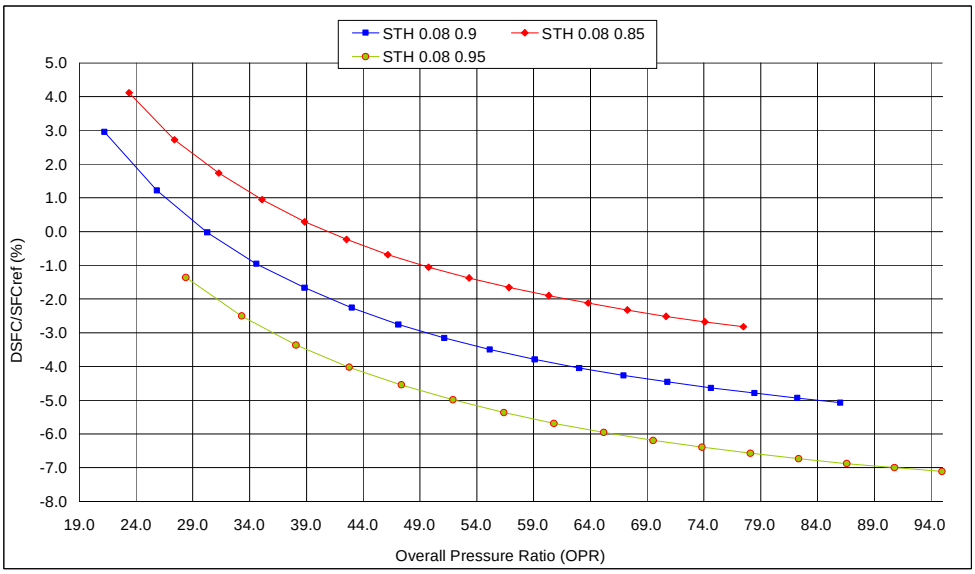

Figure 63 – Influence of the overall pressure ratio and the combustor pressure losses on SFC for CV cycle and constant ST design at TOC

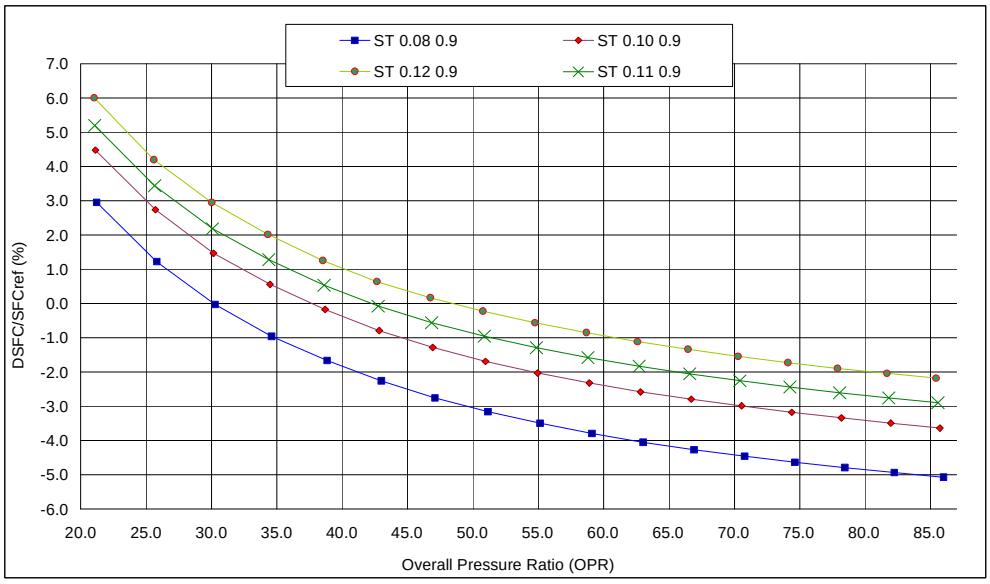

Figure 64 – Influence of the overall pressure ratio and the heat transferred to the bypass in combustor cooling process on SFC for CV cycle and constant ST design at TOC

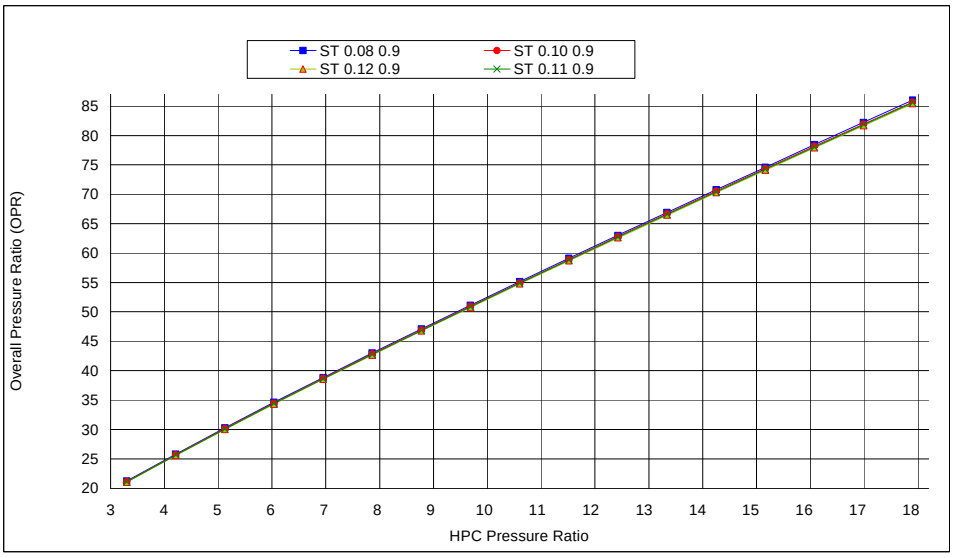

Figure 65 – Variation of the overall pressure ratio with the HPC pressure ratio for the CV cycle and constant ST design at TOC

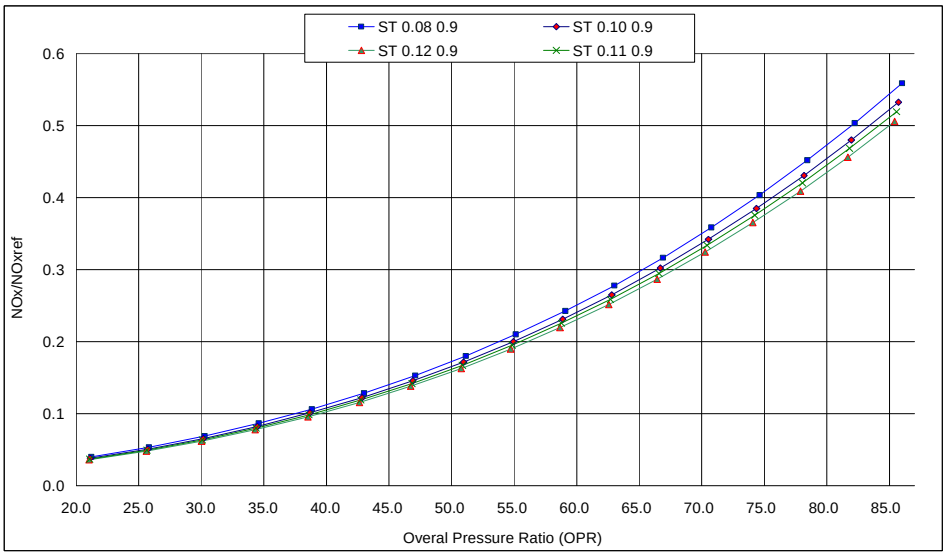

Figure 66 – Influence of the overall pressure ratio and the heat transferred to bypass in the combustor cooling process on NOx emission for the CV cycle and constant ST design at TOC

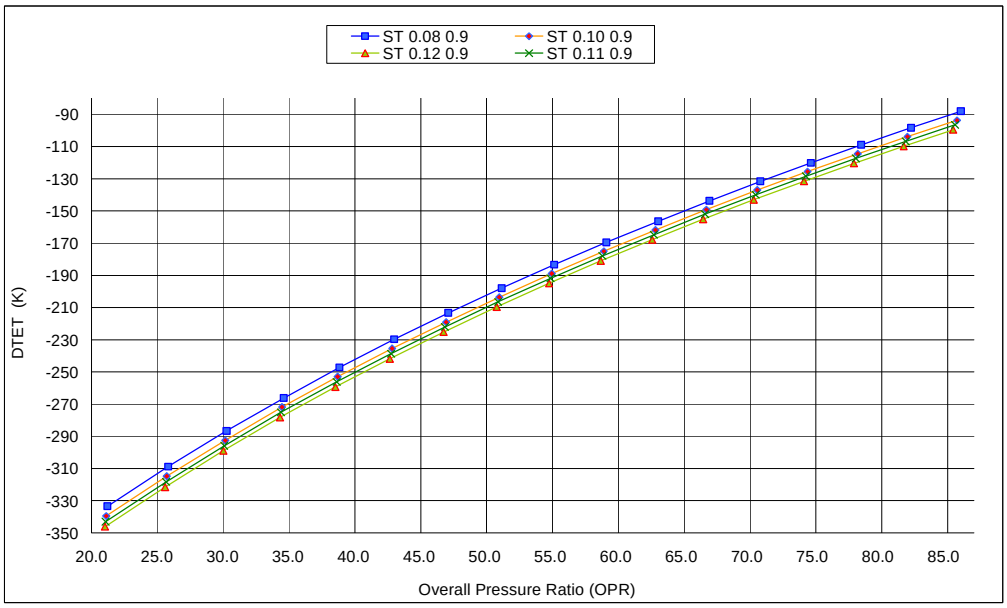

Figure 67 – Gain on turbine entry temperature with the overall pressure ratio and the heat transferred to bypass in the combustor cooling process for CV cycle and constant ST design at TOC

5.5.2 Results for cruise

The same parameter study carried out at top of climb has been also done at cruise conditions to know if the same benefits, coming from the use of the three different cycles, can be obtained at this flight conditions. Starting from the baseline engine working point at cruise conditions (10668 m M_0=0.82) and as in the study at top of climb, two possible designs have been applied to the three different cycles under consideration:

a) Design for constant TET, the same as in the baseline engine at cruise, and

b) Design for constant specific thrust ST, the same as in the baseline engine at cruise.

In both cases, we look for benefits on SFC, emissions and noise, and also if it is possible, on TET in the case of design for constant specific thrust. The variations of the different parameters, which define the new components in the

cycles and have been used in the study, coincide exactly with variation used in the study at sea level static with the exception of the pressure losses in the different heat exchangers. At cruise condition the flow capacity of the heat exchanger will be lower than at sea level static and consequently, because the pressure losses in a duct will go as the square of the flow capacity (Kays 1984), lower pressure losses are expected in heat exchangers; this pressure losses are assumed to be constant and equal to 1% instead of the 3% assumed at sea level static (Kentfield 1975). Therefore, taking into account that the results lead to the same considerations as in study at sea level static and to avoid excessive presentation of data, only some relevant results will be presented here.

From **Figure 68** to **Figure 70** are presented the benefits on SFC which could be obtained from the use of the three different cycles when they are compared with the baseline engine. We have to keep in mind that the reference values are constant and correspond to the baseline at cruise working point; this could drive us to the conclusions that at the maximum design overall pressure ratio the benefits on SFC for the IRC cycle should be cero if the regenerative heat exchanger can not be installed because the temperature at the exit of the LPT is lower than the temperature at the exit of the HPC for that overall pressure ratio; this does not happen on Figure 68. This difference comes from the fact that there is also an intercooler heat exchanger although there is no regenerative heat exchanger.

These figures show similar benefits to the ones obtained in the study at top of climb. These results were expected because, beside the parameters which define the new components and whose influence we have studied, the TET and overall pressure ratio of the baseline engine really provide the possibilities of using some new components in the case of the IRC cycle as well the possible power saving in the compression cycle phase in the case of CV cycle or the pressure ratio needed in the wave rotor to obtain the maximum benefits on thermal efficiency in the case of WRTC cycle. As an example, in IRC cycle the overall pressure ratio of the baseline is lower at top of climb than at cruise while with the TET the opposite happens; this will not permit the use of the regenerative heat exchanger at high design overall pressure at cruise as it can

be see in Figure 68. In the IRC cycle the SFC first decreases and later increases with the design overall pressure ratio until it get a maximum which represents the limit at which the RHE can be installed and then starts to decrease again, see Figure 68; this last decrease of the SFC is a consequence of the increase of the overall pressure and its influence on the thermal efficiency in a standard Brayton cycle. Finally, the same comments will be pertinent to rest of results which have not been presented to avoid excessive data presentation.

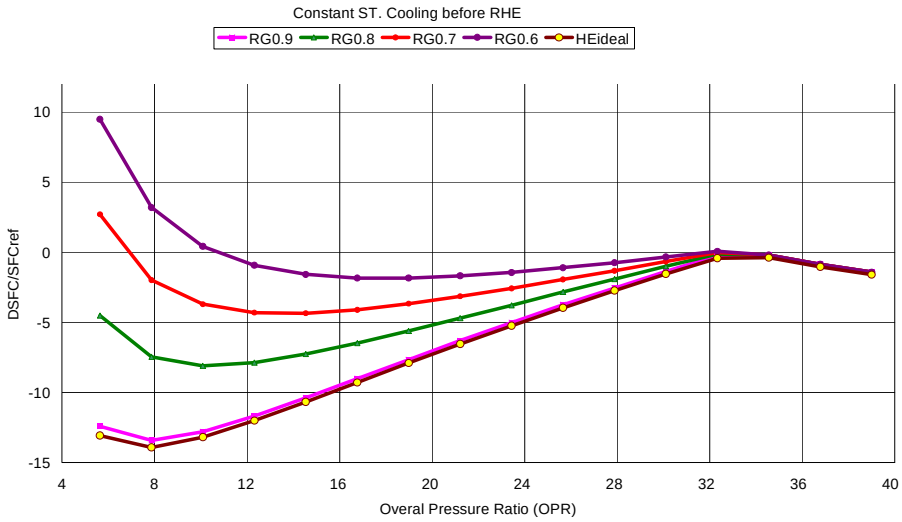

Figure 68 – Influence of the overall pressure ratio and the regenerative thermal efficiency (0.9, ..,0.7) on SFC at cruise for constant ST design and cooling bled at the entry of the RHE

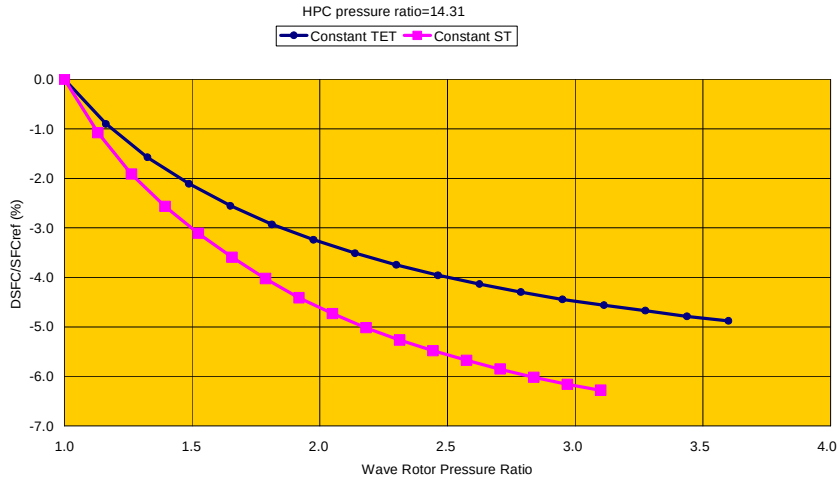

Figure 69 – Influence of the wave rotor pressure ratio on the SFC at cruise for constant ST design (ST) an for constant TET design (TET)

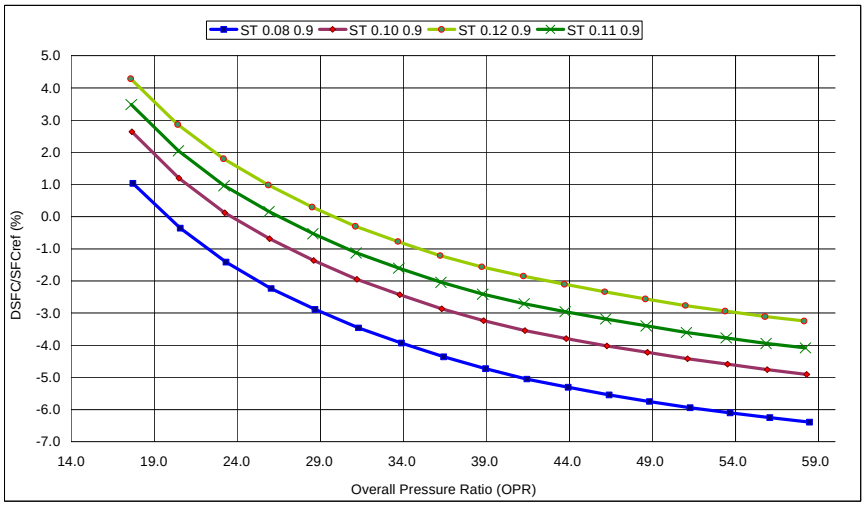

Figure 70 – Influence of the overall pressure ratio and the combustor pressure losses on SFC for CV cycle and constant ST design at cruise

5.5.3 Discussion

The parameter study, which has been presented, offers relevant results from the point of view of fuel saving, CO_2 production, as well as of NO_x emissions. An exception to NO_x emission is the WRTC, which gives a clear increase of NO_x emissions due to a significant increase of the maximum pressure and temperature, see Figure 62. Other significant results correspond to possible designs with lower TET for the case of constant ST, which translates in an increase of the engine life and consequently in manufacturing and maintenance economics, and also in an emissions spinoff during the manufacturing and maintenance process. The noise level due to jets will keep practically unchanged for constant ST design which is also offering the higher benefits on SFC and also on TET decrease. The turbo machineries keep the same or decrease their size and consequently no increase of noise is expected; for constant TET a low noise increase is expected as a consequence of the low increase of the specific thrust, a measure of the jet velocities, see Figure 57.

Focusing on specific fuel consumption (SFC), the range of benefits goes from about 3-6% to above 15%, depending on the design cycle and on the overall pressure ratio used in the design. The best benefits correspond to the IRC and worse benefits correspond to the WRTC, while the CV will be in between but

close to the IRC. A handicap on the CV comes from the fact that a high pressure loss is expected due to the closing-opening combustor system; a possible configuration to compensate these pressure losses could consist in the use of a wave rotor with combustion inside the rotor, which could compensate these losses; additionally the use of multiple ducts could also mitigate the problems due to the CV unsteady process. Considering exclusively the possible benefits on SFC the IRC and the CV cycles promise similar values while for an ultra high bypass ratio turbofan the WRTC promises clearly lower benefits; the IRC benefits go down when the design pressure ratio increases. From the point of view of NO_x emission, the IRC and the CV provide clear benefits decreasing these emissions while the WRTC increases drastically the NO_x emissions; this is an important handicap of the WRTC cycle.

An additional important benefit, presented in the previous section, consists in the possibility of using lower TETs in the design. These benefits are nil for the IRC and designs for minimum SFC, while they are high in the cases of WRTC and CV cycles, especially in the case of CV cycle; see Figure 54, Figure 61, and Figure 67. This benefit can be also relevant for the IRC and design for higher overall pressure ratio but it will be paid with lower benefits on SFC. Finally we have to keep in mind that these benefits for the IRC come from the assumption of η_R=0.9, a value which will be difficult to achieve because of the recuperative heat exchanger size needed. The heat exchanger size can be an important drawback for its use in an aero engine at the current technology level. This size means an increase of weight and volume, and the volume will translate in drag, and the increase of weight and drag will translate in an increase of the installed specific fuel consumption, the fuel consumed per unit of installed thrust, or the fuel consumed during a specified aircraft mission. The influence of the increase of weight and volume on the aircraft mission is an interesting work we expect to do in the future; it will require the real design of the heat exchangers and to link the engine and aircraft performances. Only the influence of assumed deltas of weight and drag will be considered here.

At this stage, the purpose of the work consists in estimating the possible benefits of the different studied innovative cycles and ranking them for future

development depending on their benefits. Focusing on these objectives, the sensitive of the IRC cycle to the increase of weight and drag has been also studied; this is the case when an increase of weight and drag is expected. The IRC configuration, assuming current technology for heat exchangers map, allows to compute the off-design engine performance and to link them with the aircraft mission performance. Figure 71 and Figure 72 present the influence of assumed deltas of weight and drag on the total fuel burned during the whole aircraft mission, and for three regenerative efficiency values; η_R=0.7 and η_R=0.9 can represent the current and the target values respectively. To estimate the weight and drag influence, the IRC design point is fixed at Top of Climb ISA+10 for an overall pressure ratio of 25, three η_R values and the design condition, constant ST, joint to a reasonable value for the SFC; then the off-design performance are computed at any flight condition needed to be linked with aircraft performance. TURBOMACH and HERMES codes have been used for off-design engine and aircraft performance calculation during the mission respectively, being applied to the baseline engine and the three IRC designs for the standard VITAL short range aircraft mission. TURBOMACH and HERMES are codes developed and widely used at Cranfield University. These figures show that the final benefits, when using the IRC engines, will be highly dependant on heat exchanger technology level, the regenerative efficiency and the heat exchanger size; low regenerative efficiency and high exchanger size, volume and weight can mitigate their benefits.

The Figure 71 and Figure 72 show that:

a) The increase of weight and drag can nullify all benefits on SFC for η_R=0.7, and
b) For η_R=0.8, which could represent an achievable value with the appropriate technologic development, important benefits can be got even for important increases of weight and size;

A 100% increase of drag translates into an increase of engine diameter of 41%, assuming that the drag goes as the square of the engine diameter. The maximum benefits on total fuel consumption correspond to η_R=0.9, but it

represents a difficult value to be achieved even in terrestrial application where the weight and size of the heat exchangers do not represent a critical constraint.

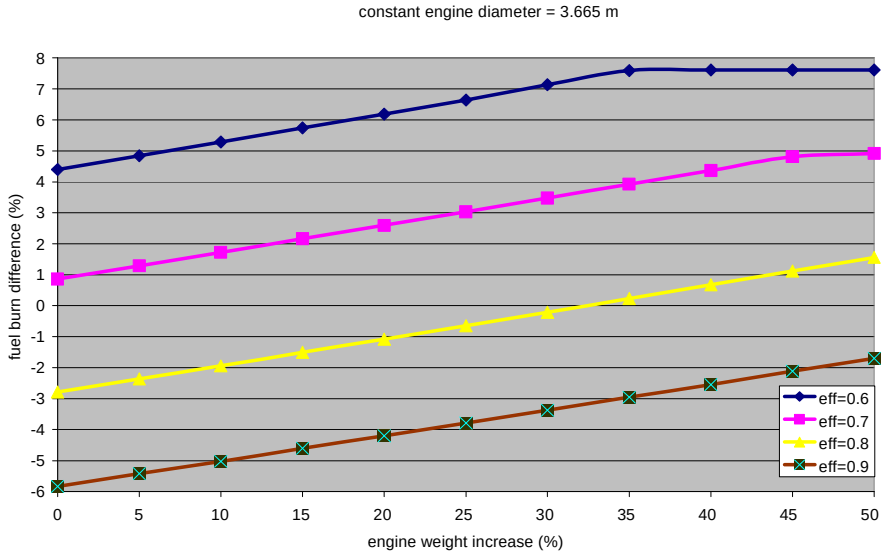

Figure 71 – Influence of the increase of weight on the total fuel burned during the whole mission, for three regenerative efficiency (η_R=0.7, 0.8 and 0.9)

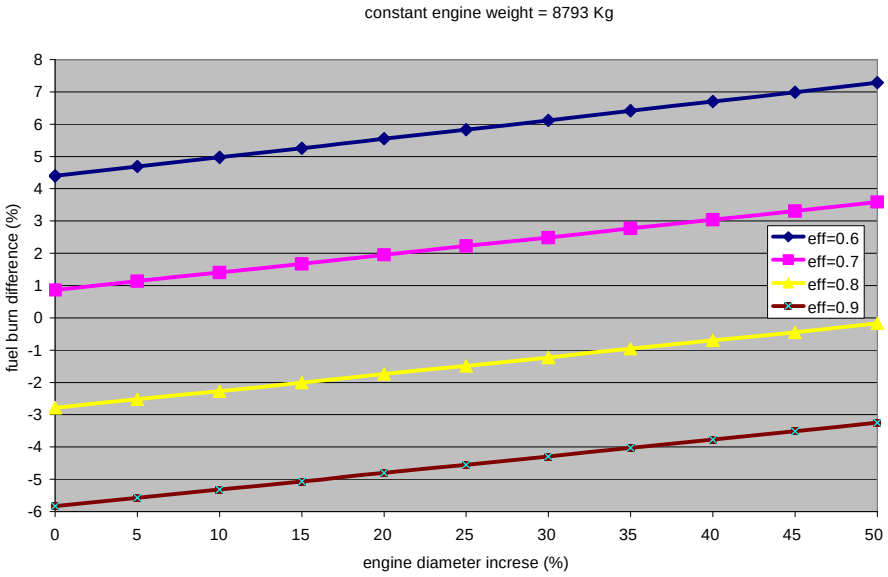

Figure 72 – Influence of the increase of drag on the total fuel burned during the whole mission, for three regenerative efficiency (η_R=0.7, 0.8 and 0.9)

These results are really promising but they will need some additional considerations. In this way:

The IRC

This cycle seems to be the most promising at the current technology level. In any case there are two points, which need to be considered:

a) Small heat exchangers and high recuperative efficiencies are essential to obtain all the shown benefits, but they really are a difficult task and will require important further developments. The heat exchanger size could mitigate completely the benefits.

b) Heat exchanger reliability and life are also an important concern in the IRC cycle for aero engine application. Any heat exchanger fail could be critical in aircraft propulsion.

The WRTC

The wave rotor topping cycle is also unsteady as it also happens with the CV cycle; this unsteadiness was solved using multiple ducts in the study by NASA. In any case higher aerodynamic developments are needed to improve its efficiency and achievable pressure ratio. Most of the recent publications on wave rotor are devoted to wave rotor aerodynamic design (Paxson 1996 & 1999, Welch 1997, Nagashima et al. 2007, Resler 1994).

The CV

It promises high benefits, but it offers also strong issues. Some of these concerns are:

a) The unsteadiness, which translates into performance loss as well as in turbine unsteady working conditions, could be also an important drawback. Perhaps, a way to avoid it could be the use of multiple chambers with some delay time between each others; a similar solution to one used in the case of the wave rotor with multiple ducts.

b) The cooling process. How to implement it? Fins immersed in the bypass stream as in air cooling reciprocating engines could be a possibility. The value

of k_{cool}=0.08 was taken as a characteristic value from these kind of engines (Ferguson 2001).

c) The combustion system. The combustion system is complex system to be study. It will require a further in-depth study. Nalim (1996 & 1999) is devoted to this crucial topic.

Summarizing, and looking at future development, and attending to the benefits on SFC and NO_x emissions the IRC and the CV are located at a quite similar level, while for these application the WRTC is clearly at a lower place especially if we have a look at the NO_x emissions. If we consider the benefits on TET and increase of weight and volume the CV seems to be above the IRC, although it is complicate to imagine the weight and volume of the CV at this stage. If we consider the current technological level it is possible to think that the IRC is located above the CV; the heat exchanger technology for terrestrial application is well known. Finally the WRTC seems to be a good option for small engines with low overall pressure to reach a high efficiency with no high penalty on NO_x emission because of a lower maximum pressure and temperature.

5.6 The internal combustion wave rotor (ICWR)

5.6.1 Assumptions

As all models, this engine performance model relies on assumption and simplifications, which are listed below:

- Everything is modeled across engine “bricks” (components) only: on dimension-related variation is to be taken into account;
- Every engine “brick” is tuned with a given set of fixed coefficients;
- Only the components aiming at modifying airflows are modeled: mechanical (bearings, seals, gearboxes…) and electrical components are not taken into account;

- Friction and heat transfers along walls are not precisely taken into account, but are rather included in overall pressure losses;
- Airflow modifications are modeled through isentropic relations, but adjusted with isentropic efficiencies;
- Cooling air extraction is modeled at a single location (the chosen compressor exit) rather than spread over several compressor stages as in a real engine;
- In the same way, the same amount of this cooling air is delivered in a single location (burner outlet) rather than spread over several turbine stages;

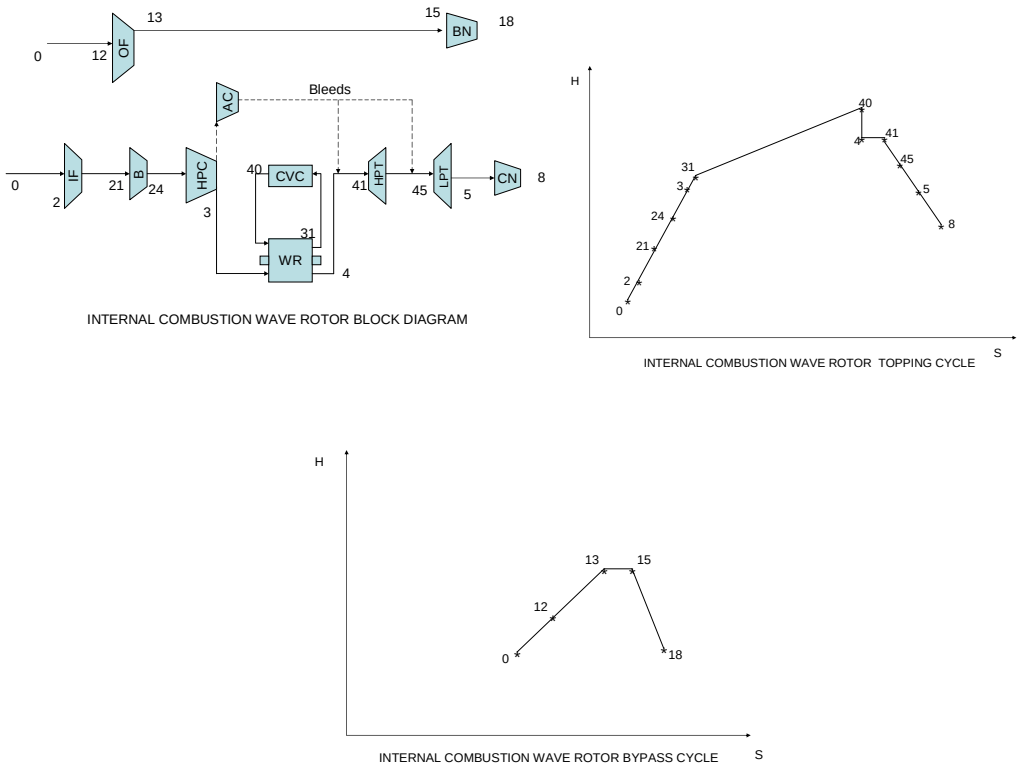

Figure 73 the INTERNAL COMBUSTION WAVE ROTOR

5.6.2 Result

Figure 74 represents the change of SFC and SPT with the BPR as we can see beyond a BPR of 18 there is no more improvement of fuel consumption, in fact it's quite the opposite, which is because of the increase of the drag generated by the bigger and bigger nacelle of the engine. Figure 75 shows, as expected,

that losses need to be low, this means that the design of the mechanical valves has to be the most accurate. But from Figure 76 we can see the variation of the pressure ratio of the cooling compressor with the pressure losses in the wave rotor – constant volume combustion system. This figure shows how the higher the losses the smaller needs to be the compressor used to compress the cooling air that come from the compressor; higher the pressure ratio of this compressor higher will be the weight of the engine, and this weight increase will affect the SFC. A trade off analysis needs to be done in order to understand the magnitude of the acceptable losses in the wave rotor. Figure 77 shows the variation of SFC and ST against OPR.

After this parametric study a design configuration has been chosen for the ICWR in order to do a comparison against the VITAL and the advanced engines. As exemplar for the VITAL engines the GTFLR has been chosen. The ICWR and the GTF have the following same values (see Table 6, Table 9 and annex C):

- FPR
- Fan efficiency
- BPR
- Booster PR
- Booster Efficiency
- Turbines efficiencies
- Thrust
- cooling bleed
- OPR
- Mass flow

The following table shows the results of the comparison for the four engines for the SFC and NOx. As we can see in **Table 13** the ICWR shows better results than all the other engines. Once all the technical problems connected shall be solved this engine seems to be the best solution to the reduction of

fuel consumption and emissions, although a noise analysis is needed in order to understand the noise impact.

%	ICR	WR	CVC	ICWR
SFC	-2.5	-3.2	-2.5	-4
NOX	+0.3	+4	+0.2	-4

Table 13 Comparison between the advanced engines and the GTF

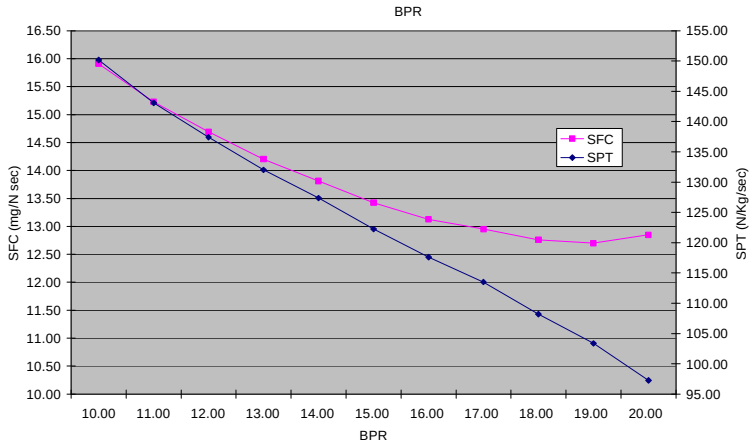

Figure 74: variation of SFC and ST with the BPR

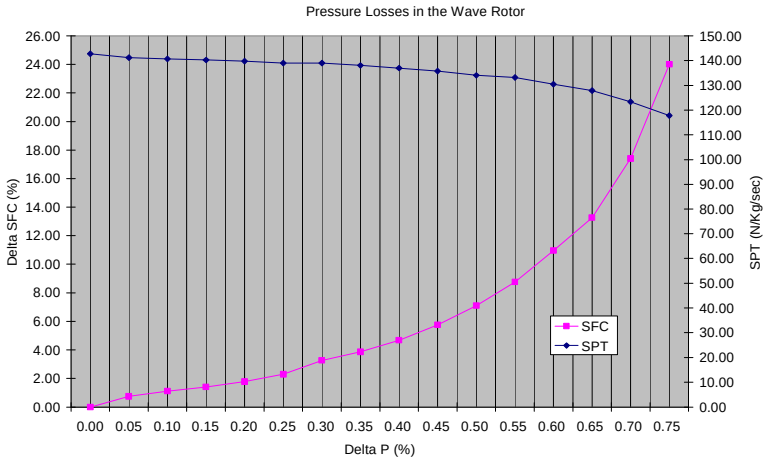

Figure 75 influence of the pressure losses in the ICWR system on the SFC and ST

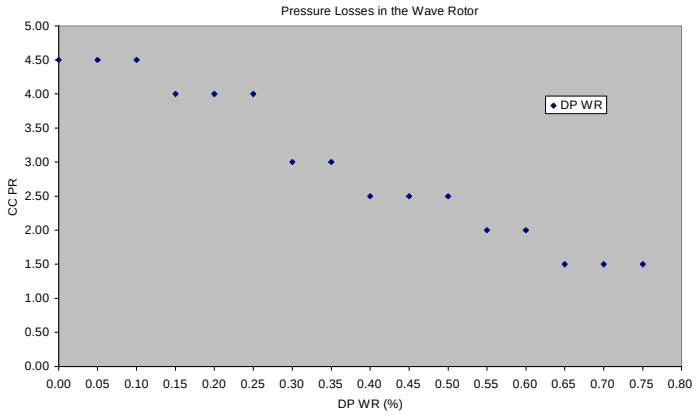

Figure 76 variation of the pressure ratio of the cooling compressor with the pressure losses in the ICWR system

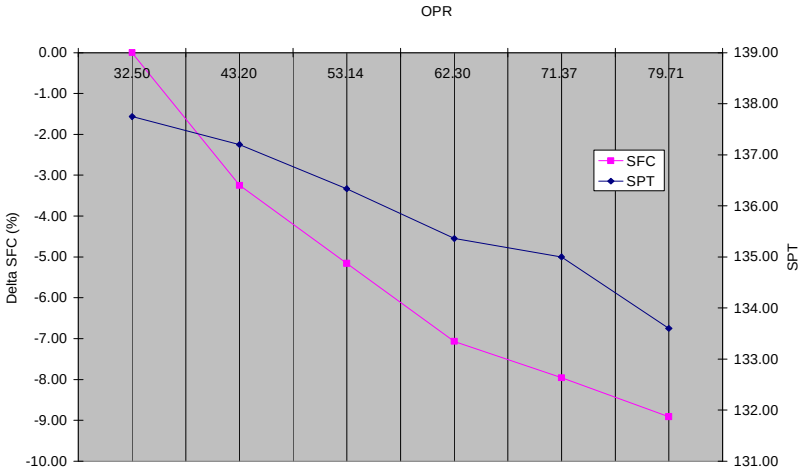

Figure 77 SFC and ST against OPR.

6. Conclusions and Recommendations

6.1 Conclusions

This work describes a method for calculating the direct operating cost of engines that has been validated using data from public sources and also by comparison with already existing and well accredited methods. As we have seen from the results shown, the accuracy of the economic model in DOC estimation is good (within about 15%), considering the great scattering of data that can be found for a very large variety of engines, and so can be adapted for use in the cost analysis of today and future type of engines, such as ultra high bypass ratio turbofans, with little modifications.

A method for calculating the direct operating cost of aero engines has been applied to three different types of configurations of advanced type of turbofans used for long and short range applications: the direct drive, the geared and the counter rotating turbofans. The model shows that, if any type of future engines would be considered economically advantageous, current technology has to be improved and costs of production have to decrease by around 35%, because they are the main driving factors for the cost of operation of engines.

Using the risk module a sensitivity analysis has been done in order to understand the impact of the different economic parameters on the operational costs. Considering today legislation and common core technology for the different VITAL engines the bigger drivers are fuel burn and carbon tax, instead NOx and noise have quite low impact. But we need to keep in mind that for sure the legislation will soon change then a study has been done in order to understand which would be the main drivers in the design of future engines. The analysis has shown that noise will be most probably the main constraint to be taken into consideration.

Weibull distributions have been used into the life analysis of different parts of the engine in order to estimate the cost of maintenance, the direct operating costs (DOC) and net present cost (NPC) of future type turbofan engines.

The Weibull risk assessment has been applied to four different engines of different thrust in order to show the applicability of the method to all type of engines.

Five Weibull distributions have been used for five important sources of interruption of the working life of the engine: Combustor, Life Limited Parts (LLP), High Pressure Compressor (HPC), General breakdowns and High Pressure Turbine (HPT).

As it was shown in the results, the components that are more likely to breakdown are the HPT and the HPC, keeping in mind that general causes of breakdown are very difficult to predict.

The distributions used in the work are the same for all the engines, so the results are quite similar for all of them. But the use of more specified distributions will led to more accurate predictions. In this thesis it has been proved that the Weibull method can be used with great success in forecasting the possible breakdown causes of gas turbines. The analysis of the life of the different components done with the Weibull is one-dimensional and quite general, but it still is useful to help the designer in order to do a risk assessment of the engine.

Optimisation was done on the VITAL engines in order to improve them. It was done using two numerical gradient based techniques. Firstly the *Sequential Quadratic Programming – NLPQL* and secondly the *Mixed Integer Optimization – MOST*; the objectives of the optimisation were two: minimum fuel burn and minimum direct operating costs. Because the engines were already designed for minimum fuel burn, the optimization for minimum fuel burn showed only a slight improvement; instead the results for minimum DOC showed that the engines can be greatly got better, between 2 and 6 percent.

As can also be seen by the input files the new engines cannot achieve the decrease in noise and gaseous emissions required by ACARE. Then it has been presented a parametric study of three possible configurations that could accomplish the task. The three engines are:

- Intercooled recuperated
- Wave rotor topped cycle
- Constant volume combustion

These three cycles have been applied to a characteristic next generation long range aero engine looking for a possible future evolution and searching for benefits on specific thrust fuel consumption, emissions and economics. The parametric study has been applied to TOC (Top of Climb) and cruise conditions, and considering two possible designs:

a) Design for constant specific thrust and

b) Design for constant TET considering the current technology level limit;

Both values correspond to the baseline engine at respective flight conditions.

The study leads to the following conclusions:

a) A significant decrease of specific fuel consumption can be obtained for the new three cycles. These benefits can reach values close to 10%, depending on the cycle.

b) The benefits on SFC can also be translated into benefits on NO_x emissions. An exception is the wave rotor topping cycle which will increase NO_x emissions due to a high increase of maximum cycle pressure and temperature.

c) The case of design condition for constant specific thrust also leads to significant lower engine TETs, which will increase the engine life. These benefits are extremely high in the case of CV cycle.

d) The three cycles will need important technological developments, especially the wave rotor topping cycle and the CV cycle. The intercooled recuperated cycle seems to be the most achievable at the current technological level; we have to keep in mind it comes from typical applications in sea and terrestrial power generation.

e) About the impact of weight in the ICR it can be said:

- The increase of weight and drag can nullify all benefits on SFC for η_R=0.7
- Instead for values of η_R=0.8 or higher, which could represent an achievable value with the appropriate technologic development, important benefits can be got even for important increases of weight and size; a 100% increase of drag translates into an increase of engine diameter of 41%, assuming that the drag goes as the square of the engine diameter.
- The maximum benefits on total fuel consumption correspond to η_R=0.9, but it represents a difficult value to be achieved even in terrestrial application where the weight and size of the heat exchangers do not represent a critical constraint.
- Small heat exchangers and high recuperative efficiencies are essential to obtain all the shown benefits, but they really are a difficult task and will require important further developments. The heat exchanger size could mitigate completely the benefits.
- Heat exchanger reliability and life are also an important concern in the IRC cycle for aero engine application. Any heat exchanger fail could be critical in aircraft propulsion.
- Considering the existing experience on later recuperated engines the author believes that this engine can achieve the ACARE goals of 2020.

6.2 Recommendations for future works

Being a study about future engines, done using the innovative approach of coupling all the main aspects of first design engines, many things can be done in the future.

First of all the lifing code can be improved in several ways. Some suggestions are here mentioned:

- having talked about and described carefully how temperature really affects the results, playing a primary role in the failure mechanism, a useful and recommended improvement would be the implementation of a more sophisticate cooling mechanism;
- Another issue to cope with is the changing in the material mechanical properties with the temperature: this phenomenon is even more evident at elevated temperature, as it is in the 'hot section' of the engine, causing the material to behave totally different from what it would have done at room temperature.
- The lifing analysis can be improved including all the possible type of stress that affect the HPT blades and disk
- And also introducing life analysis of other engine components, like compressor or, for the future configurations, the counter rotating fan, the gear, the wave rotor, the CVC and the heat exchangers.
- The Weibull distributions can be improved using real data for each component of each engine.

Also a risk analysis should be conducted in order to see the impact of different type of legislations on the operating costs.

Detailed performance analysis of the design point and off design point operation of engines fitted with ICWR's. Accounting for the various losses that occur in

ICWR's would lead to better design procedures. Analysis of the noise generated and the various noise abatement techniques that can be used to reduce the aforementioned noise levels need to be investigated.

The types of materials required along with various failure modes and a feasibility study would need to be conducted. This would help engineers decide as to whether ICWR's are reliable and feasible.

Numerically simulating a complete ICWR with combustion along with various losses would need to be conducted. This would need to thorough understanding of the various flow characteristic that are present within a working ICWR.

More work can be done also under the optimisation point of view. Different optimisation techniques could be used and a comparison between the results can be done. An optimisation of the intercooled recuperated, wave rotor and constant volume combustion engines should be done in order to further improve them. A multi trade – off analysis should be done in order to see which kind of design is preferable: one with minimum fuel burn or minimum direct operating costs, and also to see if it is possible to find a configuration that can achieve both results.

6.3 Author's contributions to knowledge

The contribution to knowledge that the author thinks can give to the scientific community with his research comes in two forms:

1. The creation of a tool that can optimise the one dimensional design of aero engines in a new way. Thermo Economic and Risk Analysis (TERA) will be in fact a new way to optimise all the characteristics that are needed to be taking into account in the design of an engine, such as engine and aircraft performance, weight, noise, emissions and the operating costs. In TERA my scope is the creation of an economic and a performance models that can study the operating costs and the

performance of aero engines. The economic model is divided into three modules: a lifing module, a risk module and an economic module.

2. The performance analysis of new cycle engines that can achieve the goals of ACARE to decrease the emissions of CO, NOX and CO_2 by 50%. With the help of TERA the design of this new type of engine will be much facilitated.

References

1. Aircraft Commerce: Issues No. 5, 23, 30, 38, 39, 44
2. Barrett, M. J., Expectations of Closed-Brayton-Cycle Heat Exchangers in Nuclear Space Power Systems, *J. of Propulsion and Power*, 21 (1), January-February 2005, 152-157.
3. Baudier, D. and Piquet, F., 2004. Snecma, a VITAL player. *Snecma Magazine*, November, p.28.
4. Beck, D. S., Optimization of Regenerated Gas Turbines, *J. of Engineering for Gas Turbine and Power*, 118, July 1996, 654-660.
5. Bhargava, R., Bianchi, M., Peretto, A., Spina, P. R., A Feasibility Study of Existing Gas Turbines for Recuperated, Intercooler, an Reheat Cycle, *J. of Engineering for Gas Turbine and Power*, 126, July 2004, 531-544.
6. Cai, R., A new Analysis of Recuperative Gas Turbine Cycles, *Proc. Instn. Mech Engnrs Vol 212 Part A*, 1998, 289-296.
7. Cambier, J. L., Tegner, J. K., Strategies for Pulsed Detonation Engine Performance Optimization, *J. of Propulsion and Power*, 14 (4), July-August 1998, 489-498.
8. Corchero, G., Montañes, J. L., An Approach to the Use of Hydrogen for Commercial Aircraft Engines, *Proc. IMechE Vol. 219 Part G: J. Aerospace Engineering*, 2005, 35-43.
9. Dellenback, P. A., Improved Gas Turbine Efficiency through Alternative Regenerator Configuration, *J. of Engineering for Gas Turbine and Power*, 124, July 2002, 441-446.
10. Environmentally Friendly Aero Engine (VITAL). *Sixth Framework Program of the European Communities*, contract AIP4-CT-2004-012271, 2004.
11. ETBX *Strain-Life Fatigue Analysis* [online]. EngineersToolbox. http://www.engrasp.com/doc/etb/mod/fm1/strainlife/strainlife_help.html
12. Ferguson, C., R., Kirkpatrick, *Internal Combustion Engines, Applied Thermosciences*, John Willey & Son, Inc, New York, 2001, chap. 8.
13. Flight international: Issues no. 5022-5050

14. Haslam “Fracture and fatigue course notes” Cranfield University.
15. Haslam “Mechanical design of turbo machinery course notes” Cranfield University.
16. Heiser, W. H., Pratt, D. T., Thermodynamic Cycle Analysis of Pulse Detonation Engines, *J. of Propulsion and Power*, 18 (1), January-February 2002, 68-76.
17. Henry T. Won and Mark Waters, *Constant Volume Combustor implementation on a 50 passenger Commercial Regional Transport Mission Simulation*, 39th AIAA/ASME/SAE/ASEE Joint Propulsion Conference and Exhibit 20-23 July 2003, Huntsville, Alabama.
18. Hill, P. G., Peterson, C. B., *Mechanics and Thermodynamics of Propulsion*, Addison-Wesley, London, 1965.
19. Howse, M., Rolls-Royce and Gas Turbine,16th *ISABE International Symposium on Air Breathing Engines*, Cleveland, Ohio, USA, September 2003, AIAA paper 2003-1002.
20. http://www.boeing.com/commercial/noise/index.html
21. Jenkinson, Lloyd R. Paul Simpkin, Darren Rhodes: “Civil jet aircraft Design” London: Arnold, 1999.
22. Johnsen, A., Bullock, R. O., Aerodynamic Design of Axial-Flow Compressors, NASA SP-36, 1965, chap. II.
23. Kays, W. M., London, A. L. *Compact Heat Exchangers,* Krieger Publishing Company, Malabar, Florida, 1984.
24. Kentfield, J. A. C., Fundamentals of Idealized Airbreathing Pulse-Detonation Engines, *J. of Propulsion and Power*, 18 (1), January-February 2002, 77-83.
25. Kentfield, J. A. C., Regenerative Turbofans; A Comparison with Non regerative Units, *J. of Aircraft*, 12 (3), March 1975, 174-181.
26. Klug, H. G., Reinhard, F., CRYOPLANE: Hydrogen Fuelled Aircraft – Status and Challenges, *Air&Space Europe*, 2001, 3 (3), 252-254.
27. Lefebvre, A. H., Fuel Effects on Gas Turbine Combustion-Liner Temperature, Pattern Factor, and Pollutants Emissions, *J. of Aircraft*, 21(11), November 1984, 887-898.
28. Lefebvre, A. H., *Gas Turbine Combustion*, Taylor & Francis,

Philadelphia, London, 1998.

29. Lenoble G. Performance Analysis of a Wave Rotor Topping Unit with Constant Volume Combustion, Cranfield University MSc Thesis, 2008
30. Lewis, G. D., A new Understanding of NOx formation, 10th *ISABE International Symposium on Air Breathing Engines*, Nottingham, England, 1991, paper ISABE 91-7064.
31. Liquid Hydrogen Fuelled Aircraft – System Analysis (CRYOPLANE), Part B Proposal GRD1-1999-10014, *Fifth Framework Program of the European Communities*, contract G4RD-CT-2000-00192, June 1999.
32. Liu, F., Sirignano, W. A., Turbojet and Turbofan Engine Performance Increases through Turbine Burners, *J. of Propulsion and Power*, 17 (3), May-June 2001, 695-705.
33. Management for technology course notes Cranfield University.
34. Manson, S. S., 1965. Fatigue: A Complex Subject—Some Simple Approximations. Experimental Mechanics. *Journal Society For Experimental Stress Analysis*, 5 (7),193–226.
35. Martinez-Frias, J., Aceves, S. M., Brandt, H., Thermodynamic Analysis of Zero- Atmospheric Emissions Power Plant, *J. of Engineering for Gas Turbine and Power*, 126, January 2004, 2-8.
36. Mattingly, J. D., Heiser, W. H., Prat, D. T., *Aircraft Engine Design*, AIAA Education Series, American Institute of Aeronautics and Astronautics, Inc, Reston, Virginia, 2002.
37. Meggiolaro, J.T.P. Castro: “Statistical evaluation of strain-life fatigue Crack initiation predictions”, 2004, International Journal of Forecasting
38. Missirlis, D., et al, Experimental and Numerical Investigation of Flow Field through a Heat Exchanger for Aero-engine Applications, *Int. J. of Heat and Fluid Flow*, 26, 2005, 440-458.
39. Nagashima, T., Okamoto, K., Simple Numerical Modelling for Gasdynamic Design of Wave Rotors, *J. of Propulsion and Power*, 23 (1), January-February 2007, 99-107.
40. Nalim, M. R., Assessment of Combustion Modes for Internal Combustion Wave Rotors, *J. of Engineering for Gas Turbine and Power*, April 1999, 121, 265-271

41. Nalim, M. R., Paxson, D. E., A Numerical Investigation of Premixed Combustion in Wave Rotors, NASA TM-107242, 41st *Gas Turbine and Aero engine Congress*, Birmingham, UK, June 10.13, 1996, paper ASME-96-GT-116.
42. Nalim, M. R., Thermodynamic Limits of Work and Pressure Gain in Combustion and Evaporation Processes, *J. of Propulsion and Power*, 18 (6), November-December 2002, 1176-1182.
43. Nalim, R. M., Resler Jr, E. L., Wave Cycle Design for Wave Rotor Gas Turbine Engines with Low NOx Emissions, *J. of Engineering for Gas Turbine and Power*, July 1996,118, 474-480.
44. New Aero Engine Concept (NEWAC). *Sixth Framework Programme of the European Communities*, 2006.
45. Paxson, D. E., Lindau, W. J., Numerical Assessment of Four-Port Through-Flow wave Rotor Cycles with Passage Height Variation, NAS TM-107490, 33rd *Joint Propulsion Conference and Exhibit*, Seattle, Washington, July 1997.
46. Paxson, D. E., Nalim, M. R., Modified Through-Flow Wave-Rotor Cycle with Combustor- Bypass Ducts, *J. of Propulsion and Power*, 151 (3), May-June 1999, 462-467.
47. Paxson, D. E., Numerical Simulation of Dynamic Wave Rotor Performance, *J. of Propulsion and Power*, 12 (5), September-October 1996, 949-957.
48. Pilidis “Gas turbine performance course notes” Cranfield University.
49. Ramsden “Turbo machinery course notes” Cranfield University.
50. Resler Jr, E. L., Moscari, J. C., Nalim, M. R., Analytic Design Methods for Wave Rotor Cycles, *J. of Propulsion and Power*, 10 (5), Sept.-Oct. 1994, 683-689.
51. Roskam, Jan: “Airplane design. Part VIII, Airplane cost estimation: design, Development, manufacturing and operating” Ottawa, Kansas: Roskam Aviation and Engineering Corporation, 1990.
52. Rubini, P., 2006. *Turbine Blade Cooling*. MSc course notes. Cranfield University.
53. Saravanamamuttoo, H. I. H., *Gas Turbine Theory*, Pearson, England,

2001.

54. Sawyer, W. J., Sawyer's *Gas Turbine Engineering Handbook*, Gas Turbine Publications, Inc, Stamford, Connecticut, USA, 1972.
55. Sehra, A. K., Shin, J., Revolutionary Propulsion Systems for 21st Century Aviation, NASA TM-2003-212615, I*nternational Gas Turbine Congress 2003*, Tokyo, Japan, November 2-7, 2003, paper IGTC03-ABS-066b.
56. Sirignano, W. A., Liu, F., Performance Increases for Gas-Turbine Engines through Combustion inside the Turbine, *J. of Propulsion and Power*,15(1), January-February 1999, 111-118.
57. Smith, C. P., The environmental Challenge – Bringing Technology to Market, 17th *ISABE International Symposium on Air Breathing Engines*, Munich, Germany, September 2005, paper ISABE-2005-1008.
58. Smith, C.F., Snyder, P.H., Emmerson, C.W. Nalim, M.R., *Impact of the CVC on a Supersonic Turbofan Engine*, 38th AIAA/ASME/SAE/ASEE Joint Propulsion Conference & Exhibit 7-10 July 2002, Indianapolis, Indiana.
59. Sourmail, T., no date. *Coatings for Turbine Blades* [online]. University of Cambridge. Available from: http://www.msm.cam.ac.uk/phase-trans/2003/Superalloys/coatings/index.html [Accessed July 2006].
60. Steffen, K., Walter, R., Driving the Technological Edge in Airbreathing Propulsion, 16th *ISABE International Symposium on Air Breathing Engines*, Cleveland, Ohio, USA, September 2003, AIAA paper 2003-1002.
61. TERA high level specification document
62. Thomas N. R. Preliminary Design and Analysis of an Internal Combustion Wave Rotor, Cranfield University MSc Thesis, 2008
63. Vigna Suria O., "*A Flexible Lifing Model for Gas Turbines: Creep and Low Cycle Fatigue Approach",* Cranfield University, master thesis, 2006.
64. Walsh, P. P., Fletcher, P., *Gas Turbine Performance*, Blackwell Science, Ltd, London, 1998.
65. Weekly Petroleum Status Report/Energy Information Administration January 2005, February 2006

66. Welch, G. E., Jones, S. M., Paxson, D. E., Wave-Rotor-Enhancement Gas Turbine Engines, *J. of Engineering for Gas Turbine and Power*, 119, April 1997, 469-477.
67. Welch, G. E., Macroscopic Balance Model for Wave Rotor, *J. of Propulsion and Power*, 13 (4), July-August 1997, 508-516.
68. Welch, G. E., Paxson, D. E., Wave-Rotor-Enhanced Gas Turbine Engine Demonstrator, NASA TM-1999-209459, *Gas Turbine Operation and Technology for Land, Sea and Air Propulsion and Power System Symposium*, Ottawa, Canada, October 18-21, 1999.
69. Welch, G. E., Wave Engine Topping Cycle Assessment, NASA TM-107371, 35th *Aerospace Science Meeting and Exhibit*, paper AIAA-97-0707, Reno, Nevada, January 1997.
70. Wilson, J., an Experiment on Losses in a Three-Port Wave Rotor, NAS CR-19508, 1997.
71. Wilson, J., Paxson, D. E., Jet Engine Performance Enhancement through Use of a Wave-Rotor Topping Cycle, NASA TM-4486, 1993.
72. Wilson, J., Paxson, D. E., Wave Rotor Optimization for Gas Turbine Engine Topping Cycles, *J. of Propulsion and Power*, 12 (4), July-August 1996,778-785.
73. Wulff, A., Hourmouziadis,J., An Universal Combustor Model for the Predictions of Pollutant Emissions, 15th *ISABE International Symposium on Air Breathing Engines,* paper ISABE 99-7162, 1999.
74. www.icaodata.com
75. www.weibull.com
76. Yakinthos, et al, Optimization of the Design of Recuperative Heat Exchangers in the Exhaust Nozzle of an Aero-Engine, *Appli Math Mod*, 2006, doi: 10.1016/J.a.p.m.2006.10.008.

Appendix A – Economic Model Input Files

! EcoModuleInput.dat

! Input file for the Economic Program

! This file requires both user defined variables for a given power plant/aircraft. It has been separated into SR and LR

! Some of the parameters are regularly updated parameters during the optimisation done and explained in paragraph 5.4. In red are shown the parameters obtained by other modules and passed to the economic through iSight and then changed during the optimisation.

```
BASELR                  : Engine configuration
Rene80              :blade MATERIAL
Rene95              :disk material
23000               :TBO (Hr) (This value is used when the Lifing cannot do the  calculations)
316.296000             :Take-off Thrust,AcToFN (kN)
7.877100                        :Block Time,AcBlockTime (Hr)
5879.780000                     :Plant Cost,PCost (k€)
82533.090000         :WEIGHT OF FUEL USED,AcBlockFuel (Kg)
817                             :Fuel density (Kg/cubic meter)
27000                           :Threshold for the Carbon Tax (Kg)
5                               :Carbon Tax Charge (€/kg)
12048.410000         :BLOCK DISTANCE (RBL),AcBlockRng (Km)
0.005                           :INSURANCE PERCENTAGE (ISP)
103.210000             :EPNLarr (dB)
99.                 :EPNLdep (dB)
24419.485400         :NOX, MNoxLto (g)
0.8222                          :exchange rate $ -> € (ROC)
22.065300               :D/Foo CO, DFCO (-)
30                              :EXPECTED OPERATING ENGINE LIFE (NYEARS)
1                   :NUMBER OF SCENARIOS
5.                              :NOX TAX CHARGE (€/kg)
172.                            :FUEL PRICE (FP)
0.1                             :INTEREST PERCENTAGE (IP)
0.02                            :INFLATION (INF)
89.9                :NOISE TAX Limit (dB)
100                 :Unit of cost of Decibel (€/dB)
1.5                             :NOX FACTOR (B)
10.                             :DOWNTIME
70.                             :MAINTENANCE labour Rate Per Man Hour (RLENG) (€/Hr)
1                               :Selector of IP (1:constant for every scenario; 2:change every scenario)
2                               :SELECTOR OF FUEL PRICE
2                               :SELECTOR OF NOX FACTOR
2                               :SELECTOR OF DOWNTIME
2                               :SELECTOR OF INFLATION
2                               :SELECTOR OF MAINTENANCE labour RATE PER MAN HOUR
2                               :Selector of Threshold for the Carbon Tax (Kg)
2                               :Selector of NOISE TAX Limit
2                               :selector of weibull
60.                             :Minimum Value of FUEL Price (c$/US gallon)
200.                            :Maximum Value OF FUEL PRICE
0.05                            :Minimum Value of INTEREST PERCENTAGE
0.2                             :Maximum Value OF INTEREST PERCENTAGE
0.01                            :Minimum Value of INFLATION
0.03                            :Maximum Value OF INFLATION
1.1                             :Minimum Value of NOX FACTOR
2.                              :Maximum Value OF NOX FACTOR
1.                              :Minimum Value of DOWNTIME (days)
90.                             :Maximum Value OF DOWNTIME
50.                             :MINIMUN Value of Maintenance labour Rate Per Man Hour
70.                             :MAXIMUM Value of Maintenance labour Rate Per Man Hour
21000.              :minimum Value of Threshold for the Carbon Tax (Kg)
27000.              :Maximum Value of Threshold for the Carbon Tax (Kg)
89.                 :MINIMUN VALUE OF NOISE TAX Limit
94.                 :Maximum Value of NOISE TAX Limit
```

Below are shown the typical input file for the lifing module, first for creep with analysis of the stresses for the blades and the disk of the high pressure

turbine that is the element in a gas turbine that most limit the life of the engine and then the input data necessary for the analysis of fatigue also applied to the blades of the high pressure turbine:

! blade_stress_input.dat

```
1               :number of section the blade has been split into
0.347156        :inner radius
0.392258        :outer radius
0.000273        :inner cross area
0.000191        :outer cross area
```

!disc_input.dat

```
1.        :disc type selector (1 = constant thickness disc; 2 = varying thickness disc)
1.        :rim stress selector (1 = Rim stress to be calculated using the blade stress subroutine; 2 = Rim stress
to be calculated knowing number of blades, balde mass and radius of the centre of gravity; 3 = rim stress known)
0.694311            :rim diameter
0.171014             :bore diameter
0.030068            :disc constant thickness
68.000000             :number of blades
4.                  :number of rings into which the disc is discretized
0.09820             :inner radius (m) of the first ring
0.03710             :thickness (m) of the first ring
0.12840             :inner radius (m) of the second ring
0.02000             :thickness (m) of the second ring
0.15590             :inner radius (m) of the third ring
0.00930             :thickness (m) of the third ring
0.27670             :inner radius (m) of the fourth ring
0.01836             :thickness (m) of the fourth ring
0.32150             :radius (m) of the boundary
0.01836             :thickness (m) of the boundary
```

! indat_creep.dat

```
3.        :number of segments into which the flight envelope has been split
221.098000          :HPT rpm @ design point
1.             :blade stress selector (1 = stress unknown, a stress subroutine will calculate it; 2 = stress known)
1.             :disk stress selector (1 = stress unknown, a stress subroutine will calculate it; 2 = stress known)
1.        :cooling selector (1 = blade cooled; 2 = no cooling)
0.5       :cooling effectiveness
150.      :Delta of Temperature due to Termal Barrier Coating on the blade
1.             :blade Larson-Miller selector (1 = insert values to be interpolated; 2 = LMP known for each segment)
1.             :disk Larson-Miller selector (1 = insert values to be interpolated; 2 = LMP known for each segment)
0.980000            :relative rpm during the climb
0.914550            :relative rpm acting during the cruise
0.807730            :relative rpm acting during the descent
923.660000            :cooling temperature during climb
830.630000            :cooling temperature during cruise
710.960000            :cooling temperature during descent
1888.000000           :temperature in K acting during the climb
1640.000000           :temperature in K acting during the cruise
1278.000000           :temperature in K acting during the descent
16.001550            :time in hours spent during the climb
339.655600             :time in hours spent during the cruise
21.267750            :time in hours spent during the descent
```

If the stresses are known for each segment for the blade and/or the disk put below all the stresses in MPa first for the blade and/or then for the disk, the same applies if the Larson-Miller parameter for each segment of flight is known. First put all the stresses and then all the LMPs for the blade and then do the same for the disk

! Indat_fatigue.dat

```
288.                        :Ambient temperature in Kelvin
2011.000000                 :Component maximum operating temperature in Kelvin
1.                          :cooling selector (1 = blade cooled; 2 = no cooling)
997.240000                  :cooling flow temperature
0.5                         :cooling effectiveness
150                         :delta temperature for coating
```

! INPUTweibull.txt

```
5      :NUMBER OF DISTRIBUTIONS
0.0        :ETA HPT
0.12       :ETA COMBUSTOR
0.20        :ETA LLP
0.22      :ETA HPC
0.45      :ETA GENERAL
6      :BETA HPT
4.5    :BETA COMBUSTOR
4      :BETA LLP
3      :BETA HPC
1.5    :BETA GENERAL
```

! material_database.txt

```
DSCM247              :Material specifier
 20.0                    :Larson Miller (LM) constant
  6                  :Number of data in LM curve
    51.84    20.5   :LM curve (stress in (Ksi)). LM parameters in decreasing order.
    50.1     30.0   :
    48.0     47.0   :
    46.9     55.0   :
    45.9     65.0   :
    44.9     74.0   :
 8910.0             :Material density (kg/m^3)
 1                  :No data in yield stress (ys) curve. Temp. in K. ys in MPa
   300.00  890.0    :
  215000.0              :Elastic modulus of the material in MPa
  0.15                  :Fatigue ductility coefficient in mm
  1573.0      :Fatigue strength coefficient in MPa
  -0.08                 :Fatigue strength exponent
  -0.59                 :Fatigue ductility exponent
  11.0E-6           :Linear coefficient of thermal expansion in mm/°C
  0.29                  :Poisson's ratio
 1           :LM equation selector (1 = equation in Imperial Units, 2 = equation in SI)
!---------------------------------
Nimo118             :Material specifier
 20.0                    :Larson Miller (LM) constant
  6                  :Number of data in LM curve
    28.7     80.0   :LM curve (stress in (MPa)). LM parameters in decreasing order
    28.4     90.0   :
    28.0    100.0   :
    27.0    150.0   :
    26.4    200.0   :
    25.7    250.0   :
 8190.0             :Material density (kg/m^3)
 1                  :No data in yield stress (ys) curve. Temp. in K. ys in MPa
   300.00  800.0    :
  222000.0              :Elastic modulus of the material in MPa
  0.40                  :Fatigue ductility coefficient in mm
  1820.0      :Fatigue strength coefficient in MPa
  -0.08                 :Fatigue strength exponent
  -0.59                 :Fatigue ductility exponent
  12.7E-6           :Linear coefficient of thermal expansion in mm/°C
  0.32                  :Poisson's ratio
 2           :LM equation selector (1 = equation in Imperial Units, 2 = equation in SI)
!---------------------------------
MarM247             :Material specifier
 20.0                    :Larson Miller (LM) constant
  6                  :Number of data in LM curve
    53.1     11.5   :LM curve (stress in (Ksi)). LM parameters in decreasing order.
    49.0     30.0   :
    46.56    50.0   :
    44.0     66.0   :
    42.5     84.0   :
    41.0    100.0   :
 8540.0             :Material density (kg/m^3)
 1                  :No data in yield stress (ys) curve. Temp. in K. ys in MPa
   300.00  827.0    :
  221000.0              :Elastic modulus of the material in MPa
  0.177                 :Fatigue ductility coefficient in mm
  1351.0      :Fatigue strength coefficient in MPa
  -0.12                 :Fatigue strength exponent
  -0.6                  :Fatigue ductility exponent
  11.0E-6           :Linear coefficient of thermal expansion in mm/°C
  0.29                  :Poisson's ratio
 1           :LM equation selector (1 = equation in Imperial Units, 2 = equation in SI)
!---------------------------------
IMI_829            :Material specifier
 20.0                    :Larson Miller (LM) constant
  0                 :Number of data in LM curve
 4540.0             :Material density (kg/m^3)
 1                  :No data in yield stress (ys) curve. Temp. in K. ys in MPa
   300.00  996.7    :
  109000.0              :Elastic modulus of the material in MPa
  0.5                   :Fatigue ductility coefficient in mm
  1913.3      :Fatigue strength coefficient in MPa
  -0.10                 :Fatigue strength exponent
  -0.69                 :Fatigue ductility exponent
   9.5E-6           :Linear coefficient of thermal expansion in mm/°C
  0.33                  :Poisson's ratio
 1          :LM equation selector (1 = equation in Imperial Units, 2 = equation in SI)
!---------------------------------
Inco718             :Material specifier
```

```
 25.0                  :Larson Miller (LM) constant
  6                   :Number of data in LM curve
    36      50.0    :LM curve (stress in (MPa)). LM parameters in decreasing order.
    34      100.0   :
    32      172.0   :
    30      303.0   :
    28      400.0   :
    26      500.0   :
 8220.96             :Material density (kg/m^3)
 1                  :No data in yield stress (ys) curve. Temp. in K. ys in MPa
   300.00  1122.64  :
  205000.0              :Elastic modulus of the material in MPa
  0.35                  :Fatigue ductility coefficient in mm
  1736.0      :Fatigue strength coefficient in MPa
  -0.08                 :Fatigue strength exponent
  -0.59                 :Fatigue ductility exponent
  11.5E-6           :Linear coefficient of thermal expansion in mm/°C
  0.29                  :Poisson's ratio
 2            :LM equation selector (1 = equation in Imperial Units, 2 = equation in SI)
!-----------------------------------
Rene95              :Material specifier
 20.0                :Larson Miller (LM) constant
 6                   :Number of data in LM curve
    30       50.0   :LM curve (stress in (MPa)). LM parameters in decreasing order
    28.4    100.0   :
    26.3    300.0   :
    25      500.0   :
    23      620.0   :
    21      850.0   :
 8248.64             :Material density (kg/m^3)
 1                  :No data in yield stress (ys) curve. Temp. in K. ys in MPa
   300.00  1274.99  :
218000.0            :Elastic modulus of the material in MPa
 0.15                :Fatigue ductility coefficient in mm
 1785.0              :Fatigue strength coefficient in MPa
 -0.08               :Fatigue strength exponent
 -0.59               :Fatigue ductility exponent
 11.3E-6                 :Linear coefficient of thermal expansion in mm/°C
 0.3                 :Poisson's ratio
 2            :LM equation selector (1 = equation in Imperial Units, 2 = equation in SI)
!-----------------------------------
Udimet720           :Material specifier
 20.0                :Larson Miller (LM) constant
 6                   :Number of data in LM curve
    29.9     50.0   :LM curve (stress in (MPa)). LM parameters in decreasing order.
    28.8    100.0   :
    27.7    200.0   :
    26      300.0   :
    25      400.0   :
    24      700.0   :
 8080.0              :Material density (kg/m^3)
 1                  :No data in yield stress (ys) curve. Temp. in K. ys in MPa
  300 1150.0 :
220000.0            :Elastic modulus of the material in MPa
 0.15                :Fatigue ductility coefficient in mm
 1561.0              :Fatigue strength coefficient in MPa
 -0.08               :Fatigue strength exponent
 -0.59                 :Fatigue ductility exponent
 12E-6                 :Linear coefficient of thermal expansion in mm/°C
 0.3                 :Poisson's ratio
 2            :LM equation selector (1 = equation in Imperial Units, 2 = equation in SI)
!-----------------------------------
 Waspalloy           :Material specifier
 20.0                 :Larson Miller (LM) constant
 6                   :Number of data in LM curve
    30.3       50.0   :LM curve (stress in (MPa)). LM parameters in decreasing order.
    28.2    100.0   :
    27.1    200.0   :
    25.4    327.5   :
    23.7    517.0   :
    21.5    700.0   :
 8190.0              :Material density (kg/m^3)
 1                  :No data in yield stress (ys) curve. Temp. in K. ys in MPa
   294.26   792.86  :
211000.0            :Elastic modulus of the material in MPa
 0.15                :Fatigue ductility coefficient in mm
 1118.0              :Fatigue strength coefficient in MPa
 -0.08               :Fatigue strength exponent
 -0.59               :Fatigue ductility exponent
 12.2E-6             :Linear coefficient of thermal expansion in mm/°C
 0.3                 :Poisson's ratio
 2            :LM equation selector (1 = equation in Imperial Units, 2 = equation in SI)
!-----------------------------------
 CMSX4               :Material specifier
 20.0                 :Larson Miller (LM) constant
 6                   :Number of data in LM curve
    30.9    120.0   :LM curve (stress in (MPa)). LM parameters in decreasing order
    30.2    137.2   :
    29.4    160.0   :
    28.8    200.0   :
    27.5    300.0   :
    26.9    392.0   :
 8700.0              :Material density (kg/m^3)
 8                   :No data in yield stress (ys) curve. Temp. in K. ys in MPa
  297.15   942.0    :
250000.0            :Elastic modulus of the material in MPa
 0.15                :Fatigue ductility coefficient in mm
 1413.0              :Fatigue strength coefficient in MPa
 -0.08               :Fatigue strength exponent
 -0.59               :Fatigue ductility exponent
 11E-6               :Linear coefficient of thermal expansion in mm/°C
 0.3                 :Poisson's ratio
```

```
 2            :LM equation selector (1 = equation in Imperial Units, 2 = equation in SI)
!----------------------------------
 ReneN5              :Material specifier
 20.0                 :Larson Miller (LM) constant
 6                   :Number of data in LM curve
    29.4    141.0    :LM curve (stress in (MPa)). LM parameters in decreasing order.
      28    237.0    :
      27    324.0    :
      26    427.0    :
      25    549.0    :
      24    676.0    :
 8630.0              :Material density (kg/m^3)
 1                   :No data in yield stress (ys) curve. Temp. in K. ys in MPa
   300.00  1260      :
 219000.0            :Elastic modulus of the material in MPa
 0.17                :Fatigue ductility coefficient in mm
 1770.0              :Fatigue strength coefficient in MPa
 -0.1                :Fatigue strength exponent
 -0.61               :Fatigue ductility exponent
 11.8E-6             :Linear coefficient of thermal expansion in mm/°C
 0.3                 :Poisson's ratio
 2            :LM equation selector (1 = equation in Imperial Units, 2 = equation in SI)
!----------------------------------
Rene80              :Material specifier
 20.0                :Larson Miller (LM) constant
 6                   :Number of data in LM curve
    31.4       50    :LM curve (stress in (MPa)). LM parameters in decreasing order
    30.2      100    :
      29      150    :
   28.04      200    :
   27.24      250    :
   26.52      300    :
 8160.0              :Material density (kg/m^3)
 1                   :No data in yield stress (ys) curve. Temp. in K. ys in MPa
   300.00  1274.99   :
 217000.0            :Elastic modulus of the material in MPa
 0.16                :Fatigue ductility coefficient in mm
 1780                :Fatigue strength coefficient in MPa
 -0.09               :Fatigue strength exponent
 -0.60               :Fatigue ductility exponent
 11.5E-6             :Linear coefficient of thermal expansion in mm/°C
 0.3                 :Poisson's ratio
 2            :LM equation selector (1 = equation in Imperial Units, 2 = equation in SI)
```

Appendix B – Economic Model Output Files

Amongst the outputs the economic model would give are:

- Direct operating cost, DOC (k€)
- Engine maintenance cost (k€)
- Net present cost, NPC.

The NPC would be obtained over a time frame defined by the user to depict the engine operating life.

A typical output from the economic model is show below:-

! EcoModuleOutput.dat

```
*********************************************************************
 OUTPUT, Courtesy of:
 09-APR-08
 13:08:45
 Configuration:  BASELR
*********************************************************************
ANNUAL UTILIZATION /YEAR (Hr)                              =   4400.000
COST OF LANDING FEES /FLIGHT (k€)                          =   1.380000
COST OF NAVIGATIONAL FEES /FLIGHT (k€)                     =   5.168192
COST OF GROUND HANDLING CHARGES /FLIGHT (k€)               =   3.30000
XXXXXXXXXXXXX SCENARIO STUDIES XXXXXXXXXXXXXXXXXXXX
 SCENARIO =1

XXXXXXXXXXXXXXX SUMMARY OF RESULTS FOR YEAR 1 XXXXXXXX
Labour/Eng/BlockHr (k€/Hr)              =  0.6296688
NOx Tax (k€/Flight)                     =  0.1868091
CarbonTax (k€/Flight)                   =   283.2188
Mtrls/Eng/BlockHr (k€/Hr)               =  0.2746555
DoCMtce/Eng/Hr (k€/Hr)                  =  0.9043242
DoC/Eng/Yr (k€/Year)                    =   123957.1
CFUEL/Yr (k€/Year)                      =   14350.40
NoiseTax (k€/Flight)                            =   9.143278
AirportTax (k€/Year)                    =   103854.9
XXXXXXXXXXXXXXXXXXXXXXXXXXXXXXXXXXXXXXXXXXXXXXX

WEIBULL TIME BETWEEN OVERHAUL =   995.0844
ENGINE NPC FOR          30  YEARS (k€)   =       17347
```

Below it is given a typical output used to generate the cumulative curve from the economic model with the risk model changing all the variables apart from the IP for 10000 scenarios.

!NPCoutput.dat

```
ENGINE NPC
 MAXIMUM NPC (k€) =       7924
 MINIMUM NPC (k€) =       7666
 LENGHT OF INTERVALS =         23
 Medium value of interval (k€) frequency (%) cumulative frequency (%)
               7677                   3                   3
               7700                   1                   4
               7723                   8                  12
               7746                  18                  30
```

```
                7769                  28                  58
                7792                   8                  66
                7815                  19                  85
                7838                   6                  91
                7861                   0                  91
                7884                   6                  97
                7907                   1                  98
```

!blade_stress_output.dat

```
sec_cf_load =    21060.91
 tot_cf_load =   21060.91      0.0000000E+00
 cf_stress =   236.6395      0.0000000E+00
 sigma_cf =   236.6395
 sigma_cf_approx =   240.6961
```

!disc_output.dat

```
solution of equation           1  =   1.5741477E+08
 solution of equation           2  =    366787.0
 sigma_r_bore =  0.0000000E+00
 sigma_r_rim =   33.51949
 sigma_h_bore =   297.9690
 sigma_h_rim =   108.6580
 sigma_eq_rim =   96.37402
```

!outdat_creep.dat

```
total blade creep life         =   305.6255     hrs

 Blade Stress (MPa)                354.30              308.55              240.70
 Blade Temperature (K)            1255.83             1085.31              844.48
 Blade Time spent (hrs)              0.27                5.66                0.35
 Blade LMP                          26.52               26.52               27.39
 Blade Time to failure (hrs)        13.11            27246.09           **********
 Blade Life fraction           0.02034707          0.00020777          0.00000000

 total disc creep life        =  5.9832259E-06 hrs

  Disc Stress (MPa)     438.61              381.97              297.97
 Disc Temperature (K)             1888.00             1640.00             1278.00
 Disc Time spent (hrs)               0.27                5.66                0.35
 Disc LMP                           25.40               25.77               26.32
 Disc Time to failure (hrs)          0.00                0.00                3.94
 Disc Life fraction            **********          **********          0.08991954
```

! Outdat_fatigue.dat

```
The temperature in K after cooling is:    1217.500
 The temperature difference acting on the component after cooling is: 929.5000
 The average temperature difference acting on the component is:    779.5000
 Numbers of block hours to failure (for the blades)                  =                                   38577.14
```

Appendix C: Turbomatch input files

TRENT 772

```
! OPR = 35.8 at TO; % Power Setting - TO==100%,
Climb out == 85%, Approach = 30%, Idle == 7%
! Rated Output at TO = 316.3KN; BPR = 5.03; Mass
flow = 919kg/s; TET (operations)= 1700; TET (type
test-incl allowance for overshoot, deterioration
etc)= 1810
////
OD SI KE CT FP
-1
-1
INTAKE  S1-2        D1-4         R100
COMPRE  S2-3        D5-10        R110     V5   V6
PREMAS  S3,4,20     D11-14                V11
MIXEES  S20,24,21
DUCTER  S21,22      D15-18       R120
NOZCON  S22,23,1    D19          R130
COMPRE  S4-5        D20-25       R140     V20   V21
PREMAS  S5,6,24     D26-29
PREMAS  S6,7,25     D90-93
COMPRE  S7-8        D30-35       R150     V30   V31
DUCTER  S8-9        D36-39       R160
PREMAS  S9,10,19     D40-43
PREMAS  S10,11,26    D95-98
BURNER  S11-12       D44-46       R170
MIXEES  S12,19,13
TURBIN  S13-14      D47-54,150            V48
TURBIN  S14-15      D60-67,140            V61
TURBIN  S15-16      D80-87,110            V81
DUCTER  S16-17      D69-72       R190
NOZCON  S17,18,1    D73          R200
OUTPBD              D110,140,145
PERFOR  S1,0,0  D74-77,130,100,120,200,0,170,0,0,0
CODEND

TRENT 772 DATA
////
1 10668.0                ! INTAKE DATA : ALTITUDE !
INTAKE
2 10.0                  ! DEV FROM STANDARD TEMP
3 0.82                  ! MA-NUMBER
4 0.995                 ! PRESSURE RECOVERY
5 0.90178                 ! COMP : Z ! FAN
6 0.9951                 ! RELATIVE ROTATIONAL SPEED
7 1.925                 ! PRESSURE RATIO (OPR=44)
8 0.82302               ! ISENTROPIC EFFICIENCY
9 0.0                  ! ERROR SELECTOR
10 1.0                 ! MAP-NUMBER
11 0.184                ! LAMBDA(BPR=5.03 @ TO, 4.435
TOC) ! BYPASS split
12 0.0                 ! DELTA
13 0.93                 ! LAMBDA
14 0.0                 ! DELTA
15 0.0                 ! NO REHEAT ! FAN DUCT
16 0.0                ! DELTA(P)/Pin
17 0.0                 ! COMBUSTION EFFICIENCY
18 0.0                 ! FUEL FLOW LIMIT
19 -1.0                ! AREA FIXED !FAN NOZZLE
20 0.88197                ! Z  ! BOOSTER
21 0.9484               ! DESIGN SPEED PCN
22 5.736              ! PRESSURE RATIO(OPR=35.8 AT TO)
23 0.87055               ! ISENTROPIC EFFICIENCY
24 1.0                 ! ERROR SELECTION
25 2.0                 ! MAP-NUMBER
26 1.0                    ! LAMBDA W  ! HANDLING AIR
BLEED. Typically 10% from core during descent and
idle
27 0.0                 ! DELTA W
28 1.0                 ! LAMBDA P
29 0.0                 ! DELTP
90 1.000               ! LAMBDA W  ! CABIN AIR BLEED
91 -1.50               ! Cabin air bleed (2.5kg/s@low
alt and about 1.5kg/s at high alt)
92 1.0               ! Lambda P
93 0.000               ! DELTP
30 0.62217                ! COMP : Z  !HPC COMPRESSOR
31 1.0               ! RELATIVE ROTATIONAL SPEED
32 4.546                ! PRESSURE RATIO(OPR=46.45)
33 0.88453                ! ISENTROPIC EFFICIENCY
34 1.0                 ! ERROR SWITCH
35 5.0                 ! MAP-NUMBER
36 0.0                 ! NO REHEAT  !HPC OUTLET DUCT
37 0.0                ! DELTA (P)/PIN
38 0.0                 ! COMBUSTIONEFFICIENCY
39 0.0                 ! FUEL FLOW LIMIT
40 0.8                ! LAMBDA W  !HPC COOLING BLEED
41 0.0                 ! DELTA W
42 1.0                 ! LAMBDA P
43 0.0                 ! PRESSURE LOSS
95 1.000               ! LAMBDA W  ! CABIN AIR BLEED
96 0.000                ! Cabin air bleed (2.5kg/s@low
alt and about 1.5kg/s at high alt)
97 1.000               ! Lambda P
98 0.000               ! DELTP
44 0.05                ! BURNER: PRESSURE LOSS
45 0.99                ! COMB. EFF.
46 -1.0                ! FUEL FLOW
47 0.0                      ! TURBINE DATA: AUXWORK
!TURBINE-HPT
48 0.7                 ! DESIGN NON DIM FLOW / MAX
49 0.7                 ! DESIGN NON DIM SPEED
50 0.88025                ! ISENTROPIC EFF
51 -1.0                ! ROT SPEED OF PT
52 3.0                 ! NUMBER OF COMPRESSOR DRIVEN
53 3.0                 ! MAP NUMBER
54 -1.0                ! POWER LAW INDEX
60 156600.0              ! TURBINE DATA: AUXWORK  !IP
TURBINE
61 0.6                 ! DESIGN NON DIM FLOW / MAX
62 0.7                 ! DESIGN NON DIM SPEED
63 0.89695                ! ISENTROPIC EFF
64 -1.0                ! ROT SPEED OF PT
65 2.0                 ! NUMBER OF COMPRESSOR DRIVEN
66 3.0                 ! MAP NUMBER
67 -1.0                ! POWER LAW INDEX
69 0.0                 !NO  REHEAT !CORE EXHAUST DUCT
70 0.01                !DELTA
71 0.0                 !COMBUSTION EFFICIENCY
72 0.0                 !FUEL FLOW LIMIT
!CORE EXHAUST NOZZLE
73 -1.0                !AREA FIXED
!PERFORMANCE
74 -1                  ! POWER(-1=TURBOJET/FAN)
75 -1                  ! PROPELLER EFFICIENCY
76 0.0                 ! SCALING INDEX
77 0.0
!TURBINE FOR FAN
80 0.0                    ! TURBINE DATA: AUXWORK  !LP
TURBINE
81 0.5                 ! DESIGN NON DIM FLOW / MAX
82 0.55                 ! DESIGN NON DIM SPEED
83 0.90858                ! ISENTROPIC EFF
84 -1.0                ! ROT SPEED OF PT
85 1.0                 ! NUMBER OF COMPRESSOR DRIVEN
86 3.0                 ! MAP NUMBER
87 -1.0                ! POWER LAW INDEX
-1
1  2    400.0        !INLET AIR MASS FLOW
12  6   1705.0        !Turbine inlet temperature
-1
```

CRTFLR

```
! OPR = 52,09 @ TOC; % Power Setting - TO==100%,
Climb out == 85%, Approach = 30%, Idle == 7%
! Rated Output at TOC = 67.429KN; BPR = 9,24; Mass
flow = 511,16
////
OD SI KE CT FP
-1
-1
INTAKE  S1-2        D1-4         R100
COMPRE  S2-3        D5-10        R110     V5   V6
PREMAS  S3,4,19     D11-14                V11
MIXEES  S19,25,20
DUCTER  S20,21      D15-18       R120
NOZCON  S21,22,1    D19          R130
ARITHY              D80-87
COMPRE  S4-5        D20-25       R140     V20
PREMAS  S5,6,25     D26-29
PREMAS  S6,7,23     D55-58
COMPRE  S7-8        D30-35       R150     V30   V31
PREMAS  S8,9,24     D36-39
PREMAS  S9,10,18    D40-43
BURNER  S10-11      D44-46       R170
MIXEES  S11,18,12
TURBIN  S12-13      D47-54,150            V48
DUCTER  S13-14      D218-221
ARITHY              D88-94
TURBIN  S14-15      D60-67,145            V61
DUCTER  S15-16      D69-72       R190
NOZCON  S16,17,1    D73          R200
OUTPBD              D110,140,145
PERFOR  S1,0,0  D74-77,130,100,170,200,0,120,0,0,0
CODEND

SNM DATA
```

```
////
1 10668.0                  ! INTAKE DATA : ALTITUDE !
INTAKE
2 10.0                      ! DEV FROM STANDART TEMP
3 0.82                      ! MA-NUMBER
4 1.0                     ! PRESSURE RECOVERY
5 0.97                    ! COMP : Z ! FAN
6 1.12                      ! RELATIVE ROTATIONAL SPEED
7 1.55                      ! PRESSURE RATIO (OPR=52.09 @
ToC )
8 0.828                   ! ISENTROPIC EFFICIENCY
9 0.0                     ! ERROR SELECTOR
10 1.0                    ! MAP-NUMBER
11 0.09766                  ! LAMBDA(BPR=9.24) ! BYPASS
split
12 0.0                    ! DELTA
13 1.075                    ! LAMBDA
14 0.0                    ! DELTA
15 0.0                    ! NO REHEAT ! FAN DUCT
16 0.0                   ! DELTA(P)/Pin
17 0.0                    ! COMBUSTION EFFICIENCY
18 0.0                    ! FUEL FLOW LIMIT
19 -1.0                   ! AREA FIXED !FAN NOZZLE
20 0.6                    ! Z  ! BOOSTER
21 0.5                    ! DESIGN SPEED PCN
22 1.92         ! PRESSURE RATIO((OPR=52.09 AT TOC))
23 0.85                    ! ISENTROPIC EFFICIENCY
24 1.0                    ! ERROR SELECTION
25 1.0                    ! MAP-NUMBER
26 1.0                  ! LAMBDA W  ! HANDLING AIR BLEED
27 0.0                    ! DELTA W
28 1.0                    ! LAMBDA P
29 0.0                    ! DELTP
55 1.0                  ! LAMBDA W  ! CABIN AIR BLEED
56 0.0                    ! Cabin air bleed (2.5kg/s@low
alt and about 1.5kg/s at high alt)
57 1.0                  ! Lambda P
58 0.0                  ! DELTP
30 0.8                   ! COMP : Z  !HPC COMPRESSOR
31 1.12                   ! RELATIVE ROTATIONAL SPEED
32 29.5                  ! PRESSURE RATIO(OPR=52.09 )
33 0.92                    ! ISENTROPIC EFFICIENCY
34 1.0                    ! ERROR SWITCH
35 5.0                    ! MAP-NUMBER
36 1.0                  ! LAMBDA W  ! CABIN AIR BLEED
37 0.0                    ! Cabin air bleed (2.5kg/s@low
alt and about 1.5kg/s at high alt)
38 0.9                  ! Lambda P
39 0.0                  ! DELTP
40 0.78                    ! LAMBDA W  !HPC BLEED
41 0.0                    ! DELTA W
42 0.95                    ! LAMBDA P
43 0.06                    ! PRESSURE LOSS
44 0.05                   ! BURNER: PRESSURE LOSS
45 0.99                   ! COMB. EFF.
46 -1.0                   ! FUEL FLOW
47 123040.0        ! TURBINE DATA: AUXWORK
!TURBINE-HPT
48 0.3                    ! DESIGN NON DIM FLOW / MAX
49 0.8                    ! DESIGN NON DIM SPEED
50 0.94                   ! ISENTROPIC EFF
51 -1.0                   ! ROT SPEED OF PT
52 3.0                    ! NUMBER OF COMPRESSOR DRIVEN
53 3.0                    ! MAP NUMBER
54 -1.0                   ! POWER LAW INDEX
218 0.0                   !NO  REHEAT !CORE EXHAUST DUCT
219 0.0                   !DELTA
220 0.0                    !COMBUSTION EFFICIENCY
221 0.0                    !FUEL FLOW LIMIT
60 0.0                    ! TURBINE DATA: AUXWORK
!LP TURBINE
61 0.6                    ! DESIGN NON DIM FLOW / MAX
62 0.4                    ! DESIGN NON DIM SPEED
63 0.938                   ! ISENTROPIC EFF
64 -1.0                   ! ROT SPEED OF PT
65 1.0                    ! NUMBER OF COMPRESSOR DRIVEN
66 3.0                    ! MAP NUMBER
67 -1.0                   ! POWER LAW INDEX
69 0.0                    !NO  REHEAT !CORE EXHAUST DUCT
70 0.0                   !DELTA
71 0.0                    !COMBUSTION EFFICIENCY
72 0.0                    !FUEL FLOW LIMIT
!CORE EXHAUST NOZZLE
73 -1.0                   !AREA FIXED
!PERFORMANCE
74 -1                     ! POWER(-1=TURBOJET/FAN)
75 -1                     ! PROPELLER EFFICIENCY
76 0.0                    ! SCALING INDEX
77 0.0
!ARITHY:BOOSTER SPEED=FAN SPEED* K
80  3.0                   !multiply
81 -1.0
82  21.0                  !booster SPEED
83 -1.0
84  6.0                   !fan     SPEED
85 -1.0
86  87                    ! K
87  1                     ! value of K
!ARITHY:LPTWORK=BOOSTER WORK+FAN WORK
88  1.0                   !ADD
89 -1.0
90  145.0                 !LPT WORK
91 -1.0
92  110.0                 !FAN WORK
93 -1.0
94  140.0                 !BOOSTER WORK
-1
1  2    511.16      !INLET AIR MASS FLOW
11  6   1750        !TET
-1
```

DDTFLR

```
! OPR = 60.118 at TOC; % Power Setting - TO==100%,
Climb out == 85%, Approach = 30%, Idle == 7%
! Rated Output at TOC = 67.42918KN; BPR = 13.85;
Mass flow = 601.87;
////
OD SI KE CT FP
-1
-1
INTAKE  S1-2        D1-4         R100
COMPRE  S2-3        D5-10        R110     V5   V6
PREMAS  S3,4,20     D11-14               V11
MIXEES  S20,24,21
DUCTER  S21,22      D15-18       R120
NOZCON  S22,23,1    D19          R130
COMPRE  S4-5        D20-25       R140     V20   V21
PREMAS  S5,6,24     D26-29
PREMAS  S6,7,25     D90-93
COMPRE  S7-8        D30-35       R150     V30   V31
DUCTER  S8-9        D36-39       R160
PREMAS  S9,10,19     D40-43
PREMAS  S10,11,26    D95-98
BURNER  S11-12       D44-46       R170
MIXEES  S12,19,13
TURBIN  S13-14      D47-54,150           V48
TURBIN  S14-15      D60-67,140           V61
TURBIN  S15-16      D80-87,110           V81
DUCTER  S16-17      D69-72       R190
NOZCON  S17,18,1    D73          R200
OUTPBD              D110,140,145
PERFOR  S1,0,0  D74-77,130,100,120,200,0,170,0,0,0
CODEND

DDTFLRDATA
////
1 10668.0              ! INTAKE DATA : ALTITUDE
! INTAKE
2 10.0                  ! DEV FROM STANDARD TEMP
3 0.82                  ! MA-NUMBER
4 1.0                 ! PRESSURE RECOVERY
5 0.65                  ! COMP : Z ! FAN
6 0.95                  ! RELATIVE ROTATIONAL SPEED
7 1.497                 ! PRESSURE RATIO (OPR=60.118)
8 0.927                 ! ISENTROPIC EFFICIENCY
9 0.0                   ! ERROR SELECTOR
10 1.0                  ! MAP-NUMBER
11 0.06734        ! LAMBDA(BPR=13.85) ! BYPASS split
12 0.0                  ! DELTA
13 0.91                  ! LAMBDA
14 0.0                  ! DELTA
15 0.0                  ! NO REHEAT ! FAN DUCT
16 0.0                 ! DELTA(P)/Pin
17 0.0                  ! COMBUSTION EFFICIENCY
18 0.0                  ! FUEL FLOW LIMIT
19 -1.0                 ! AREA FIXED !FAN NOZZLE
20 0.90                  ! Z  ! BOOSTER
21 1.15                 ! DESIGN SPEED PCN
22 10.07         ! PRESSURE RATIO(OPR=60.118 AT TOC)
23 0.851                 ! ISENTROPIC EFFICIENCY
24 1.0                  ! ERROR SELECTION
25 1.0                  ! MAP-NUMBER
26 1.0               ! LAMBDA W  ! HANDLING AIR BLEED.
Typically 10% from core during descent and idle
27 0.0                  ! DELTA W
28 1.0                  ! LAMBDA P
29 0.0                  ! DELTP
90 1.000                ! LAMBDA W  ! CABIN AIR BLEED
91 0.0                  ! Cabin air bleed (2.5kg/s@low
alt and about 1.5kg/s at high alt)
92 1.0                ! Lambda P
93 0.000                ! DELTP
30 0.95                 ! COMP : Z  !HPC COMPRESSOR
31 1.1                ! RELATIVE ROTATIONAL SPEED
32 3.987983             ! PRESSURE RATIO(OPR=51.011)
33 0.89                 ! ISENTROPIC EFFICIENCY
34 1.0                  ! ERROR SWITCH
35 5.0                  ! MAP-NUMBER
36 0.0                  ! NO REHEAT  !HPC OUTLET DUCT
37 0.0                ! DELTA (P)/PIN
38 0.0                  ! COMBUSTIONEFFICIENCY
39 0.0                  ! FUEL FLOW LIMIT
40 0.8                ! LAMBDA W  !HPC COOLING BLEED
41 0.0                  ! DELTA W
42 0.96                  ! LAMBDA P
43 0.0                  ! PRESSURE LOSS
95 1.000                ! LAMBDA W  ! CABIN AIR BLEED
96 0.00                  ! Cabin air bleed (2.5kg/s@low
alt and about 1.5kg/s at high alt)
97 1.0                ! Lambda P
98 0.000                ! DELTP
```

```
44 0.05                ! BURNER: PRESSURE LOSS
45 0.998                ! COMB. EFF.
46 -1.0                ! FUEL FLOW
47  123040.0                 !  TURBINE  DATA:  AUXWORK
!TURBINE-HPT
48 0.8                ! DESIGN NON DIM FLOW / MAX
49 0.6                ! DESIGN NON DIM SPEED
50 0.95               ! ISENTROPIC EFF
51 -1.0               ! ROT SPEED OF PT
52 3.0                ! NUMBER OF COMPRESSOR DRIVEN
53 3.0                ! MAP NUMBER
54 -1.0               ! POWER LAW INDEX
60 0.0          ! TURBINE DATA: AUXWORK
!IP TURBINE
61 0.7                ! DESIGN NON DIM FLOW / MAX
62 0.58                ! DESIGN NON DIM SPEED
63 0.94               ! ISENTROPIC EFF
64 -1.0               ! ROT SPEED OF PT
65 2.0                ! NUMBER OF COMPRESSOR DRIVEN
66 3.0                ! MAP NUMBER
67 -1.0               ! POWER LAW INDEX
69 0.0                !NO  REHEAT !CORE EXHAUST DUCT
70 0.05               !DELTA
71 0.0                !COMBUSTION EFFICIENCY
72 0.0                !FUEL FLOW LIMIT
!CORE EXHAUST NOZZLE
73 -1.0               !AREA FIXED
!PERFORMANCE
74 -1                 ! POWER(-1=TURBOJET/FAN)
75 -1                 ! PROPELLER EFFICIENCY
76 0.0                ! SCALING INDEX
77 0.0
!TURBINE FOR FAN
80 0.0                   ! TURBINE DATA: AUXWORK  !LP
TURBINE
81 0.9                ! DESIGN NON DIM FLOW / MAX
82 0.3                ! DESIGN NON DIM SPEED
83 0.95               ! ISENTROPIC EFF
84 -1.0               ! ROT SPEED OF PT
85 1.0                ! NUMBER OF COMPRESSOR DRIVEN
86 3.0                ! MAP NUMBER
87 -1.0               ! POWER LAW INDEX
-1
1  2    601.87        !INLET AIR MASS FLOW
12  6   1910.0        !Turbine inlet temperature
-1
```

GTFLR

```
!  OPR  =  58.3  @  TOC;  %  Power  Setting  -  TO==100%,
Climb out == 85%, Approach = 30%, Idle == 7%
! Rated Output at TOC = 67.43 kN; BPR = 12.45; Mass
flow = 575.58kg/s
////
OD SI KE CT FP
-1
-1
INTAKE  S1-2        D1-4         R100
COMPRE  S2-3        D5-10        R110     V5   V6
PREMAS  S3,4,19     D11-14               V11
MIXEES  S19,25,20
DUCTER  S20,21      D15-18       R120
NOZCON  S21,22,1    D19          R130
ARITHY              D80-87
COMPRE  S4-5        D20-25       R140     V20
PREMAS  S5,6,25     D26-29
PREMAS  S6,7,23     D55-58
COMPRE  S7-8        D30-35       R150     V30   V31
PREMAS  S8,9,24     D36-39
PREMAS  S9,10,18    D40-43
BURNER  S10-11      D44-46       R170
MIXEES  S11,18,12
TURBIN  S12-13      D47-54,150           V48
DUCTER  S13-14      D218-221
ARITHY              D88-94
TURBIN  S14-15      D60-67,145           V61
DUCTER  S15-16      D69-72       R190
NOZCON  S16,17,1    D73          R200
OUTPBD              D110,140,145
PERFOR  S1,0,0  D74-77,130,100,170,200,0,120,0,0,0
CODEND

mtu DATA
////
1 10668.0                 ! INTAKE DATA : ALTITUDE !
INTAKE
2 10.0                 ! DEV FROM STANDART TEMP
3 0.82                ! MA-NUMBER
4 1.0                ! PRESSURE RECOVERY
5 0.7                ! COMP : Z ! FAN
6 1.04                ! RELATIVE ROTATIONAL SPEED
7 1.517                ! PRESSURE RATIO (OPR=58.3)
8 0.911                ! ISENTROPIC EFFICIENCY
9 0.0                ! ERROR SELECTOR
10 1.0                ! MAP-NUMBER
11 0.07435        ! LAMBDA(BPR=12.45) ! BYPASS split
12 0.0                ! DELTA
13 0.86                ! LAMBDA
14 0.0                ! DELTA
15 0.0                ! NO REHEAT ! FAN DUCT
16 0.0                ! DELTA(P)/Pin
17 0.0                ! COMBUSTION EFFICIENCY
18 0.0                ! FUEL FLOW LIMIT
19 -1.0               ! AREA FIXED !FAN NOZZLE
20 0.8                ! Z  ! BOOSTER
21 1.02                ! DESIGN SPEED PCN
22 2.527               ! PRESSURE RATIO(((OPR=58.3))
23 0.91                ! ISENTROPIC EFFICIENCY
24 1.0                ! ERROR SELECTION
25 4.0                ! MAP-NUMBER
26 1.0             ! LAMBDA W  ! HANDLING AIR BLEED
27 0.0                ! DELTA W
28 1.0                ! LAMBDA P
29 0.0                ! DELTP
55 1.0              ! LAMBDA W  ! CABIN AIR BLEED
56 0.0                ! Cabin air bleed (2.5kg/s@low
alt and about 1.5kg/s at high alt)
57 1.0              ! Lambda P
58 0.0              ! DELTP
30 0.9               ! COMP : Z  !HPC COMPRESSOR
31 0.98               ! RELATIVE ROTATIONAL SPEED
32 15.21              ! PRESSURE RATIO (OPR=58.3)
33 0.8853             ! ISENTROPIC EFFICIENCY
34 1.0                ! ERROR SWITCH
35 5.0                ! MAP-NUMBER
36 1.0              ! LAMBDA W  ! CABIN AIR BLEED
37 0.0                ! Cabin air bleed (2.5kg/s@low
alt and about 1.5kg/s at high alt)
38 1.0              ! Lambda P
39 0.0              ! DELTP
40 0.75               ! LAMBDA W  !HPC BLEED
41 0.0                ! DELTA W
42 1.0                ! LAMBDA P
43 0.0                ! PRESSURE LOSS
44 0.05               ! BURNER: PRESSURE LOSS
45 0.99               ! COMB. EFF.
46 -1.0               ! FUEL FLOW
47  123030.0                 !  TURBINE  DATA:  AUXWORK
!TURBINE-HPT
48 0.2                ! DESIGN NON DIM FLOW / MAX
49 0.7                ! DESIGN NON DIM SPEED
50 0.92               ! ISENTROPIC EFF
51 -1.0               ! ROT SPEED OF PT
52 3.0                ! NUMBER OF COMPRESSOR DRIVEN
53 1.0                ! MAP NUMBER
54 -1.0               ! POWER LAW INDEX
218 0.0               !NO  REHEAT !CORE EXHAUST DUCT
219 0.0               !DELTA
220 0.0                !COMBUSTION EFFICIENCY
221 0.0                !FUEL FLOW LIMIT
60 0.0                ! TURBINE DATA: AUXWORK
!LP TURBINE
61 0.9               ! DESIGN NON DIM FLOW / MAX
62 0.3                ! DESIGN NON DIM SPEED
63 0.934               ! ISENTROPIC EFF
64 -1.0               ! ROT SPEED OF PT
65 1.0                ! NUMBER OF COMPRESSOR DRIVEN
66 1.0                ! MAP NUMBER
67 -1.0               ! POWER LAW INDEX
69 0.0                !NO  REHEAT !CORE EXHAUST DUCT
70 0.02               !DELTA
71 0.0                !COMBUSTION EFFICIENCY
72 0.0                !FUEL FLOW LIMIT
!CORE EXHAUST NOZZLE
73 -1.0               !AREA FIXED
!PERFORMANCE
74 -1                 ! POWER(-1=TURBOJET/FAN)
75 -1                 ! PROPELLER EFFICIENCY
76 0.0                ! SCALING INDEX
77 0.0
!ARITHY:BOOSTER SPEED=FAN SPEED* K
80  3.0               !multiply
81 -1.0
82  21.0              !booster SPEED
83 -1.0
84  6.0               !fan     SPEED
85 -1.0
86  87                ! K
87  1                 ! value of K
!ARITHY:LPTWORK=BOOSTER WORK+FAN WORK
88  1.0               !ADD
89 -1.0
90  145.0             !LPT WORK
91 -1.0
92  110.0             !FAN WORK
93 -1.0
94  140.0             !BOOSTER WORK
-1
1  2    575.58       !INLET AIR MASS FLOW
11  6   1888.        !TET
-1
```

Constant Volume Combustion Turbofan

```
SIMULATION OF WAVE ROTOR DETONATION COMBUSTOR BY
SEPARATING THE WAVE ROTOR AND THE CONSTANT VOLUME
COMBUSTOR
WAVE ROTOR SIMULATED BY A VIRTUAL (4 Spools)
```

```
////
OD SI KE VA FP
-1
-1
INTAKE  S1-2         D1-4            R100
COMPRE  S2-3         D5-11           R101   V5    V6
PREMAS  S3,4,18      D12-15                 V12
NOZCON  S18-19,1     D20             R103
COMPRE   S4-5           D21-27             R104    V21
V22
PREMAS  S5,6,20      D35-38
COMPRE   S20-21         D28-34             R105    V28
V29
PREMAS  S21,22,23    D39-42
COMPRE  S6-7         D110-116      R106   V110  V111
BURNER  S7-8         D43-45          R107
ARITHY               D46-52          R108
ARITHY               D53-59
TURBIN  S8-9         D117-124,106,125       V118
MIXEES  S9,22,10
DUCTER  S10-11           D130-133
ARITHY               D134-140
TURBIN  S11-12       D60-67,145,68          V61
MIXEES  S12,23,13
TURBIN  S13-14       D69-76,104,77          V70
TURBIN  S14-15       D78-85,101,86          V79
DUCTER  S15-16       D16-19
NOZCON  S16-17,1     D87             R109
ARITHY               D92-99
PERFOR        S1,0,0                              D88-
91,103,100,0,109,0,107,0,0,0
CODEND
////
 ! INTAKE - Aeroplane inlet
  1    10686.000
  2        10.000
  3        0.820
  4        1.0
!Fan
  5        0.850
  6        1.00
  7        1.517
  8        0.911
  9        0.000
 10        1.000
 11        0.
 ! PREMAS -  Bypass - Main
 12        0.07435    ! BPR=12.45
 13        0.000
 14        1.000
 15        0.0
 !Bypass Convergent Nozzle
 20       -1.000
 !  IP COMPRESSOR
 21        0.850
 22        1.000
 23        2.450000000 !
 24        0.898046820
 25        1.000
 26        4.000
 27        0.
 !  HPT Turbine COOLING BYPASS
 35        0.75
 36        0.000
 37        1.000
 38        0.0
!  COMPRESSOR for cooling air
 28        0.850
 29        1.000
 30        2.25
 31        0.91
 32        1.000
 33        5.000
 34        0.
 !  PREMAS FOR COOLING
 39        0.66
 40        0.0
 41        1.0
 42        -0.01
!VIRTUAL COMPRESSOR: wave rotor
110        0.850
111        1.000
112        1.8
113        0.83
114        1.
115        5.000
116        0.
!  BURNER
 43        0.0
 44        0.998
 45       -1.000
!  CONSTANT VOLUME ARITHY I
 46        4.
 47        -1
 48        108     !TET/CIT
 49        8
 50        6
 51        7
 52        6
! CONSTANT VOLUME ARITHY II
 53        3.
 54        8
 55        4        !P8=P8*TET/CIT
 56        8
 57        4
 58        -1
 59        108
!VIRTUAL TURBINE
117        0.000
118        0.800
119        0.600
120        0.83
121       -1.000
122        4.000
123        1.000
124       -1.000
125        0.000
!  Ducter
 130        000
 131        0.5
 132        0.000
 133        0.0
 !  TURBINE-HP
 60        150000.0
 61        0.800
 62        0.600
 63        0.88
 64       -1.000
 65        4.000
 66        1.000
 67       -1.000
 68        0.000
 !  TURBINE-IP
 69        0.000
 70        0.800
 71        0.600
 72        0.88
 73       -1.000
 74        2.000
 75        1.000
 76       -1.000
 77        0.000
 !  TURBINE-LP
 78        0.000
 79        0.800
 80        0.600
 81        0.93
 82       -1.000
 83        1.000
 84        1.000
 85       -1.000
 86        0.000
! NOZZLE duct
 16        0.000
 17        0.15
 18        0.000
 19        0.0
 !  Core CONVERGENT NOZZLE
 87       -1.000
 !  PERFORMANCE
 88       -1.000
 89       -1.000
 90        0.000
 91        0.000
!ARITHY FOR THE GAMMA CORRECTION OF FUEL FLOW
92   4.
93   -1
94   107
95   -1
96   107
97   -1
98   99
99   1.33            !GAMMA OF HOT GASES
!ARITHY: HPTW=VCW+CCW
134 1.0
135 -1
136 145    !HPTW
137 -1
138 105    !VCW
139 -1
140 106    !CCW
-1
  1   2  575.6
  8   6  1825
-1
-3
```

Appendix D: iSight

ISight is the integrator and optimizer that have been used in order to put together all the different modules (performance, aircraft, weight, plant costs, noise, emissions, economics and environmental) that were needed in order the 0-dimension analysis of the advanced engines presented in this work. Below is done a short presentation of what is iSight.

ISight is a generic software shell that improves productivity in the design process. In iSight, design problems are specified, and simulation codes from multiples disciplines are coupled, in a description file. After a description file is created, you can use the iSight interface to set up, monitor, and analyse a design run.

The iSight Graphical User Interface (GUI) is comprised of four modules that address different aspects of specifying, formulating, monitoring, and analysing a design problem. Figure 78 illustrate the four iSight modules.

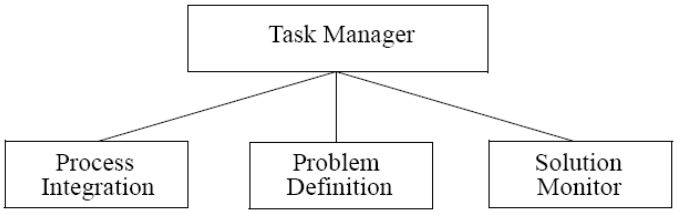

Figure 78 iSight Modules [iSight]

D.1 Task Manager

The main iSight interface is the Task Manager. From here you can launch any of the iSight interfaces. Task Manager also allows you to set up and run a design problem.

D.2 Process Integration

Process Integration is the iSight module that enables you to couple simulation programs to iSight and specifies their execution sequence. Process Integration provides a GUI that acts as a front end for creating an iSight description file.

A subcomponent of Process Integration, Advanced Parser, conveys information to iSight that is needed to provide inputs for simulation programs as well as read outputs. The Advanced Parser interface provides a set of buttons to allow easy navigation within input and output files, regardless of their format, and without writing code. Another parsing interface, Fast Parser, is also available.

D.3 Problem Definition

Problem Definition is a collective term for three iSight interfaces: the Parameters dialog box, the Task Plan dialog box, and the Database dialog box. These interfaces provide a convenient mean for defining problem formulation information.

Problem Definition also includes the design exploration tools used by iSight to reach an optimum during design exploration. The following tools are available in iSight:

- Optimisation
- Design of Experiments (DOE)
- Quality Engineering Methods (QEM)
- Multi-criteria Trade-off Analysis (MTA)
- Approximation

- Knowledge Rules

D.4 Solution Monitor

Solution Monitor provides a visual mean to monitor the design process as it moves through the design space. Solution Monitor provides several tables and graphs that can be used to view the runtime changes.

Appendix E - PUBLICATIONS

CONFERENCES:

- "*An Economic and Risk Analysis Model for Aircraft and Engines*". **Pascovici**, **D.S.**, Colmenares, F., Ogaji, and Pilidis, P. ASME Turbo Expo 2007 GT2007 – 27236.
- "*A Preliminary Parametric Study for Geared, Intercooler and/or Recuperated Turbofan for Short Range Civil Aircrafts*". F. Colmenares, **D.S. Pascovici**, S.O.T. Ogaji, P. Pilidis. ASME Turbo Expo 2007 GT2007 – 27234.
- "*Operating Cost and Risk Analysis for Aircraft and Engines*". Pascovici, D.S., Colmenares, F., Ogaji, S.O.T., and Pilidis, P. ISABE 2007 – 1106.
- "*A Feasibility Study for Future Aero Engines*". Colmenares, F., Gomez, J., **Pascovici, D.S.,** Ogaji, S.O.T. ISABE 2007 – 1194.
- "*Weibull Distributions Applied to Cost and Risk Analysis for Aero Engines*", **Pascovici**, **D.S.**, Colmenares, F., Ogaji, and Pilidis, P. ASME Turbo Expo 2008 GT2008-51060.
- "*EVA – A Tool for EnVironmental Assessment of Novel Propulsion Cycles*", K. G. Kyprianidis, F. Colmenares, **D.S. Pascovici**, S.O.T. Ogaji, P. Pilidis, A. Kalfas. ASME Turbo Expo 2008 GT2008-50602.
- "*Future Aero-Engines' Optimisation for Minimal Operating Costs*", F. Colmenares, **D.S. Pascovici**, S.O.T. Ogaji, P. Pilidis. ASME Turbo Expo 2008 GT2008-50127.

Journals:

- *"Overview of coupling noise prediction for turbofan with engine and aircraft performance*", **D.S. Pascovici**, S. Sorato, S.O.T. Ogaji, P. Pilidis, Proc. IMechE, Part G: J. Aerospace Engineering, 2008, **222**(G4), 515-529.

- *"Investigating the emissions and performance of High Bypass Ratio aero-engines"*, S. Sorato, **D.S. Pascovici**, S.O.T. Ogaji, P. Pilidis, Proceedings of the Institution of Mechanical Engineers, Part G: Journal of Aerospace Engineering, vol. 222(G4), 463-471.
- *"An Inside into some Innovative Cycles for Aircraft Propulsion",* G. Corchero, J. L. Montañés, **D.S. Pascovici**, S. Ogaji, *Proc. IMechE, Part G: J. Aerospace Engineering*, 2008, **222**(G6), 731-747.

Appendix F – Equations Used in the Economic Module

F.1 Economic Module

The main equations used in the economic module are taken from Roskam, only the factors have been changed in order to match the trends of the costs of current engines.

NUMBER OF AIRFRAME MAINTENANCE HOURS/BLOCK HOURS:

```
MHRMAPBL = (OEW**(1/3.1))/10.5
```

Number of hour of annual utilization for short range engines (for long range the value is fixed at 4400):

```
UANNBL = 1000*(3.4536*TBL+2.994-SQRT(12.289*TBL**2-5.6626*TBL+8.964))
```

COST OF CREW /FLIGHT (k€):

```
CCREW = 4*TBL*(NP/35*CCS+2*CFCM)/1000        short range
CCREW = 2*TBL*(NP/35*CCS+2*CFCM)/1000        long range
```

COST OF LANDING FEES /FLIGHT (k€):

```
CLF0 = 0.006*MTO/1000
```

COST OF NAVIGATIONAL FEES /FLIGHT (k€):

```
CNF0 = RBL/5*SQRT(MTO/50000)/1000
```

COST OF GROUND HANDLING CHARGES /FLIGHT (k€):

```
CGHC = 11*NP/1000
```

NUMBER OF ENGINE MAINTENANCE HOURS NEEDED PER BLOCK HOUR PER ENGINE:

```
MHRMENGBL = 24.8*TT0/HEM+0.936
```

ATTAINED PERIOD BETWEEN ENGINE OVERHAUL FACTOR:

```
KHEM = 0.021*HEM/100+0.769
```

Cost of labour per engine:

```
CLABENG = MHRMENGBL*RLENG
```

Cost of fuel:

```
CPOL = 1.05*WF*FP/FD
```

Cost of flight:

```
DOCFLT = CCREW*1000+CPOL
```

engine price:

```
EP = PC*(1+DOWNTIME/(HEM+DOWNTIME))*1000
```

Cost of the Materials for the Engine:

```
CMATENG = (5E-05*EP*ESPPF)/KHEM      short range
CMATENG = (2.5E-05*EP*ESPPF)/KHEM    long range
```

Cost of maintenance:

```
DOCMAINTENG = CLABENG+CMATENG
```

Direct Operating Costs

```
((CPOL+TAXN+NOXTAX+CarbonTax)*355+IP*EP*1.6*ESPPF+ISP*EP*ESPPF+DOCMAINTENG*UANNBL)*NA/10
00
```

Net Present Cost

```
NPCENG = NPCENG+DOCENG/(1+IP)**I
```

F.2 Gaussian Distribution Module

```
double precision FUNCTION VARIABILE (MINVAR,MAXVAR)        !Subroutine for the Gaussian distribution

          INTEGER :: I
double precision:: X,MINVAR,MAXVAR,STADEV,V1,V2,V3,V4,V5,V6,V7,V8,V9,V10,V11

          STADEV=(MAXVAR-MINVAR)/6.0   ! Standar Deviation
          V1=MINVAR
          V2=MINVAR+STADEV
          V3=MINVAR+2.0*STADEV
          V4=MINVAR+2.5*STADEV
          V5=MINVAR+3.0*STADEV
          V6=MINVAR+3.5*STADEV
          V7=MINVAR+4.0*STADEV
          V8=MINVAR+4.5*STADEV
          V9=MINVAR+5.0*STADEV
          V10=MINVAR+5.5*STADEV
          V11=MINVAR+6.0*STADEV

    call random_seed ()

          DO I =1,10000

                    call RANDOM_NUMBER (x)   ! Put random number (0.0<=x<1.0) into x

                        if (x<=0.005) then
                                VARIABILE=V1

               else if (x<=0.015) then
                                VARIABILE=V2

                                else if (x<=0.085) then
                                VARIABILE=V3

                                else if (x<=0.155) then
                                VARIABILE=V4

                                else if (x<=0.325) then
                                VARIABILE=V5

                                else if (x<=0.495) then
                                VARIABILE=V6

                                else if (x<=0.665) then
                                VARIABILE=V7

                                else if (x<=0.835) then
                                VARIABILE=V8

                                else if (x<=0.905) then
                                VARIABILE=V9

                                else if (x<=0.985) then
                                VARIABILE=V10

                                else if (x<1.0) then
                                VARIABILE=V11

                                endif
    ENDDO

          end FUNCTION VARIABILE
```

F.3 Weibull Distribution Module

```
subroutine weibull(HEM1,HEMPROB,component)

    implicit none
    INTEGER :: I,N,J
    double precision :: HEMPROB,HEM1
    real :: U
    CHARACTER (LEN = 10) :: component
    integer :: a(1)
    double precision,ALLOCATABLE :: X(:),BETA(:),ALFA(:),ETA(:)
```

```
    OPEN(100,FILE='INPUTweibull.txt',STATUS='UNKNOWN', ACTION = 'READ')

READ(100,*)N

ALLOCATE (X(N),BETA(N),ALFA(N),ETA(N))

DO I=1,N
   READ(100,*) ETA(I)
ENDDO

DO I=1,N
   ALFA(I) = HEM1*(1+ETA(I))
ENDDO

DO I=1,N
   READ(100,*) BETA(I)
ENDDO

   call random_seed ()
   DO I=1,N
      call random_number (U)   ! random number (0.0<U<1.0); U = reliability function
      X(I)= ALFA(I)*(-ALOG(U))**(1/BETA(I))   ! x = variate
   ENDDO

   HEMPROB=MINVAL(X)

   a=minloc(x)

   IF (minval(a)==1) COMPONENT = 'HPT'
  IF (minval(a)==2) COMPONENT = 'Burner'
   IF (minval(a)==3) COMPONENT = 'LLP'
   IF (minval(a)==4) COMPONENT = 'HPC'
   IF (minval(a)==5) COMPONENT = 'General'

CLOSE(100)
    End subroutine Weibull
```

F.4 Fatigue Module

```
! This algorithm will be able to predict low cycle fatigue life of an engine component, using the Neuberg method,
together with the Coffin-Manson Rule
! The material features has to be know and typed as inputs

Subroutine thermal_fatigue (fatigue_life_blade,blade_material_properties,time_cyc)

Implicit none

! Declaration of all the variables
! n = counter used in the iterative process to get to solution in terms of number of cycles allowable
! COOL = check used to determine whether the blade is cooled or not: 1 if it is, 2 if not
! ierror = indication of an error in the output file
! n_cycles =
! deltaT = average temperature difference acting on the component
! Tamb = ambient operating temperature in K
! TET = turbine entry temperature in K before cooling
! EPS = cooling effectiveness (assumed to be equal to 0.5)
! T_COOL = temperature in K of the coolant entering the blade
! cycles = number of cycles to failure, with an applied safety factor of 2/3
! Features of the material:
! sigma_y = yield stress of the material (0.2% proof stress) in MPa
! E = elastic modulus (in MPa)
! epsilon_f = fatigue ductility coefficient in mm
! sigma_f = fatigue strenght coefficient in MPa
! b = fatigue strength exponent
! c = fatigue ductility exponent
! exp_coeff = linear coefficient of therma expansion
! eps_max = maximum thermal strain in mm
! sigma_max = maximum stress in MPa associated to the maximum thermal strain
! neu_cost = Neuber rule constant for the superior curve, defined as the product of sigma and epsilon
! epsilon_y = ideal strain in mm at the yield condition
! epsilon_neuy = real strain in mm at the yield condition, estimated through the Neuber rule
! Characteristic point of the Neuber rule applied to cyclic loading
! epsilon_o1
! sigma_c1
! epsilon_c1
! neu_costinf = Neuber rule constant for the inferior curve, defined as the product of sigma and epsilon
! sigma_d1
! epsilon_d1
! epsilon_d
! delta_eps = derived from Neuber rule, it will be the input for the Coffin and Manson rule
! Results and iterative process:
! res = real result obtained with Neuber rule
! res1 = result obtained iteratively through Coffin and Manson method. This value will be compared to the real result
"res", and the iterations stopped when
! the residual will be <= to 1% of the real result
! fatigue_life = time to failure due to fatigue, expressed in hours

double precision :: fatigue_life_blade,fatigue_life_disc

Integer :: n,COOL,ierror,n_cycles_blade
double precision ::
deltaT,sigma_y_blade,E_blade,epsilon_f_blade,sigma_f_blade,b_blade,c_blade,exp_coeff_blade,eps_max_blade,time_cyc,sigm
a_max_blade,neu_cost_blade,&
&
epsilon_y_blade,epsilon_neuy_blade,epsilon_o1_blade,sigma_c1_blade,epsilon_c1_blade,neu_costinf_blade,sigma_d1_blade,e
psilon_d1_blade,epsilon_d_blade,&
& delta_eps_blade,res_blade,res1_blade,Tamb,TET,EPS,T_COOL,coating
double precision :: blade_material_properties(23)

! Opening the input file where the input data are listed
```

```
Open (UNIT=60, FILE='Indat_fatigue.dat', STATUS='OLD', ACTION='READ')

! Creation of an output file where the results will be reported

Open (UNIT=65, FILE='Outdat_fatigue.dat', STATUS='UNKNOWN', ACTION='WRITE', IOSTAT=ierror)

Read (60,*) Tamb
Read (60,*) TET
Read (60,*) COOL
READ (60,*) T_COOL
READ (60,*) EPS
read (60,*) coating

! Blade cooling section: calculation based on an equilibrium between the heat flux entering the blade and the one
leaving it, absorbed by the coolant.
! It has been assumed that the overall cooling effectiveness is equal to 0.5

SELECT CASE (COOL)
          CASE (1)
                    TET=TET-EPS*(TET-T_COOL)
                    WRITE (65,*) 'The temperature in K after cooling is: ',TET
                    deltaT=TET-Tamb
                    Write (65,*) 'The temperature difference acting on the component after cooling is: ',deltaT

          CASE DEFAULT
                    deltaT=TET-Tamb
                    WRITE (65,*) 'No cooling used'
END SELECT

deltaT = deltaT-coating

! Working condition in terms of variation of temperature

Write (65,*) 'The average temperature difference acting on the component is: ',deltaT

! Estimation of the blade fatigue

                     sigma_y_blade = blade_material_properties(22)
                     E_blade = blade_material_properties(14)
                     epsilon_f_blade = blade_material_properties(15)
                     sigma_f_blade = blade_material_properties(16)
                     b_blade = blade_material_properties(17)
                     c_blade = blade_material_properties(18)
                     exp_coeff_blade = blade_material_properties(19)

! Calculation of the maximum thermal strain in mm and of the associated stress in MPa

                    eps_max_blade=deltaT*exp_coeff_blade
                    sigma_max_blade=eps_max_blade*E_blade

                    ! We use the Neuber rule, which states that sigma*epsilon=constant

                    neu_cost_blade=sigma_max_blade*eps_max_blade

                    ! Calculation of the strain in mm at the yield stress

                    epsilon_y_blade=sigma_y_blade/E_blade

                    ! Calculation of the Neuber strain in mm at the yield stress

                    epsilon_neuy_blade=neu_cost_blade/sigma_y_blade

                    ! Calculation of the strain in mm at O'

                    epsilon_o1_blade=epsilon_neuy_blade-epsilon_y_blade

                    ! Calculation of the inferior Neuber curve

                    sigma_c1_blade=abs(sigma_y_blade-sigma_max_blade)
                    epsilon_c1_blade=sigma_c1_blade/E_blade
                    neu_costinf_blade=sigma_c1_blade*epsilon_c1_blade
                    sigma_d1_blade=sigma_y_blade
                    epsilon_d1_blade=neu_costinf_blade/sigma_d1_blade
                    epsilon_d_blade=epsilon_o1_blade-epsilon_d1_blade
                    delta_eps_blade=epsilon_neuy_blade-epsilon_d_blade

                    ! Applying Coffin and Manson rule

                    res_blade=delta_eps_blade/2.

! Iterations to get the result: the iterations stop and give the result when a residual <= 1% is reached

                    do n=1,20000

res1_blade=(sigma_f_blade*((2*n)**b_blade)/E_blade)+(epsilon_f_blade*((2*n)**c_blade))
                              n_cycles_blade=n
                              if (abs(res1_blade-res_blade)<=(res_blade*0.01)) exit
                    end do
                                                        !life given in terms of hours of flight


          fatigue_life_blade=n_cycles_blade*time_cyc

                                                                                write (65,*) 'Numbers of block hours
to failure (for the blades)            =',fatigue_life_blade

close (UNIT=60)
close (UNIT=65)

end subroutine thermal_fatigue
```

F.5 Creep Module

```
! the following subroutine will be able to estimate the creep life of an engine component, by using the larson-miller
approach.it is included also a very simple
! mechanism of cooling, where inserting the cooling effectiveness and the coolant temperature as inputs, the new
component temperature is calculated. Here in
! particular the subroutine is written for a single stage turbine, and allows the user to analyse the blade, the disc
or both.

subroutine creep (blade_creep_life,blade_material_properties,disk_material_properties)

implicit none

! Declaration of all the variables:
double precision :: blade_creep_life,disc_creep_life
integer ::
nseg,p,q,r,num_t,lmp_check_blade,lmp_type_blade,lmp_constant_blade,lmp_type_disc,lmp_constant_disc,lmp_check_disc,nlmp
_blade,nlmp_disc,&
& rpm,sf,cool,ierror,blade_stress_select,disc_stress_select,MATERIAL_BLADE,MATERIAL_DISK
double precision ::
temp,time,blade_lmp_value,blade_lmp_stress,blade_lmp,blade_tf,blade_sum_life,blade_total_life,total_time,sigma_max_bla
de,disc_lmp_value,disc_lmp_stress,&
& eps,disc_lmp,disc_tf,disc_sum_life,disc_total_life,sigma_max_disc,sigma_cf,root_cf_load,Coating
double precision, allocatable ::
t_cool(:),blade_lmp_curve(:,:),disc_lmp_curve(:,:),disc_stress_temp(:,:),blade_stress_temp(:,:),rpm_array(:),temp_arra
y(:),time_array(:)
double precision :: blade_material_properties(23),disk_material_properties(23)

! Description of all the variables:
! nseg = number of segment into which the flight envelope has been split
! sf = rpm of the high pressure turbine first stage at design point
! blade_stress_select = stress selector: 1 if the maximum stress acting will be estimated using the blade stress
subroutine, 2 if the maximum stress is inputted by the user
! cool = check used to determine whether the blade is cooled or not: 1 if it is, 2 if not
! t_cool = temperature in k of the coolant entering the blade
! eps = cooling effectiveness
! num_t = flight segment time selector: 1 if time is expressed in hours, 2 if it is expressed as percentage of the
whole envelope
! total_time = total time spent in flight from the beginning of the simulation
! time = time spent during each segment of flight, expressed in hours if num_t = 1, or as a percentage of the whole
flight envelope if num_t = 2
! lmp_check_blade = larson-miller parameter selector: 1 if the LMP are unknown and have to be calculated from the LM
curve (inputted by points), 2 if the LMP for each load condition (i.e. segment of flights) are known
! lmp_type_blade = larson-miller parameter type selector: 1 if the LM equation is expressed in Imperial Units
(temperature in °F and stress in Ksi), 2 if it is expressed in SI (temperature in °K and stress in MPa)
! lmp_constant_blade = value of the constant of the LM equation (usually 20 or 25, depending upon the material)
! nlmp_blade = number of points of the larson-miller curve known, and that will be inputted to create a curve from
where the LMP corresponding to each stress condition will be taken (by interpolation)
! blade_lmp = larson-miller parameter for each load condition
! cyc_hrs_blade = creep life selector: 1 for creep life in hours, 2 for creep life in cycles (the whole flight
envelope is considered as 1 cycle)
! blade_sum_life = sum of all the life fractions of each segment
! blade_total_life = total creep life of the blade without safety factors
! blade_creep_life = total creep life of the blade with safety factors
! disc_stress_select = stress selector: 1 if the maximum stress acting will be estimated using the disc stress
subroutine, 2 if the maximum stress is inputted by the user
! lmp_check_disc = larson-miller parameter selector: 1 if the LMP are unknown and have to be calculated from the LM
curve (inputted by points), 2 if the LMP for each load condition (i.e. segment of flights) are known
! lmp_type_disc = larson-miller parameter type selector: 1 if the LM equation is expressed in Imperial Units
(temperature in °F and stress in Ksi), 2 if it is expressed in SI (temperature in °K and stress in MPa)
! lmp_constant_disc = value of the constant of the LM equation (usually 20 or 25, depending upon the material)
! nlmp_disc = number of points of the larson-miller curve known, and that will be inputted to create a curve from
where the LMP corresponding to each stress condition will be taken (by interpolation)
! disc_lmp = larson-miller parameter for each load condition
! cyc_hrs_disc = creep life selector: 1 for creep life in hours, 2 for creep life in cycles (the whole flight envelope
is considered as 1 cycle)
! disc_sum_life = sum of all the life fractions of each segment
! disc_total_life = total creep life of the disc without safety factors
! disc_creep_life = total creep life of the disc with safety factors
! ierror = indication of an error in the output file
! p,q,r = counters used for the loop cycles
! num = check used to determine whether the larson-miller parameters will be calculated as an interpolation of at
least 6 values of the curve known, or
! they are already known and typed by the user; 1 if there are some curve's values available to interpolate, 2 if the
parameters will be inserted as input by the user
! nlmp = number of known point of the larson-miller curve, that have to be interpolated the find the current values of
the larson-miller parameter. this number has to be => 6
! cyc_hrs = check used to define wether the user wants a creep life in terms of hours (1) or cycles (2)
! stress = values of the stresses acting during each segment of the flight envelope (in mpa), determined from
turbomatch simulations
! temp = values of the temperatures acting during each segment of the flight envelope (in k), determined from
turbomatch simulations
! time = time spent for each segment of flight (in hours or percentage)
! lmp_value = larson-miller parameter known from the curve and interpolated to give the larson-miller parameter we
need
! lmp_stress = stresses in mpa correspondant to each larson-miller parameter typed before
! lmp = larson-miller parameter acting during each segment of flight. they are already known, so there's no needing to
interpolate
! tf = time to failure in hours of each segment of flight, estimated through the larson-miller method
! sum_life = sum of the life fractions
! total_life = total time to failure of the whole component
! total_time = total time (in hours) spent for the whole flight envelope
! lmp_curve = matrix that contains the larson-miller parameter and the respective stress associated, that define the
larson-miller curve
! stress_temp = matrix that contains all the data we need: stress for each segment, temperature for each segment, time
spent for each segment
! larson-miller parameter for each segment, time to failure of each segment and total life fraction of each segment
! creep_life = creep life in hours of the component
! sigma_max_blade = maximum stress acting on the blade

! -------------------opening the input files where data are listed----------------------
```

```
open (unit=50, file='indat_creep.dat', status='old', action='read')

! --------------------creation of an output file where the results will be reported-----
open (unit=55, file='outdat_creep.dat', status='unknown', action='write', iostat=ierror)

!                           --------------------creep analysis------------------
read (50,*) nseg
read (50,*) sf
read (50,*) blade_stress_select
read (50,*) disc_stress_select
read (50,*) cool
read (50,*) eps
read (50,*) Coating
read (50,*) lmp_check_blade
read (50,*) lmp_check_disc
lmp_type_disc=disk_material_properties(23)
lmp_constant_disc=disk_material_properties(21)
lmp_constant_blade=blade_material_properties(21)
lmp_type_blade=blade_material_properties(23)
sf=sf*60

                    allocate (blade_stress_temp(nseg,6))              ! A matrix which will contain all the data
needed the carry out a creep analysis is created

                    allocate (rpm_array(nseg),temp_array(nseg),time_array(nseg),t_cool(nseg))

                    ! input stress and temperatures acting during each segment of flight

                    do p=1,nseg
                       read(50,*) rpm_array(p)
                    enddo

                    do p=1,nseg
                       read(50,*) t_cool(p)
                    enddo

                    do p=1,nseg
                       read(50,*) temp_array(p)
                    enddo

                    do p=1,nseg
                       read(50,*) time_array(p)
                       time_array(p)=time_array(p)/60
                    enddo

                    read (50,'(2/)')

                    do p=1,nseg
                              select case (blade_stress_select)
                                        case (1)
                                                  rpm=rpm_array(p)*sf
          ! The rpm is the needed input file to use the blade stress subroutine
                                                  call blade_stress
(rpm,sigma_max_blade,root_cf_load,blade_material_properties)
                                        case (2)
                                                  read (50,*) sigma_max_blade
                              end select
                              blade_stress_temp(p,1)=sigma_max_blade
! The first coloumn of the matrix contains the stresses acting during each segment of flight
                              blade_stress_temp(p,2)=temp_array(p)                              ! The second
coloumn of the matrix contains the maximum temperature acting during each segment of flight
                    end do

                    ! --------------------cooling section------------------
                    ! calculation based on an equilibrium between the heat flux entering the blade and the one leaving
it, absorbed by the coolant.

                    select case (cool)
                              case (1)
                              ! calculation of the new temperature of the metal after cooling:
                                        do p=1,nseg
                                                  blade_stress_temp(p,2)=blade_stress_temp(p,2)-
eps*(blade_stress_temp(p,2)-t_cool(p))
                                        end do
                              case (2)                                  ! no cooling
                              write (55,*) 'no cooling used'
                    end select
                    ! ----------------------end of the blade cooling section------------------

!-------------------------Effect of thermal barrier coating---------------------

do p=1,nseg
          blade_stress_temp(p,2)=blade_stress_temp(p,2)-Coating
end do

                    ! ---------------------input of time spent for each flight segment--------

                              total_time=0                              ! inizialization of the variable
                              do p=1,nseg
                                        blade_stress_temp(p,3)=time_array(p)                                        ! The
third coloumn of the matrix contains the amount of time spent during each segment of flight
                                        total_time=total_time+blade_stress_temp(p,3)
                              end do

! -------------------------calculation of the larson-miller parameter--------------------

                              if (lmp_check_blade==1) then
                                        nlmp_blade = 6
                                        allocate (blade_lmp_curve(nlmp_blade,2))
          ! A matrix containing the LMP and their respective stresses is created
                    ! values of the larson-miller parameter available(at least 6), with the corresponding stress
value, read from the input file:
```

```
                  ! IMPORTANT!! The known Larson-miller parameters have to be inserted in a decreasing order, from
the higher to the lower!

          blade_lmp_curve(1,1)=blade_material_properties(1)                    ! first coloumn of the matrix
containing the LMP

          blade_lmp_curve(2,1)=blade_material_properties(3)

          blade_lmp_curve(3,1)=blade_material_properties(5)

          blade_lmp_curve(4,1)=blade_material_properties(7)

          blade_lmp_curve(5,1)=blade_material_properties(9)

          blade_lmp_curve(6,1)=blade_material_properties(11)


          blade_lmp_curve(1,2)=blade_material_properties(2)                    ! second coloumn of the matrix
containing the stress
                                                              blade_lmp_curve(2,2)=blade_material_properties(4)
                                                              blade_lmp_curve(3,2)=blade_material_properties(6)
                                                              blade_lmp_curve(4,2)=blade_material_properties(8)
                                                              blade_lmp_curve(5,2)=blade_material_properties(10)
                                                              blade_lmp_curve(6,2)=blade_material_properties(12)

                  ! interpolation of the available larson-miller curve to get the larson-miller parameter for stress
condition (i.e. each segment of flight)
                                                          select case (lmp_type_blade)
                                                                    case (1)
          ! LM equation in Imperial Units
                                                                    do p=1,nseg

blade_stress_temp(p,1)=blade_stress_temp(p,1)/6.894                ! Stress converted from MPa to Ksi, as the Larson-
Miller curve is given in Imperial Units

blade_stress_temp(p,2)=blade_stress_temp(p,2)-273.15

blade_stress_temp(p,2)=(blade_stress_temp(p,2)*9./5.)+32.    ! Temperatures in farenight
                                                                    end do
                                                                    outer: do p=1,nseg
                                                                              inner: do q=1,nlmp_blade-1

                                                                                        blade_lmp=0
                                                                                  if
(blade_stress_temp(p,1)>=blade_lmp_curve(q,2).and.blade_stress_temp(p,1)<=blade_lmp_curve(q+1,2)) then

blade_lmp=blade_lmp_curve(q+1,1)+(blade_lmp_curve(q,1)-blade_lmp_curve(q+1,1))*(blade_lmp_curve(q+1,2)-
blade_stress_temp(p,1))/(blade_lmp_curve(q+1,2)-blade_lmp_curve(q,2))

                                                                                  elseif
(blade_stress_temp(p,1)<blade_lmp_curve(1,2)) then

blade_lmp=blade_lmp_curve(1,1)

                                                                                  elseif
(blade_stress_temp(p,1)>blade_lmp_curve(nlmp_blade,2)) then

blade_lmp=blade_lmp_curve(nlmp_blade,1)

                                                                                  endif
                                                                        ! calculation of time to failure
for each segment (in hours)


blade_tf=10**(blade_lmp*1000/(blade_stress_temp(p,2)+460)-lmp_constant_blade)
                                                                                  blade_stress_temp(p,4)=blade_lmp
                                                ! fourth coloumn of the matrix containing the LMP corresponding to the load
condition
                                                                                  blade_stress_temp(p,5)=blade_tf
                                                                    ! fifth coloumn of the matrix
containing the time to failure corresponding to each load condition

blade_stress_temp(p,6)=blade_stress_temp(p,3)/blade_tf               ! sixth coloumn containing the life fraction of
each load condition
                                                                        if (blade_lmp/=0) exit
                                                                              end do inner
                                                                    end do outer
                                                              case (2)
          ! LM equation in SI
                                                                        do p=1,nseg
                                                                        do q=1,nlmp_blade
                                                                                  blade_lmp=0
                                                                                        if
(blade_stress_temp(p,1)>=blade_lmp_curve(q,2).and.blade_stress_temp(p,1)<=blade_lmp_curve(q+1,2)) then

          blade_lmp=blade_lmp_curve(q+1,1)+(blade_lmp_curve(q,1)-blade_lmp_curve(q+1,1))*(blade_lmp_curve(q+1,2)-
blade_stress_temp(p,1))/(blade_lmp_curve(q+1,2)-blade_lmp_curve(q,2))

                                                                                                    elseif
(blade_stress_temp(p,1)<blade_lmp_curve(1,2)) then

                  blade_lmp=blade_lmp_curve(1,1)

                                                                                                    elseif
(blade_stress_temp(p,1)>blade_lmp_curve(nlmp_blade,2)) then

                  blade_lmp=blade_lmp_curve(nlmp_blade,1)
                                                                                          endif


          blade_stress_temp(p,4)=blade_lmp                                   ! fourth coloumn of the matrix
containing the LMP corresponding to the load condition
```

```
                              ! calculation of time to failure for each segment (in hours)

          blade_tf=10**(blade_lmp*1000/blade_stress_temp(p,2)-lmp_constant_blade)

          blade_stress_temp(p,5)=blade_tf
! fifth coloumn of the matrix containing the time to failure corresponding to each load condition

          blade_stress_temp(p,6)=blade_stress_temp(p,3)/blade_tf               ! sixth coloumn containing the life
fraction of each load condition
                                                                                        if (blade_lmp/=0) exit
                                                                                        end do
                                                                               end do
                                                          end select

                              else if (lmp_check_blade==2) then ! larson-miller parameter already known for each
segment and introduced by the user through the input file
                                        do p=1,nseg    ! larson-miller parameter acting on each segment of flight,
read from the input file
                                                  read (50,*) blade_lmp
                                                  blade_stress_temp(p,4)=blade_lmp

                              ! calculation of time to failure for each segment (in hours)
                                                  select case (lmp_type_blade)
                    case (1)                                ! LM equation in Imperial Units
                                                      blade_stress_temp(p,1)=blade_stress_temp(p,1)/6.894
                                                      blade_stress_temp(p,2)=blade_stress_temp(p,2)-273.15

          blade_stress_temp(p,2)=(blade_stress_temp(p,2)*9./5.)+32.    ! Temperatures in farenight

          blade_tf=10**(blade_lmp*1000/(blade_stress_temp(p,2)+460)-lmp_constant_blade)
                                                          case (2)                                  ! LM equation in
SI

          blade_tf=10**(blade_lmp*1000/blade_stress_temp(p,2)-lmp_constant_blade)
                                                  end select

                                                  blade_stress_temp(p,5)=blade_tf
                                                  blade_stress_temp(p,6)=blade_stress_temp(p,3)/blade_tf
                                        end do
                              end if

                              ! ------------------------------calculation of creep life using the cumulative Miner's
law---------------------------------
! first of all, it is to be decided wether to estimate the creep life in hours or cycles; talking about cycles, we
assume that the sum of all the segments of
! flight (i.e. the whole flight envelope) represents 1 cycle through the variable cyc_hrs, read from the input file,
it is decided whether we want the creep life
! in hours (cyc_hrs = 1) or in cycles (cyc_hrs = 2)

! creep life in hours
                                        blade_sum_life=0                                                    !
inizialization of the variable
                                        do r=1,nseg
                                                  blade_sum_life=blade_sum_life+blade_stress_temp(r,6)
                                        end do
                                        blade_total_life=total_time/blade_sum_life

blade_creep_life=blade_total_life                         ! total creep life of the component

                              write (55,*) 'total blade creep life
          =',blade_creep_life, 'hrs'
write (55,*)
if (lmp_type_blade==1) then
   do p=1,nseg
      blade_stress_temp(p,1)=blade_stress_temp(p,1)*6.894          ! Stress converted from MPa to Ksi, as the Larson-
Miller curve is given in Imperial Units
         blade_stress_temp(p,2)=(blade_stress_temp(p,2)-32.)*5./9.    ! Temperatures in farenight
         blade_stress_temp(p,2)=blade_stress_temp(p,2)+273.15
   end do
end if
                    write (55,110) 'Blade Stress (MPa)            ',blade_stress_temp(:,1)
                    write (55,110) 'Blade Temperature (K)         ',blade_stress_temp(:,2)
                    write (55,110) 'Blade Time spent (hrs)        ',blade_stress_temp(:,3)
                    write (55,110) 'Blade LMP                     ',blade_stress_temp(:,4)
                    write (55,120) 'Blade Time to failure (hrs)   ',blade_stress_temp(:,5)
                    write (55,130) 'Blade Life fraction           ',blade_stress_temp(:,6)

!*****************************************************************************************************************

! disk creep calculations

                    allocate (disc_stress_temp(nseg,6))                                                 ! A matrix which
will contain all the data needed the carry out a creep analysis is created

                    ! input stress and temperatures acting during each segment of flight

                    do p=1,nseg
                              select case (disc_stress_select)
                                        case (1)
                                                  rpm=rpm_array(p)*sf
          ! The rpm is the needed input file to use the disc stress subroutine
                                                  call disc_stress
(rpm,sigma_max_disc,sigma_cf,sigma_max_blade,disk_material_properties,blade_material_properties)
                                        case default
                                                  read (50,*) sigma_max_disc
                              end select
                              disc_stress_temp(p,1)=sigma_max_disc                        ! The first coloumn of the
matrix contains the stresses acting during each segment of flight
                              disc_stress_temp(p,2)=temp_array(p)
          ! The second coloumn of the matrix contains the maximum temperature acting during each segment of flight
                    end do

                    ! ---------------------input of time spent for each flight segment--------
```

```
                              total_time=0                              ! inizialization of the variable
                              do p=1,nseg
                                        disc_stress_temp(p,3)=time_array(p)
! The third coloumn of the matrix contains the amount of time spent during each segment of flight
                                        total_time=total_time+disc_stress_temp(p,3)
                              end do

! ------------------------calculation of the larson-miller parameter--------------------

if (lmp_check_disc==1) then
                                        nlmp_disc = 6
                                        allocate (disc_lmp_curve(nlmp_disc,2))                                  ! A
matrix containing the LMP and their respective stresses is created

                                                  ! values of the larson-miller parameter available(at least
6), with the corresponding stress value, read from the input file:
                                                  ! IMPORTANT!! The known Larson-miller parameters have to
be inserted in a decreasing order, from the higher to the lower!

                                                            disc_lmp_curve(1,1)=disk_material_properties(1)
                              ! first coloumn of the matrix containing the LMP
                                                            disc_lmp_curve(2,1)=disk_material_properties(3)
                                                            disc_lmp_curve(3,1)=disk_material_properties(5)
                                                            disc_lmp_curve(4,1)=disk_material_properties(7)
                                                            disc_lmp_curve(5,1)=disk_material_properties(9)
                                                            disc_lmp_curve(6,1)=disk_material_properties(11)

                                                            disc_lmp_curve(1,2)=disk_material_properties(2)
                              ! second coloumn of the matrix containing the stress
                                                      disc_lmp_curve(2,2)=disk_material_properties(4)
                                                      disc_lmp_curve(3,2)=disk_material_properties(6)
                                                      disc_lmp_curve(4,2)=disk_material_properties(8)
                                                      disc_lmp_curve(5,2)=disk_material_properties(10)
                                                      disc_lmp_curve(6,2)=disk_material_properties(12)

          ! interpolation of the available larson-miller curve to get the larson-miller parameter for stress condition
(i.e. each segment of flight)
                                                  select case (lmp_type_disc)
                                                            case (1)
          ! LM equation in Imperial Units
                                                            do p=1,nseg

disc_stress_temp(p,1)=disc_stress_temp(p,1)/6.894   ! Stress converted from MPa to Ksi, as the Larson-Miller curve is
given in Imperial Units
                                                               disc_stress_temp(p,2)=disc_stress_temp(p,2)-
273.15

disc_stress_temp(p,2)=(disc_stress_temp(p,2)*9./5.)+32.
                                                            end do
                                                                     do p=1,nseg
                                                                          do q=1,nlmp_disc
                                                                          disc_lmp=0
                                                                                    if
(disc_stress_temp(p,1)>=disc_lmp_curve(q,2).and.disc_stress_temp(p,1)<=disc_lmp_curve(q+1,2)) then

          disc_lmp=disc_lmp_curve(q+1,1)+(disc_lmp_curve(q,1)-disc_lmp_curve(q+1,1))*(disc_lmp_curve(q+1,2)-
disc_stress_temp(p,1))/(disc_lmp_curve(q+1,2)-disc_lmp_curve(q,2))

                                                                                    else if
(disc_stress_temp(p,1)<disc_lmp_curve(1,2))then

disc_lmp=disc_lmp_curve(1,1)
                                                                                    else if
(disc_stress_temp(p,1)>disc_lmp_curve(nlmp_disc,2)) then

disc_lmp=disc_lmp_curve(6,1)
                                                                                    end if

          disc_stress_temp(p,4)=disc_lmp                                    ! fourth coloumn of the matrix
containing the LMP corresponding to the load condition

          ! calculation of time to failure for each segment (in hours)


          disc_tf=10**(disc_lmp*1000/(disc_stress_temp(p,2)+460)-lmp_constant_disc)

          disc_stress_temp(p,5)=disc_tf                                                                         ! fifth
coloumn of the matrix containing the time to failure corresponding to each load condition

          disc_stress_temp(p,6)=disc_stress_temp(p,3)/disc_tf               ! sixth coloumn containing the life
fraction of each load condition
                                                                                    if (disc_lmp/=0)

exit
                                                                              end do
                                                                     end do
                                                            case (2)
          ! LM equation in SI
                                                                     do p=1,nseg
                                                                        do q=1,nlmp_disc
                                                                        disc_lmp=0
                                                                                    if
(disc_stress_temp(p,1)>=disc_lmp_curve(q,2).and.disc_stress_temp(p,1)<=disc_lmp_curve(q+1,2)) then

          disc_lmp=disc_lmp_curve(q+1,1)+(disc_lmp_curve(q,1)-disc_lmp_curve(q+1,1))*(disc_lmp_curve(q+1,2)-
disc_stress_temp(p,1))/(disc_lmp_curve(q+1,2)-disc_lmp_curve(q,2))

                                                                                    else if
(disc_stress_temp(p,1)<disc_lmp_curve(1,2)) then

disc_lmp=disc_lmp_curve(1,1)
                                                                                    else if
(disc_stress_temp(p,1)>disc_lmp_curve(nlmp_disc,2)) then
```

```
disc_lmp=disc_lmp_curve(6,1)
                                                                                                    end if


          disc_stress_temp(p,4)=disc_lmp                                          ! fourth coloumn of the matrix
containing the LMP corresponding to the load condition

                    ! calculation of time to failure for each segment (in hours)

          disc_tf=10**(disc_lmp*1000/disc_stress_temp(p,2)-lmp_constant_disc)

          disc_stress_temp(p,5)=disc_tf                                                                  ! fifth
coloumn of the matrix containing the time to failure corresponding to each load condition

          disc_stress_temp(p,6)=disc_stress_temp(p,3)/disc_tf                    ! sixth coloumn containing the life
fraction of each load condition
                                                                                        if (disc_lmp/=0) exit
                                                                                        end do
                                                                                end do
                                                                end select

                              else if (lmp_check_disc==2) then    ! larson-miller parameter already known for each
segment and introduced by the user through the input file
                                        do p=1,nseg
! larson-miller parameter acting on each segment of flight, read from the input file
                                                read (50,*) disc_lmp
                                                disc_stress_temp(p,4)=disc_lmp

                    ! calculation of time to failure for each segment (in hours)
                                                select case (lmp_type_disc)
                    case (1)                                    ! LM equation in Imperial Units
                                                    disc_stress_temp(p,1)=disc_stress_temp(p,1)/6.894   !
Stress converted from MPa to Ksi, as the Larson-Miller curve is given in Imperial Units
                                                                disc_stress_temp(p,2)=disc_stress_temp(p,2)-
273.15

disc_stress_temp(p,2)=(disc_stress_temp(p,2)*9./5.)+32.

disc_tf=10**(disc_lmp*1000/(disc_stress_temp(p,2)+460)-lmp_constant_disc)

                                        case (2)                                ! LM equation in SI

          disc_tf=10**(disc_lmp*1000/disc_stress_temp(p,2)-lmp_constant_disc)
                                                end select

                                                disc_stress_temp(p,5)=disc_tf
                                                disc_stress_temp(p,6)=disc_stress_temp(p,3)/disc_tf
                                        end do
                              end if

! ------------------------------calculation of creep life using the cumulative Miner's law--------------------------
-------
! first of all, it is to be decided wether to estimate the creep life in hours or cycles; talking about cycles,
                              ! we assume that the sum of all the segments of flight (i.e. the whole flight envelope)
represents 1 cycle
! through the variable cyc_hrs, read from the input file, it is decided whether we want the creep life in hours
(cyc_hrs = 1) or in cycles (cyc_hrs = 2)

                                        ! creep life in hours
                                        disc_sum_life=0                                                 !
inizialization of the variable
                                        do r=1,nseg
                                                disc_sum_life=disc_sum_life+disc_stress_temp(r,6)
                                        end do
                                        disc_total_life=total_time/disc_sum_life
disc_creep_life=disc_total_life                         ! total creep life of the component
          write (55,*)
                              write (55,*) 'total disc creep life
          =',disc_creep_life, 'hrs'
                    write (55,*)
if (lmp_type_disc==1) then
   do p=1,nseg
      disc_stress_temp(p,1)=disc_stress_temp(p,1)*6.894   ! Stress converted from MPa to Ksi, as the Larson-Miller
curve is given in Imperial Units
      disc_stress_temp(p,2)=(disc_stress_temp(p,2)-32.)*5./9.
      disc_stress_temp(p,2)=disc_stress_temp(p,2)+273.15
   end do
end if
                    write (55,110) 'Disc Stress (MPa)       ',disc_stress_temp(:,1)
                    write (55,110) 'Disc Temperature (K)          ',disc_stress_temp(:,2)
                    write (55,110) 'Disc Time spent (hrs)         ',disc_stress_temp(:,3)
                    write (55,110) 'Disc LMP                      ',disc_stress_temp(:,4)
                    write (55,120) 'Disc Time to failure (hrs)    ',disc_stress_temp(:,5)
                    write (55,130) 'Disc Life fraction            ',disc_stress_temp(:,6)

!                                       --------------------end of creep analysis------------------

! -------------------closing the input and output units-----------------------------
close (unit=50)
close (unit=55)

! --------------------------outputs format-----------------------------
110 format (' ',A30,5(F10.2,10X))
120 format (' ',A30,F10.2,10X,F10.2,10X,F10.2,11X,F12.2,7X,F10.2,10X)
130 format (' ',A30,F10.8,10X,F10.8,10X,F10.8,11X,F12.8,7X,F10.8,10X)
end subroutine creep
```

F.6 Disk Stress Module

```
! The following subroutine will be able to estimate the maximum stress acting on the disc of a turbine stage: the disc
to be
! analysed can be a constant thickness or a varying thickness one: a subroutine is needed to proceed solving a linear
system
! of equations.

subroutine disc_stress
(rpm,sigma_max_disc,sigma_cf,sigma_max_blade,disk_material_properties,blade_material_properties)

implicit none

! Variables declaration
integer, intent(in) :: rpm
double precision, intent(out) :: sigma_max_disc,sigma_cf,sigma_max_blade
double precision ::
rim_dia,bore_dia,thick,sigma_r_bore,sigma_h_bore,sigma_r_rim,sigma_h_rim,sigma_eq_rim,rim_radial_stress,blade_mass,in_
rad,out_rad,blade_cg_rad,rim_area,&
& root_cf_load,omega,ro_disc,nu
integer :: istat,i,j,n,const_thick,n_ring,check,rim_stress,n_blades
integer, parameter :: n_eq=6            ! maximum number of equations to solve in a linear system (using a subroutine
included)
double precision, parameter :: pi=3.1415926
double precision, parameter :: iter=10000.
double precision, dimension(n_eq,n_eq) :: a
double precision, dimension(n_eq) :: b
integer :: error
double precision, allocatable ::
inner_radius(:,:),outer_radius(:,:),thickness(:,:),sigma_h_in(:,:),sigma_r_in(:,:),S_in(:,:),S_out(:,:),D_in(:,:),D_ou
t(:,:),&
& sigma_h_out(:,:),sigma_r_out(:,:),delta_sigma_r(:,:),delta_sigma_h(:,:),von_mises(:,:)
double precision :: disk_material_properties(23),blade_material_properties(23)

! Description of all the variables:
! nu = Poisson's ratio of the disc material
! ro_disc = density of the disc material (in Kg/m^3)
! const_thick = disc type selector: 1 if the disc is a constant thickness type, 2 if it is a varying thickness one
! rim_stress = rim stress selector: 1 if the centrifugal load is unknown and has to be calculated using the blade
stress subroutine, 2 if it is calculated knowing blade mass and radius of blade centre of gravity, 3 if the rim stress
is already given as input
! omega = angular velocity in rad/s
! n = number of equations to be solved in the linear system
! rim_dia = rim diameter (m) of the constant thickness disc
! bore_dia = bore diameter (m) of the constant thickness disc
! thick = thickness (m) of the constant thickness disc (or of each ring the varying thickness disc has been
discretised into)
! n_blades = number of blades carried by the disc
! rim_area = area of the disc (m^2) over which the centrifugal stress due to the presence of the blades is spread
! root_cf_load = centrifugal load of one blade (MN)
! sigma_cf = rim stress
! blade_mass = mass of a blade (Kg)
! blade_cg_rad = radius of the centre of gravity of the blade (m)
! rim_radial_stress = sigma_cf = rim radial stress
! sigma_r_bore = radial stress at the bore
! sigma_r_rim = radial stress at the rim
! sigma_h_bore = hoop stress at the bore
! sigma_h_rim = hoop stress at the rim
! sigma_eq_rim = von mises stress at the rim, obtained combining the hoop and the radial stress at the rim
! sigma_max_disc = maximum stress acting on the disc
! n_ring = number of rings into which the
! inner_radius = matrix containing the inner radius (m) of each ring the varying thickness disc has been discretised
into
! outer_radius = matrix containing the outer radius (m) of each ring the varying thickness disc has been discretised
into
! thickness = matrix containing the thickness (m) of each ring the varying thickness disc has been discretised into
! in_rad = inner radius (m) of each ring the varying thickness disc has been discretised into
! von_mises = equivalent von mises stress calculated combining the hoop and radial stress at each station

! -------------------opening the input file where data are listed-----------------------------
open (unit=1,file='disc_input.dat',status='old',action='read',iostat=istat)

! -------------------creation of the output file where the results will be written-----------------------------
open (unit=2,file='disc_output.dat',status='unknown',action='write',iostat=istat)

nu = disk_material_properties(20)
ro_disc = disk_material_properties(13)
read (1,*) const_thick
read (1,*) rim_stress
read (1,*) rim_dia
read (1,*) bore_dia
read (1,*) thick
read (1,*) n_blades

omega=(rpm/60.)*2*pi                    ! rpm transformed into angular velocity (rad/s)

!------------------Constant thickness hollow disc------------------

select case (const_thick)
          case (1)                                          ! Constant Thickness disc
                    n=2                                                 ! number of equations to solve with
the subroutine
                    select case (rim_stress)
                              case (1)                                  ! Rim stress to be calculated using
the blade stress subroutine
                                        call blade_stress (rpm,sigma_max_blade,root_cf_load,blade_material_properties)
                                        rim_area=pi*rim_dia*thick
                                        sigma_cf=root_cf_load*n_blades/rim_area
                              case (2)                                  ! Rim stress to be calculated knowing
number of blades, balde mass and radius of the centre of gravity
```

```
                                        read (1,*) blade_mass
                                        read (1,*) blade_cg_rad
                                        rim_area=pi*rim_dia*thick
                                        sigma_cf=n_blades*blade_mass*blade_cg_rad*omega**2/rim_area
                                case (3)
                                        read (1,*) sigma_cf
                        end select

                        rim_radial_stress=sigma_cf

                        ! Coefficient (a) and right-hand side (b) of the linear system of equation
                        a(1,1)=1
                        a(1,2)=-1./((bore_dia/2.)**2.)
                        b(1)=(3.+nu)*ro_disc*(omega**2)*((bore_dia/2.)**2.)/8.
                        a(2,1)=1
                        a(2,2)=-1./((rim_dia/2.)**2.)
                        b(2)=(sigma_cf*10**6)+((3.+nu)*ro_disc*(omega**2)*((rim_dia/2.)**2.)/8.)

                        ! Solve equations (using the subroutine provided)
                        call simul (a,b,n_eq,n,error)
                        do i=1,n
                                write (2,*) 'solution of equation',i,' = ',b(i)                         ! The solutions of
the equations are written
                        end do

                        sigma_r_bore=0
                        sigma_r_rim=sigma_cf
                        sigma_h_bore=(b(1)+b(2)/((bore_dia/2.)**2.)-
((1+3*nu)*ro_disc*(omega**2)*((bore_dia/2.)**2.)/8.))/10.**6
                        sigma_h_rim=(b(1)+b(2)/((rim_dia/2.)**2.)-
((1+3*nu)*ro_disc*(omega**2)*((rim_dia/2.)**2.)/8.))/10.**6

! Combination of the hoop and radial stress acting at the rim, using Von Mises equation
                        sigma_eq_rim=1/(sqrt(2.))*sqrt((sigma_h_rim-sigma_r_rim)**2.+(sigma_r_rim-0)**2.+(0-
sigma_h_rim)**2.)

                        write (2,*)         'sigma_r_bore =',sigma_r_bore
                        write (2,*)         'sigma_r_rim =',sigma_r_rim
                        write (2,*)         'sigma_h_bore =',sigma_h_bore
                        write (2,*)         'sigma_h_rim =',sigma_h_rim
                        write (2,*)         'sigma_eq_rim =',sigma_eq_rim

! Comparison of the stresses in order to get the maximum acting on the disc
                        if (sigma_r_bore>=sigma_h_bore) then
                                sigma_max_disc=sigma_r_bore
                        else
                                sigma_max_disc=sigma_h_bore
                        end if

                        if (sigma_max_disc>=sigma_eq_rim) then
                                sigma_max_disc=sigma_max_disc
                        else
                                sigma_max_disc=sigma_eq_rim
                        end if

!------------------Varying thickness hollow disc------------------

                case (2)
                        n=6                                                     ! number of equations to be solved
                        read (1,*) n_ring

allocate
(inner_radius(n_ring+1,1),outer_radius(n_ring,1),thickness(n_ring+1,1),sigma_h_in(n_ring+1,1000000),sigma_r_in(n_ring+
1,1000000),&
&
von_mises(n_ring+1,1000000),S_in(n_ring+1,1000000),S_out(n_ring,1000000),D_in(n_ring+1,1000000),D_out(n_ring,1000000),
sigma_h_out(n_ring,1000000),&
& sigma_r_out(n_ring,1000000),delta_sigma_r(n_ring,1000000),delta_sigma_h(n_ring,1000000))

                        do i=1,n_ring+1
                                read (1,*) in_rad
                                inner_radius(i,1)=in_rad
                                read (1,*) thick
                                thickness(i,1)=thick
                        end do

                        do j=1,n_ring
                                outer_radius(j,1)=inner_radius(j+1,1)
                        end do

                        select case (rim_stress)
                case (1)  ! Rim stress to be calculated using the blade stress subroutine
                                        call blade_stress (rpm,sigma_max_blade,root_cf_load,blade_material_properties)
                                        rim_area=pi*rim_dia*thick
                                        sigma_cf=root_cf_load*n_blades/rim_area
                                case (2)                                                ! Rim stress to be calculated knowing
number of blades, balde mass and radius of the centre of gravity
                                        read (1,*) blade_mass
                                        read (1,*) blade_cg_rad
                                        rim_area=pi*rim_dia*thick
                                        sigma_cf=n_blades*blade_mass*blade_cg_rad*omega**2/rim_area
                                case (3)
                                        read (1,*) sigma_cf
                        end select

                        rim_radial_stress=sigma_cf

! Boundary conditions: bore radial stress = 0 and bore hoop stress guessed to be = 100 MPa
                        sigma_h_in(1,1)=100.*10**6
                        sigma_r_in(1,1)=0.
                        S_in(1,1)=sigma_h_in(1,1)
                        D_in(1,1)=S_in(1,1)
```

```
! Iterations needed to get a calculated rim radial stress equal to the actual value of it
                    do j=1,iter
                              do i=1,n_ring
                                        ! Coefficient of the linear system to be solved
                                        a(1,1)=1.
                                        a(1,2)=0.
                                        a(1,3)=-1./2.
                                        a(1,4)=-1./2.
                                        a(1,5)=0.
                                        a(1,6)=0.
                                        a(2,1)=0.
                                        a(2,2)=1.
                                        a(2,3)=-1./2.
                                        a(2,4)=1./2.
                                        a(2,5)=0.
                                        a(2,6)=0.
                                        a(3,1)=0.
                                        a(3,2)=0.
                                        a(3,3)=1.
                                        a(3,4)=0.
                                        a(3,5)=0.
                                        a(3,6)=0.
                                        a(4,1)=0.
                                        a(4,2)=0.
                                        a(4,3)=0.
                                        a(4,4)=1.
                                        a(4,5)=0.
                                        a(4,6)=0.
                                        a(5,1)=0.
                                        a(5,2)=-(thickness(i,1)/thickness(i+1,1)-1)
                                        a(5,3)=0.
                                        a(5,4)=0.
                                        a(5,5)=1.
                                        a(5,6)=0.
                                        a(6,1)=0.
                                        a(6,2)=0.
                                        a(6,3)=0.
                                        a(6,4)=0.
                                        a(6,5)=-nu
                                        a(6,6)=1.

                    ! Right-hand side of the linear system of equations to be solved
                                        b(1)=0.
                                        b(2)=0.
                                        b(3)=S_in(i,j)-((1.+nu)/2.)*ro_disc*(omega**2)*(outer_radius(i,1)**2-
inner_radius(i,1)**2)
                                        b(4)=D_in(i,j)*(inner_radius(i,1)**2/outer_radius(i,1)**2)-(1.-
nu)*ro_disc*(omega**2)*(inner_radius(i,1)**4/outer_radius(i,1)**2-outer_radius(i,1)**2)/4.
                                        b(5)=0.
                                        b(6)=0.

                                        call simul (a,b,n_eq,n,error)

                                        ! Results got from the system of linear equations

                                        sigma_h_out(i,j)=b(1)
                                        sigma_r_out(i,j)=b(2)
                                        S_out(i,j)=b(3)
                                        D_out(i,j)=b(4)
                                        delta_sigma_r(i,j)=b(5)
                                        delta_sigma_h(i,j)=b(6)
                                        sigma_h_in(i+1,j)=sigma_h_out(i,j)+delta_sigma_h(i,j)
                                        sigma_r_in(i+1,j)=sigma_r_out(i,j)+delta_sigma_r(i,j)
                                        S_in(i+1,j)=sigma_h_in(i+1,j)+sigma_r_in(i+1,j)
                                        D_in(i+1,j)=sigma_h_in(i+1,j)-sigma_r_in(i+1,j)
                              end do

                              check=j
                              ! Check of the results: the iterations stop when the estimated rim radial stress differs
from the actual value for 0.001%
                              if ((abs((sigma_r_in(n_ring+1,j)-rim_radial_stress*10**6))<=rim_radial_stress*10) .and.
sigma_r_in(n_ring+1,j)>=0.) exit

                              sigma_h_in(1,j+1)=sigma_h_in(1,j)+1000.
                              sigma_r_in(1,j+1)=0.
                              S_in(1,j+1)=sigma_h_in(1,j+1)
                              D_in(1,j+1)=S_in(1,j+1)
                    end do

                    ! Results converted into MPa
                    sigma_h_in=sigma_h_in/10**6
                    sigma_r_in=sigma_r_in/10**6

                    ! Equivalent von mises stress calculation
                    if (check<1000000.) then
                              do i=1,n_ring
                                        von_mises(i,check)=(1./sqrt(2.))*sqrt((sigma_h_in(i,check)-
sigma_r_in(i,check))**2+(sigma_r_in(i,check)-0)**2+(0-sigma_h_in(i,check))**2)
                                        write (2,*) 'sigma (h_in,r_in,von_mises) =
',sigma_h_in(i,check),sigma_r_in(i,check),von_mises(i,check)
                              end do

                              sigma_max_disc=0.

                              ! Maximum stress identification
                              do i=1,n_ring
                                        if (sigma_max_disc < von_mises(i,check)) then
                                                  sigma_max_disc = von_mises(i,check)
                                                  write (2,*) 'von mises sigma max =',sigma_max_disc
                                        else
                                                  sigma_max_disc = sigma_max_disc
                                                  write (2,*) 'sigma max =',sigma_max_disc
                                        end if
```

```
                        end do
                    else
                        write (2,*) 'no convergence'
                    end if
end select

close (unit=1)
close (unit=2)

end subroutine disc_stress

!-------------------------------------------------------------------------------------------------------------------------
-----------------

subroutine simul (a,b,ndim,n,error)

! Purpose: subroutine to solve a set of n linear equations in n unknowns using Gaussian elimination and the maximum
pivot technique

implicit none

! Data dictionary: declare calling parameters types & definitions
integer, intent(in) :: ndim                                                                                    !
dimension of arrays a and b
double precision, intent(inout), dimension(ndim,ndim) :: a                              ! Array of coefficient (n x
n). This array is of size ndim x ndim, but only n x n of the coefficients are being used. The declare dimension must
be passed to the subroutine or it won't be able to interpret subscripts correctly. (This array is destroyed during
processing)
double precision, intent(inout), dimension(ndim) :: b                                   ! input: right-
hand side of equations.

                                    ! output: solution vector

integer, intent(in) :: n                                                                                       ! number
of equations to solve
integer, intent(out) :: error                                                            ! error flag: 0 no
error, 1 singular equations

! Data dictionary: declare constants
double precision, parameter :: epsilon = 1.0D-6                                                                ! a
"small" number for comparison when determining singular equations

! Data dictionary: declare local variable types and definitions
double precision :: factor
                        ! factor to multiply equation i-row by, before adding to equation j-row
integer  :: irow
          ! number of the equation currently being processed
integer :: ipeak
          ! pointer to equation containing maximum pivot value
integer :: jrow
                    ! number of the equation compared to the current equation
integer :: kcol
                    ! index over all columns of euqations
double precision :: temp
                        ! scratch value

! Process n times to get all equations....
mainloop: do irow=1,n

          ! Find peak pivot for column irow in rows irow to n
          ipeak=irow
          max_pivot: do jrow=irow+1,n
                    if (abs(a(jrow,irow))>abs(a(ipeak,irow))) then
                        ipeak=jrow
                    end if
          end do max_pivot

          ! Check for singular equations.
          singular: if (abs(a(ipeak,irow))<epsilon) then
                    error=1
                    return
          end if singular

          ! Otherwise, if ipeak/= irow, swap equations irow and ipeak
          swap_eqn: if (ipeak/=irow) then
                    do kcol=1,n
                        temp=a(ipeak,kcol)
                        a(ipeak,kcol)=a(irow,kcol)
                        a(irow,kcol)=temp
                    end do
                    temp=b(ipeak)
                    b(ipeak)=b(irow)
                    b(irow)=temp
          end if swap_eqn

          ! Multiply equation irow by -a(jrow,irow)/a(irow,irow), and add it to Eqn jrow (for all eqns except irow
itself)
          eliminate: do jrow=1,n
                    if (jrow/=irow) then
                        factor=-a(jrow,irow)/a(irow,irow)
                        do kcol=1,n
                            a(jrow,kcol)=a(irow,kcol)*factor+a(jrow,kcol)
                        end do
                        b(jrow)=b(irow)*factor+b(jrow)
                    end if
          end do eliminate
end do mainloop

! End of main loop over all equations. All off-diagonal terms are now zero. To get the final answer, we must divide
each
! equations by the coefficient of its non-diagonal term
divide: do irow=1,n
          b(irow)=b(irow)/a(irow,irow)
```

```
          a(irow,irow)=1
end do divide

! Set error flag to 0 and return
error=0

end subroutine simul
```

F.7 Blade Stess Module

```
!-------------------------Blade Stress Calculation using centrifugal forces only-------

subroutine blade_stress (rpm,sigma_max_blade,root_cf_load,blade_material_properties)

implicit none

integer, intent(in) :: rpm
double precision, intent(out) :: sigma_max_blade
double precision, intent(out) :: root_cf_load
double precision :: ro_blade,omega,An,rad,area,sigma_cf,sigma_cf_approx
double precision,parameter :: pi=3.1415926
double precision,allocatable :: radius(:,:)
double precision,allocatable ::
cross_area(:,:),mean_cross_area(:,:),sec_height(:,:),volume(:,:),mass(:,:),cg_radius(:,:),sec_cf_load(:,:),tot_cf_load
(:,:),cf_stress(:,:)
double precision :: blade_material_properties(23)
integer :: n_sec,t

open (40,file='blade_stress_input.dat',status='unknown',action='read')
open (45,file='blade_stress_output.dat',status='unknown',action='write')

read (40,*) n_sec
ro_blade = blade_material_properties(13)

omega=(rpm/60.)*2.*pi

allocate
(radius(n_sec+1,1),cross_area(n_sec+1,1),mean_cross_area(n_sec,1),sec_height(n_sec,1),volume(n_sec,1),mass(n_sec,1),cg
_radius(n_sec,1),&
& sec_cf_load(n_sec,1),tot_cf_load(n_sec+1,1),cf_stress(n_sec+1,1))

                    do t=1,n_sec+1
                              read (40,*) rad
                              radius(t,1)=rad
                    end do

                    do t=1,n_sec+1
                              read (40,*) area
                              cross_area(t,1)=area
                    end do

                    do t=1,n_sec
                              mean_cross_area(t,1)=(cross_area(t,1)+cross_area(t+1,1))/2.
                              sec_height(t,1)=radius(t+1,1)-radius(t,1)
                              volume(t,1)=mean_cross_area(t,1)*sec_height(t,1)
                              mass(t,1)=volume(t,1)*ro_blade
                              cg_radius(t,1)=(radius(t+1,1)+radius(t,1))/2.
                              sec_cf_load(t,1)=mass(t,1)*cg_radius(t,1)*omega**2
                    end do

                                        do t=n_sec+1,2,-1
                                                  tot_cf_load(n_sec+1,1)=0
                                        tot_cf_load(t-1,1)=sec_cf_load(t-1,1)+tot_cf_load(t,1)
                                        end do

                                        do t=1,n_sec+1
                                                  cf_stress(t,1)=(tot_cf_load(t,1)/cross_area(t,1))/1000000.
                                        end do

                    sigma_cf=cf_stress(1,1)
                    root_cf_load=tot_cf_load(1,1)/1000000.
                    An=pi*(radius(n_sec+1,1)**2.-radius(1,1)**2.)

! approximate estimate of the maximum centrifugal stress at the root

sigma_cf_approx=(2.*pi*((rpm/60.)**2.)*ro_blade*An)/1000000.                                                    !maximum
centrifugal force that occurs at the blade root

write (45,*) 'sec_cf_load = ',sec_cf_load
write (45,*) 'tot_cf_load =',tot_cf_load
write (45,*) 'cf_stress =',cf_stress
write (45,*) 'sigma_cf =',sigma_cf
write (45,*) 'sigma_cf_approx =',sigma_cf_approx

sigma_max_blade=sigma_cf_approx

close (unit=40)
close (unit=45)

end subroutine blade_stress
```